**NORTH PACIFIC RESEARCH BOARD PROJECT FINAL REPORT**

# Survey Strategies for Assessment of Bering Sea Forage Species

## NPRB Project 401 Final Report

**Michael F. Sigler[1], Mark C. Benfield[2], Evelyn D. Brown[3], James H. Churnside[4], Nicola Hillgruber[5], John K. Horne[6], Sandra Parker-Stetter[6]**

[1] National Oceanic & Atmospheric Administration, National Marine Fisheries Service, Alaska Fisheries Science Center, 11305 Glacier Highway, Juneau, AK 99801. (907) 789-6037, Mike.Sigler@noaa.gov.
[2] Lousiana State University, Department of Oceanography and Coastal Sciences Coastal Fisheries Institute, 2179 Energy, Coast & Environment Bldg., Baton Rouge LA 70803, (225) 578-6372, mbenfie@lsu.edu
[3] University of Alaska, Fairbanks, School of Fisheries and Ocean Sciences Institute of Marine Science P.O. Box 757220, Fairbanks AK 99775-7220, (907) 590-2462, ebrown@ims.uaf.edu
[4] NOAA Environmental Technology Lab, 325 Broadway R/E/ET 1, Boulder CO 80303, (303) 497-6744, James.H.Churnside@noaa.gov
[5] School of Fisheries and Ocean Sciences, University of Alaska Fairbanks, 11120 Glacier Highway, Juneau, AK 99801, (907) 796-6288, n.hillgruber@uaf.edu
[6] University of Washington, School of Aquatic and Fishery Sciences, Box 355020, Seattle WA 98195, (206) 221-6890, jhorne@u.washington.edu and slps@u.washington.edu

**July 2006**

**Abstract**

Lack of information on forage species composition, distribution, and movements hinders our understanding of their ecological role in the Bering Sea. Recognizing the need for development of forage species survey strategies, this study characterized forage species in the slope, shelf, and nearshore regions of the Bering Sea using direct (midwater trawl, MultiNet, beach seine, jig, ROV) and indirect (acoustics, LIght Detection And Ranging (LIDAR)) sampling technologies. Forage species distribution and quantity differed between shelf (6-100 m) and slope (6-100 m, 100-300 m, 300 m-bottom) regions. Acoustics suggest that shallow and deep layers contained dispersed backscatter while the middle layer contained patchy schools. LIDAR and visual measurements from aircraft documented a patchy distribution of surface plankton and densely shoaling fish that exhibited a high degree of temporal and spatial variability within the 10 d study period. In the nearshore, Pacific sand lance dominated catches and other commonly captured forage fish were YOY Pacific sandfish and gadids. Zooplankton density in the upper 100 m of the water column was significantly higher in nearshore waters. Though copepods were the most abundant taxa, euphausiids, second most abundant, provided more energy to predators due to their large size. We identified several potential candidate species/groups for assessment with acoustics and direct sampling. Other potential, near-surface species/groups could be surveyed with LIDAR and direct sampling. Our results suggest that shelf, slope, and nearshore regions should be surveyed separately and that additional work, in the form of species-or group-specific temporal studies, should be undertaken to refine survey designs.

**Key Words**

bathylagids, myctophids, Pacific sandfish, Pacific sand lance, squid, euphausiids, copepods, acoustics, aerial remote sensing, LIDAR

**Citation**

Sigler, M. F., M. C. Benfield, E. D. Brown, J. H. Churnside, N. Hillgruber, J. K. Horne, S. Parker-Stetter. 2006. Survey Strategies for Assessment of Bering Sea Forage Species. North Pacific Research Board Final Report 401, 137 p.

## Table of Contents

## Study Chronology

This project began October 1, 2004 and ended April 30, 2006. The first study year was devoted to study design and cruise preparation. Fieldwork occurred during June 2005. The second study year was devoted to laboratory analysis, quantitative data analysis, and report writing. Progress reports were submitted January 2005, July 2005, and January 2006.

## Introduction

While the importance of forage species to a healthy ecosystem is widely accepted, targeted and comprehensive studies in the Bering Sea and Gulf of Alaska are limited or lacking. In 1999, amendments to Alaskan groundfish management plans created a forage fish category to allow for specific management actions intended to conserve and manage forage species resources. Without critical life history, distribution, and abundance information the effects of management actions on these species cannot be understood and may not be detectable given the assessment tools currently used. Forage species occupy all major habitats of the Bering Sea: demersal, pelagic, meso- and epi-pelagic, and nearshore. The diverse life histories, distributions, and population dynamics of these species likely will require a diverse array of survey designs and assessment techniques to manage and protect forage species.

Mesopelagic species such as squids and myctophids are an important component of the Bering Sea ecosystem (Sinclair and Stabeno, 2002). Most species are found in water deeper than 250 m during the day and vertically migrate towards the surface at night, often reaching the 100 m upper layer (Watanabe et al., 1999). Few assessment or ecological studies have targeted these species, despite their importance in the diet of many predators including pinnipeds, cetaceans, seabirds, and finfish (Kajimura and Loughlin, 1988; Hunt et al., 1996; Brodeur et al., 1999). Standard research assessment surveys by the Alaska Fisheries Science Center (AFSC) usually operate during daylight hours during the summer, using sampling techniques that do not explicitly census mesopelagic species.

Information also is scarce on the use of nearshore habitats (e.g., eelgrass, kelp) by forage species. The rugged Alaskan coastline combined with adverse weather makes extensive sampling in nearshore habitats difficult. Of the few studies done within the Bering Sea, key forage species captured include capelin (*Mallotus villosus*), Pacific cod (*Gadus macrocephalus*), Pacific herring (*Clupea pallasi*), Pacific sand lance (*Ammodytes hexapterus*), surf smelt (*Hypomesus pretiosus*),

and walleye pollock (*Theragra chalcogramma*) (Isakson et al., 1971; Hancock, 1975; Naumenko, 1996; Robards, 1999; Robards and Schroeder, 2000). It is known that various smelt species migrate to nearshore areas to spawn. In the southeastern Bering Sea, capelin spawning has been reported in Port Moller (Warner and Shafford, 1978), and the Togiak area, beginning in mid-May and lasting until late June (Pahlke, 1985). In Prince William Sound, age-0 and age-1 capelin are found in nearshore nursery areas (Brown, 2002). In addition to providing habitat for spawning adults of some species, nearshore areas also function as migratory pathways and nursery environments for larval and juvenile forage fish, particularly those areas that offer structured habitat (e.g., eelgrass beds).

Assessing distributions and abundances of forage species requires the use of single or multiple sampling technologies depending on the species and/or habitat of interest. Catches of forage species have occurred during annual bottom trawl surveys (Livingston, 2002), acoustic-trawl surveys (Honkalehto et al., 2002), and surface trawl surveys (Farley et al., 2000). Dedicated survey efforts have not been directed towards forage species. In this pilot study, we applied, compared, and potentially integrated a suite of survey techniques over a continuum of forage species habitats. These technologies consisted of high-frequency acoustics (38 and 120 kHz), mid-water trawling, seining, MultiNet zooplankton sampling[1], in-situ imaging, and aerial remote sensing including airborne LIDAR.

## Goal and Objectives

The goal of this project was to assess the distribution, species composition, and ecological role of forage species within nearshore, continental shelf, and continental slope habitats, and the technologies and techniques used to collect the data. Specific objectives included:

*1) Apply a suite of survey techniques to assess the distribution, species composition, and diet of forage species from nearshore to continental slope habitats.*

*2) Identify strengths and constraints of integrating survey techniques to optimize habitat-specific survey effort.*

[1] Unfortunately, components of our in-situ imaging system (ZOOVIS-SC) were damaged during shipping and the system was not operational during our research cruise.

**Manuscripts**

***Chapter 1***. Characterizing distribution and identity of nekton in shelf and slope habitats of the Bering Sea

***Chapter 2***. Forage fish in shallow nearshore habitats of the Bering Sea

***Chapter 3***. Distribution, composition and energy density of zooplankton in the southeastern Bering Sea

***Chapter 4.*** Aerial remote sensing and ecological hot spots in the southeastern Bering Sea

***Chapter 5.*** Mesozooplankton distributions in the southeastern Bering Sea estimated using a Multinet sampler and an evaluation of semi-automated processing with ZooImage software

**Conclusions**

Assessing forage species in the slope, shelf and nearshore regions of the Bering Sea is essential for both ecological understanding and effective resource management. Our study results suggest that these regions differ in their species composition and distribution over time and space. We identified several potential candidate species/groups for population abundance estimates with acoustics and direct sampling. Other potential, near-surface species/groups could be surveyed with LIDAR and direct sampling. Based on our results, in general we recommend that shelf, slope and nearshore regions should be surveyed separately and that additional work, in the form of species-specific temporal studies should be undertaken to refine survey designs. Specific recommendations by habitat follow.

***Nekton in Shelf and Slope Habitats***

Population abundance assessment of mesopelagic species in the Bering Sea is important from an ecosystem and resource management perspective. Previous studies, such as Sinclair and Stabeno (2002), provide a limited picture of nekton distribution due to the use of single trawl hauls. By combining acoustics, LIDAR, and direct sampling, our June 2005 survey highlights

aspects of nekton distribution that will assist in the development of assessment strategies and quantitative abundance estimates for Bering Sea mesopelagic nekton species.

*Shelf and Slope Habitats*

1. Shelf and slope regions should be surveyed separately. Nekton horizontal and vertical distribution differed between the two regions, making it necessary to design region-specific surveys.

*Technology Comparisons*

2. In this study, backscatter measurements from acoustics and LIDAR did not match and could not be combined to provide a full water column numeric/biomass estimate. Additional LIDAR calibration and experimental measurements are needed to facilitate direct comparison between acoustic and optic backscatter data.
3. Acoustics samples backscatter from transducer face through the entire water column. Time needed to sample any area is restricted by platform speed.
4. LIDAR should be restricted to assessment of near-surface (<30 m) forage species or species that vertically migrate into surface waters at night. Aircraft-mounted LIDAR can synoptically sample large areas.
5. Surveys of Bering Sea mesopelagic species must include direct sampling for target identification and specimen collection.
6. Several potential candidate species/groups for population abundance estimates were identified: deepwater myctophids and bathylagids, shelf break squid and Pacific ocean perch (*Sebastes alutus*), shelf herring, walleye pollock, and slope pelagic walleye pollock.
7. Dedicated species- or group-specific pilot surveys are necessary to obtain accurate target strength estimates for separating: myctophids versus bathylagids, herring or capelin versus walleye pollock, and squid versus Pacific ocean perch.
8. Target species or groups should be observed at different times -daylight, crepuscular, and dark - as the effect of vertical or horizontal migration on assessment results cannot be determined at this time. Predictable diel movements could also provide additional ways to characterize the mesopelagic community composition.

9. Appropriate transect spacing must be determined for target species or groups. Ranges observed during our spatiotemporal analyses (2.4 – 5.6 km) suggest that 1 nmi transect spacing was too large to capture backscatter spatial structure in some depth layers.
10. Specific surveys should be undertaken to evaluate the contribution of jellyfish to the mesopelagic community. Midwater trawl catches frequently included jellyfish, but our gear did not effectively sample these organisms

*Biological Hotspots*

11. Airborne estimates of birds and mammals were obtained and high concentrations of these predators were associated with the moving masses of fish (presumably capelin) and large aggregations of swarming euphausiids (e.g., hot spots). Hot spots were approximately 5 nmi in diameter and were concentrated on the shelf near the shelf break. Several formed and disappeared within our relatively short survey period. Assessments of horizontally migrating concentrations should not be done within pre-determined, fixed regions, but rather within adaptively moving grids that can track the biomass.
12. Moving masses of fish schools resembling capelin and Atka mackerel (*Pleurogrammus monopterygius*) (identified by local fishing vessels) were observed from the aircraft but were not directly sampled. Most of these schools were outside the region sampled by the ship.

*Zooplankton Composition and Energetics*

13. Zooplankton and micronekton in the southeastern Bering Sea was dominated by copepods, followed by euphausiids, pteropods, and larvaceans, all of which represent important prey items of forage taxa diet.
14. Since estimates of species abundance and composition varied substantially between shelf and slope stations, assessment of forage taxa prey field needs to be stratified by sampling area.
15. Since many prey taxa migrate vertically on a diurnal basis, it is essential to survey them at different times of the day in order to accurately assess abundance and availability of prey to forage species.
16. The predominance of juvenile stages of euphausiids in the samples might be an artifact of increased net avoidance behavior with ontogeny, making it necessary to employ nets with a larger opening to accurately assess euphausiids abundance.

17. When assessing the zooplankton standing stock as a food resource for forage fish, the inclusion of energy content is important because variation amongst species in energy density (kJ $g^{-1}$) and size result in a different relative importance of taxa than estimated from abundance measures alone.
18. Species-specific measures of energy content are better than grouping taxa, given that the two pteropod species we analyzed had the most disparate energy density amongst all species examined.

***Nearshore Habitat***

Our study showed that shallow nearshore fish assemblages on Akutan, Akun, and Unalaska Islands in June were dominated by forage fish, particularly Pacific sand lance. Most sand lance we captured were juveniles and were from sand habitat, whereas all Pacific sandfish and gadids were young-of-the-year and most were from cobble habitat. The fewest number of fish were captured in bedrock habitat.

The survey approach and sampling techniques we applied were successful at sampling nearshore habitats. We recommend that this approach be continued in studies of nearshore habitats of Bering Sea forage species. One unsurprising result was that some potential nearshore species such as capelin were not found. This lack likely is due to timing of the survey as some nearshore species occupy nearshore habitats only seasonally and only one time period was sampled in this pilot study. Our second recommendation is to expand sampling to multiple time periods in future nearshore sampling. Seasonal studies would help define temporal use of shallow nearshore habitats in the Bering Sea by forage fish species and is a common approach for nearshore habitat sampling (Johnson et al., 2005).

## Publications

The five chapters are intended for publication in peer-reviewed journals.

## Outreach

Benfield, M.C. N. Hillgruber, P. Grosjean, M. Alford, S. Arndt, J. Bacon, and S.F. Keenan. 2006. Semi-automated processing of Bering Sea zooplankton samples using ZooImage software. Poster presented at the 2006 Alaska Marine Science Symposium, 22-25 Jan 2006, Anchorage, AK.

Parker-Stetter, S. 2006. Forage species in the Bering Sea. Webpage http://www.acoustics.washington.edu/current_research.php#Stetter

Parker-Stetter, S., M. Benfield, E. Brown, J. Churnside, N. Hillgruber, J. Horne, S. Johnson, C. Kenaley, M. Sigler, J. Thedinga, J. Vollenweider. 2006. Survey strategies for Bering Sea forage species. Poster presented at the 2006 Alaska Marine Science Symposium, 22-25 Jan 2006, Anchorage, AK. http://www.acoustics.washington.edu/images/ParkerStetter_poster.pdf

Parker-Stetter, S., J. Horne, and J. Churnside. 2006. Acoustic and optic characterization of forage fish distribution in the Bering Sea. Abstract submitted to Acoustical Society of America.

Thedinga, J. F., S.W. Johnson, M.R. Lindeberg, and A.D. Neff. 2006. Bering Sea forage fish: Do they use the shallow nearshore?. Poster presented at the 2006 Alaska Marine Science Symposium, 22-25 Jan 2006, Anchorage, AK.

## Acknowledgements

We would like to thank the captains and crews of the F/V “Great Pacific” and the F/V “Kema Sue” for their invaluable support at sea. Funding for this research was supported with a grant from the North Pacific Research Board, project # F0401.

**Literature Cited**

Brodeur, R.D., Wilson, M.T., Walters, G.E., and Melnikov, I.V. 1999. Forage fishes in the Bering Sea: distribution, species associations, and biomass trends. In: Loughlin, T.R. and Ohtani, K. (Eds.). Dynamics of the Bering Sea. University of Alaska Sea Grant, Fairbanks, pp. 509-536.

Brown, E. D. 2002. Life history, distribution, and size structure of Pacific capelin in Prince William Sound and the northern Gulf of Alaska. ICES J. Mar. Sci. 59: 983-996.

Farley, E.V., Jr., Haight, R.E., Guthrie, C.M., and Pohl, J.E. 2000. Eastern Bering Sea (Bristol Bay) coastal research on juvenile salmon, August 2000. (NPAFC Doc. 499).

Hancock, M. J. 1975. A survey of the fish fauna in the shallow marine waters of Clam Lagoon, Adak, Alaska. M.S. Thesis, Florida Atlantic University, Boca Raton, FL.

Honkalehto, T., N. Williamson, D. McKelvey, and S. Stienessen. *2002. Results of the echo integration-trawl survey for walleye pollock (Theragra* chalcogramma) on the Bering Sea shelf and slope in June and July 2002. NOAA/AFSC Processed Rep. 2002-04.

Hunt Jr., G. L., Decker, M.B., and Kitaysky, A.S. 1996. Fluctuations in the Bering Sea ecosystem as reflected in the reproductive ecology and diets of kittiwakes on the Pribilof Islands, 1975 to 1990. In: Greenstreets, S., and Tasker, M. (Eds.), Aquatic predators and their prey. Blackwell, London, pp. 142-153.

Isakson, J.S., Simenstad, C.A., and Burgner, R.L. 1971. Fish communities and food chains in the Amchitka area. Bio. Sci. 21: 666-670.

Johnson, S.W., A.D. Neff, and J.F. Thedinga. 2005. An atlas on the distribution and habitat of common fishes in shallow nearshore waters of southeastern Alaska. U.S. Dep. Commer., NOAA Tech. Memo. NMFS-AFSC-139, 89 p.

Kajimura, H., and Loughlin, T.R. 1988. Marine mammals in the oceanic food web of the eastern subarctic Pacific. In Nemoto, T., Pearcy, W.G. (Eds), The biology of the subarctic Pacific. Bulletin of the Ocean Research Institute, University of Tokyo, 26 (II): 87-223.

Livingston, P. (ed.) 2002. Ecosystem considerations for 2003. Available http://www.fakr.noaa.gov/npfmc/safes/safe.htm.

Naumenko, E. A. 1996. Distribution, biological condition and abundance of capelin (*Mallotus villosus*) in the Bering Sea. In: Ecology of the Bering Sea: A review of Russian Literature, p. 237-256. Ed. O. A. Mathisen and K. O. Coyle. UA Sea Grant Program.

Pahlke, K. A. 1985. Preliminary study of capelin (*Mallotus villosus*) in Alaskan waters. ADFG Info. Lflt. 250. 64 p.

Robards, M. 1999. Assessment of nearshore fish around Unalaska using beach seines during July 1999. USGS Biological Resources Division, Alaska.

Robards, M. and Schroeder, M. 2000. Assessment of nearshore fish around Akutan Harbor using beach seines during March and July 2000. USGS Biological Resources Division, Alaska.

Sinclair, E.H. and Stabeno, P.J. 2002. Mesopelagic nekton and associated physics in the southeastern Bering Sea. Deep-Sea Res. II 49: 6127-6146.

Warner, I. M. and Shafford P. 1978. Forage fish spawning surveys – southern Bering Sea. Alaska marine environmental assessment project. Project completion report. ADFG Kodiak.

Watanabe, H., Masatoshi, M., Kawaguchi, K., Ishimaru, K., and Ohno, A. 1999. Diel vertical migration of myctophid fishes (Family Myctophidae) in the transitional waters of the western North Pacific. Fish. Oceanogr. 8(2): 115-127.

# *Characterizing distribution and identity of nekton in shelf and slope regions of the Bering Sea*

Sandra Parker Stetter[1], John Horne[1], James Churnside[2], Nicola Hillgruber[3], Michael Sigler[4]

[1]School of Aquatic and Fisheries Sciences, University of Washington, Seattle, WA 98195
[2]NOAA, Environmental Technology Laboratory, Boulder, CO 80303
[3]School of Fisheries and Ocean Sciences, University of Alaska Fairbanks, Juneau, AK 99801
[4]NOAA, Auke Bay Laboratory, Juneau, AK 99801

## Abstract

Mesopelagic forage fish species are important components of the Bering Sea ecosystem, but information on species distribution and identity is limited. Recognizing the need for development of forage species survey strategies, we undertook this study to characterize nekton in the slope and shelf regions of the Bering Sea using direct (midwater trawl, MultiNet) and indirect (acoustics, LIght Detection And Ranging (LIDAR)) sampling technologies. Forage species distribution and quantity differed between shelf (6-100 m) and slope (6-100 m, 100-300 m, 300 m-bottom) regions. Acoustic results suggest that shallow and deep depth zones contained dispersed backscatter while the middle slope layer contained patchy schools associated with the shelf break. Variogram results for repeated LIDAR surveys of the shelf and slope regions indicate that backscatter distribution between 6-30 m was dynamic at the scale of days. This result was expected given the strong frontal nature of the area. When LIDAR results were compared with coincident acoustic transects on the shelf and slope, differences were found in gear detection of backscatter. Acoustic results suggest that 25-63% of forage fish in the shelf and slope regions were deeper than the LIDAR detection range. Although both LIDAR and acoustics are constrained to portions of the water column, the utility of remote sampling technologies is dependent on survey objectives. We identified several potential candidate species/groups for population abundance estimates with acoustics and direct sampling. Other potential, near-surface species/groups could be surveyed with LIDAR and direct sampling. Our

results suggest that shelf and slope regions should be surveyed separately and that additional work, in the form of species-or group-specific temporal studies, should be undertaken to refine survey designs.

## Introduction

Mesopelagic forage species such as myctophids, bathylagids, herring, and squid are important components of the Bering Sea ecosystem (Sinclair and Stabeno 2002). Important in the diets of many predators including pinnipeds, cetaceans, seabirds, skates, and finfish (e.g., Sinclair and et al. 1993, Hunt et al. 1996, Orlov 1998, Ohizumi et al. 2003), mesopelagic species may influence predator foraging behavior with their dynamic diel movement patterns (e.g., Ohizumi et al. 2003, Sterling and Ream 2004).

While some work has addressed mesopelagic forage species in the Bering Sea (e.g., Balanov and Il'inskii 1992, Nagasawa et al. 1997, Watanabe et al. 1999, Sinclair and Stabeno 2002), comprehensive studies on forage species are limited. Existing information, based on trawling, provides species composition (Sinclair and Stabeno 2002) and spatially discrete biomass estimates of biomass (Nagasawa et al. 1997, Watanabe et al. 1999), but provides an incomplete characterization of mesopelagic species. As a result, few large-scale estimates of mesopelagic biomass exist (Balanov and Il'inskii 1992). This data gap limits Bering Sea ecosystem models (Cianelli et al. 2004) and provides no context for estimates of marine mammal consumption (e.g., Ohizumi et al. 2003).

In 1999, amendments to the National Marine Fisheries Service (NMFS) Alaskan groundfish management plans created a specific category to conserve and manage forage species resources. This forage fish category includes 59 fish species belonging to 8 families.

Ecosystem-based management approaches require information on species distribution, abundance, and life history attributes.

Single gear types (e.g., pelagic trawl, bottom trawl, gill nets, seines) have traditionally been used to collect data for population estimates of single species. In this context, NMFS research assessment surveys usually operate during daylight hours in the summer, using sampling techniques that do not explicitly census mesopelagic species. As forage species occupy all major habitats (bathy-, meso-, and epi-pelagic), the development of new, or modification of existing, techniques is needed to directly assess the contribution of forage species to the Bering Sea.

## Methods

### *Study site*

Systematic surveys of nekton were conducted at locations in continental shelf (<100 m) and slope (100-1200 m) regions of the Bering Sea near Unalaska and Akutan Islands (Figure 1). The slope region was surveyed 10-13 June 2005 and shelf region during 14-19 June 2005. Shelf transects were spaced 0.5 nmi apart and slope transects were spaced 1.0 nmi apart (Figure 1). To increase sampling intensity, higher resolution, adaptive surveys were intermittently conducted at locations with high acoustic backscatter. Adaptive transect spacing varied with the target assemblage. All data were collected aboard the *F/V Great Pacific*, a 38-m stern trawler with a main engine of 1450 horsepower and a cruising speed of 10 kts.

### *Acoustic data collection and processing*

*Acoustic data collection*

Acoustic data were collected using a 38 kHz splitbeam echosounder (Simrad 38-12, input power 2000 W, pulse length 1.024 ms, ping rate 1 $sec^{-1}$), from 10-19 June 2005. We installed the transducer on an YSI towed body suspended 2.5 m below the water surface and towed it at approximately 6.0 kt. The echosounder was calibrated before our survey with a standard tungsten carbide sphere using procedures outlined in Foote et al. (1987). Interference from hydraulic winches and other machinery prevented acoustic data collection during deployment of towed gear (midwater trawl, MultiNet).

*Acoustic data processing*

Echoview (v 3.30, SonarData 2005) was used to analyze all acoustic data. Transect files were inspected for bottom delineation, vessel noise spikes, and electrical interference prior to processing. CTD cast data were used to estimate absorption coefficients (Francois and Garrison 1982) and sound speed (Chen and Millero 1977).

*EDSU selection and geostatistical approaches*

We used a horizontal elemental distance sampling unit (EDSU) of 250 m for all analyses. To determine this value, we initially exported slope-water-column and shelf Sv_mean for 10 m horizontal cells. We assumed that spatial correlation in our data would not be at scales <10 m. Preliminary variograms were inspected for nonstationarity and data sets were examined for trends with direction (Northing, Easting, Northing•Easting) using forward stepping linear regression. Final trend models were significant at $R^2 \geq 0.05$ and each parameter was significant at $P < 0.05$. Trend effects were removed using a generalized linear model (GLM) with a Gaussian error structure. Residuals were used to model the empirical spatial relationship among

data points with classical or robust variogram procedures (Matheron 1963, Cressie and Hawkins 1980). Each variogram was fit, using a weighed least squares procedure (Cressie 1993), with both exponential and spherical models. The best theoretical model was selected visually and the fit of parameters was examined. The range of a spherical model and the effective range of an exponential model indicate the distance (m) at which data are no longer spatially correlated. Our EDSU data had ranges of 3.8 km in the slope region and 3.4 km in the shelf region. Horizontal EDSU's should not exceed one-half the range of the data (Rivoirard et al. 2000). A single horizontal bin size of 250 m was chosen as the EDSU for both shelf and slope regions.

***Nekton distribution***

*Acoustic data processing*

Vertical depth strata, corresponding to shelf/shallow, shelf break, and deep-water regions, were used in our analyses. We refer to these strata as shelf (6 m-bottom, where bottom ≤ 100), slope-shallow (6-100 m), slope-middle (100-300 m), and slope-deep (300 m-bottom). For comparison, we also included a slope-water-column stratum (6 m-bottom).

Two steps were taken to remove noise and restrict data to large nekton (i.e., fish and squid). First, vessel noise was modeled through the water column with a 20•log(Range) time-varied-threshold (TVT) using Sv @ 1m. Second, to restrict our analyses to large nekton (e.g., fish, squid), we applied a Sv minimum threshold to each depth strata. To do this, we calculated the expected amount of volume backscatter (Sv) from an individual myctophid (the smallest fish captured in trawl samples) in a single vertical sample (0.2 m). A target strength (TS, in dB) of -52.5 dB (McClatchie and Dunford 2003) was selected based on similar sized myctophids to our study. Expected Sv was calculated for each 1 m vertical bin within our 3 depth strata, compensating for beam spreading and volume insonified. The median Sv value in each depth

stratum was used as our minimum threshold: -66 dB (6-100 m), -77 dB (100-300 m), and -87 dB (300 m-bottom). Samples with Sv less than either our vessel noise TVT or our Sv minimum threshold were considered to have no detectable backscatter and were assigned -999 dB (equivalent to 0 backscatter in linear domain, SonarData 2005).

*Acoustic analysis of nekton distribution*

We used daytime systematic transects in this analysis. Each depth stratum was treated separately and data were exported by depth stratum in 250 m horizontal bins. Output values included Sv_mean, Nautical Area Scattering Coefficient (NASC≡$s_A$), and Area Backscattering Coefficient (ABC≡$s_a$). In the slope region, where data were exported in three depth strata, a water column Sv_mean was calculated in each horizontal segment weighted by the proportion of the water column occupied by each depth stratum.

We were interested in determining how large nekton, measured using Sv_mean, were distributed in our survey area. We removed trends with direction (Northing, Easting, and/or Northing•Easting), used the residuals to generate empirical variograms, and fit the empirical variogram with theoretical models as outlined under *EDSU selection and geostatistical approaches.*

Using trend (from GLM results) and spatial structure (from variogram models), we predicted Sv_mean throughout our study area. Slope and shelf transects were surrounded with a 1-2 km box from the outer edges of the transects. A smaller box was created for the slope-deep region. Bounding boxes were selected to provided outside distances of ~½ the transect spacing. We then divided boxes into 250 m x 250 m grid cells. Using trend and variogram parameters (sill, range, nugget), we predicted Sv_mean in boxes with universal kriging (Cressie 1993). All geostatistical analyses were conducted using S-Plus 6.1 (Insightful Corporation 2002).

***Acoustic and optic spatiotemporal characterization of backscatter***

Acoustics provided a detailed profile of the water column in slope and shelf regions over several days. LIDAR offered a repeated, synoptic look at the same areas. We used the two data sets to examine nekton distribution patterns among days or within depth layers. We were also interested in comparing results and applications of the two techniques. Due to LIDAR depth penetration, our comparative analyses were limited to the top 30 m of the water column.

*Acoustic data processing*

We used the same horizontal EDSU of 250 m determined for previous analyses. Five vertical bins were used in all acoustic analyses: 6-12 m, 12-18 m, 18-24 m, 24-30 m, and 30 m-bottom. For acoustics, the backscatter value exported was ABC. Data were transformed to $\log_e$ (≡lnABC) as ABC values span several orders of magnitude within each analysis.

For this analysis, we removed vessel noise and then exported data both with and without an Sv minimum threshold. Vessel noise (Sv @ 1m) was modeled through the water column with a 20•log(R) TVT and samples below this threshold were identified. Our first data set had no Sv minimum thresholds to make it comparable to the LIDAR data. The second data set used median Sv minimum thresholds for large nekton (-52.5 dB fish, based on McClatchie and Dunford 2003), calculated at a 1 m vertical resolution within the 6-30 m depth range: -50 dB (6-12 m), -54 dB (12-18 m), -57 dB (18-24 m), -60 dB (24-30 m), -66 dB (30-100 m), -77 dB (100-300 m), and -87 dB (300 m-bottom). Samples with Sv less than our vessel noise TVT or our nekton Sv minimum threshold were considered to have no detectable backscatter and were assigned -999 dB (equivalent to 0 backscatter in linear domain, SonarData 2005).

*LIDAR data collection*

Aerial surveys of the slope/break systematic transects were performed 8, 9, 11, and 14 June during the day. A nighttime survey of the same region was performed in the early morning of 13 June. Shelf systematic transects were surveyed during the day on 13, 17, 18, and 19 June and at night on 17 June. A total of 12 flights were made between 8 and 19 June, with much of the flight time devoted to covering a larger area of the shelf and slope. In total, almost 7900 km were surveyed, with about 11% in the slope/break region and 16% in the shelf region as defined in Fig. 1.

The LIDAR was the NOAA Fish LIDAR that has been described in detail elsewhere (Churnside, et al, 2001; 2003; Churnside and Thorne, 2005). The system transmits a 12-nsec pulse of linearly-polarized green (532 nm) light into the water. The return is detected in the orthogonal linear polarization, and the temporal shape of the return is used to infer a depth profile of scattering. The sampling swath is 5 m in diameter, which spreads out the energy so that it is safe for marine mammals (Zorn, et al, 2000).

*LIDAR data processing*

Attenuation was inferred from the average slope of the logarithm of the signal decay over a depth range chosen to minimize the effects of surface returns and noise. The magnitude of the return from any depth was corrected for attenuation using this value. We then processed the data to obtain the total backscatter level. Total return includes layers of zooplankton or phytoplankton, diffuse aggregations of fish, and fish schools. The results within the boundaries of the two acoustic-survey regions were selected. All data were exported with an

ESDU of 250 m, and separated the data into 5 vertical bins: 2-6 m, 6-12 m, 12-18 m, 18-24 m, and 24-30 m.

*Spatiotemporal nekton distribution - 6 to 30 m*

We compared backscatter distribution in acoustic and LIDAR data using trend and geostatistical parameters. Analyses were restricted to depths (6-30 m) common to acoustics and LIDAR and to the surface layer (2-6 m) from LIDAR analyses. Each depth layer was treated separately in analyses. We removed trends with direction (Northing, Easting, and/or Northing•Easting), used the residuals to generate empirical variograms, and fit the empirical variogram with theoretical models as outlined under *EDSU selection and geostatistical approaches.* Variogram parameters (sill, range, nugget) were used to characterize aggregation structure in each analysis (Mello and Rose 2005).

Patterns in nekton distribution were compared among days and depths using agglomerative hierarchical cluster analysis. Cluster parameters included theoretical variogram sill, range (or effective range for exponential models), and nugget. All variables were standardized by subtracting the variable mean value and dividing by the variable mean absolute deviation. Distances between objects were calculated using a Euclidean distance metric and linkages were based on an unweighted pair-group method using averages.

*Vertical distribution of backscatter*

We were interested in backscatter vertical distribution observed by the two technologies. For each 250 m horizontal bin, we calculated the percent of total acoustic or LIDAR backscatter in each depth layer: 2-6 m (LIDAR only), 6-12 m, 12-18 m, 18-24 m, 24-30 m, 30m-bottom (acoustics only). A mean percent of total backscatter was calculated for each depth layer.

Next we determined the contribution of large nekton to observed backscatter by treating acoustics as the baseline observation. We used our nekton-thresholded acoustic ABC data to determine the proportion of observed backscatter in each depth bin (6 m-bottom) that was attributed to large nekton. The proportion of large nekton in each depth layer ($P_j$ ) was calculated as:

$$P_j = \frac{\sum_{j=1}^{j=n} \frac{\ln(ABC)_{thr}}{\ln(ABC)_{total}}}{n}$$

where $\ln(ABC)_{thr}$ is thresholded backscatter, $\ln(ABC)_{total}$ is unthresholded backscatter, and $n$ is the number of 250 m horizontal bins in depth layer $j$.

***Characterizing aggregations***

Target aggregations were identified on the echosounder and characterized using acoustics, midwater trawl, and MultiNet. We were interested in describing composition and common attributes of observed assemblages.

*Acoustic characterization of aggregations*

Vessel noise was removed from each aggregation data set by modeling Sv at 1m through the water column with a 20•log(R) TVT and masking out any sample values that fell below this threshold at depth. As we were interested in only sample bins that contained measurable backscatter, cells with backscatter less than our TVT were not included. No Sv minimum thresholds were applied to this data.

Target aggregations were visually classified using the acoustic typology of Reid et al. (2000). Categories, modified to reflect large and small nekton, were:

1. scattered nekton (large numbers of single echoes, not structured)
2. schools of nekton (discrete and identifiable)

3. nekton in aggregations (may be diffuse, not definable as distinct schools)
4. pelagic nekton layers (may be fairly dense, continuous, midwater)
5. demersal nekton layers (similar to pelagic layer but close or in contact with seabed)
6. other unique aggregations

Estimates of the approximate or representative horizontal and vertical extent of all aggregations were made from echograms. Sv_mean was measured within individual schools or from representative sections of pelagic/demersal nekton layers or scattered nekton regions.

*Midwater trawl*

Target aggregations observed in acoustic echograms were sampled using a Cantrawl 400/580 midwater trawl (5.0 $m^2$ alloy doors, 12 mm mesh codend liner, 15-18 m height, 55-60 m width). Trawl depth was monitored real-time using a netsonde on the headrope. Trawl duration lasted between 10 and 81 minutes. Upon net retrieval, all species were identified and counted. When catch volume was high, we subsampled by selecting a random portion of the trawl catch to count and weigh. The remainder of the catch was weighed.

*MultiNet*

The water column around target aggregations was also sampled for zooplankton and ichthyoplankton with a 0.25 $m^2$ multiple opening/closing MultiNet®, (MN, HydroBios) equipped with five 333 µm mesh net bags. Two flow meters, one located inside the net opening and one located outside, were used to monitor volume of water filtered. The MN was fished in a double oblique manner and plankton was collected over five depth ranges on the up-cast. Upon retrieval, the five nets were rinsed down, cod-ends were detached, and samples concentrated in sieves. Concentrated samples were fixed in 5% buffered formalin seawater solution.

In the lab, zooplankton samples were rinsed with tap water and displacement volume to the nearest 1.0 ml was determined. Whole samples were then scanned for large organisms (e.g., jellyfish and cephalopods) that were removed, identified to the lowest feasible taxonomic level, and counted. The remaining samples were split with a Folsom plankton splitter until a sample of approximately 100 specimens of the most abundant taxonomic group was achieved. In this split, all individuals of the abundant groups were identified to the lowest feasible taxonomic group and developmental stage and counted. Larger sub-samples were scanned for less abundant taxa, which were identified and counted.

Abundance of zooplankton was computed as # • $m^{-3}$ using flowmeter values. Since MN casts were conducted to different maximum depths and varying depth intervals were sampled, # • $m^{-2}$ was calculated by multiplying # • $m^{-3}$ with the depth ranged sampled with each net. Total # • $m^{-2}$ was computed by summing the values from each depth stratum.

*Environmental parameters*

At each station, hydrographic data were recorded with a SeaBird SBE-19 Seacat CTD (conductivity, temperature, density) profiler, equipped with a Wetstar fluorometer and a D&A Instruments transmissometer. Sea surface temperature (SST) and sea surface salinity (SSS) were determined for each station and depths of the thermocline and halocline were calculated as the point of maximum rate of change.

## Results

### *Nekton distribution*

*Acoustic analysis of nekton distribution*

A total of 375 km of acoustic data were collected during slope and shelf systematic survey transects (Figure 1). The shelf region had a higher Sv_mean (-63 dB) than the slope-water-column or any individual slope depth layers. In the slope region, the shallow (6-100 m) layer had the highest mean volume backscatter (-68 dB). On an areal basis, the slope-deep layer had the highest integrated acoustic backscatter (ABC = $6.6 \bullet 10^{-5}$ $m^2 \bullet m^2$).

Our predictions of Sv_mean emphasize patterns in distribution in the shelf and slope regions (Figure 2) and within slope depth strata (Figure 3). Sv_mean data had trends with location (Northing, Easting, and/or Northing•Easting, $p < 0.05$) in forward-stepping regression for all strata, but not consistently among strata (Table 1). When we removed these trends, all data sets still had spatial structure. Variogram results are presented in Table 1.

### *Acoustic and optic spatiotemporal characterization of backscatter*

*Spatiotemporal nekton distribution - 6 to 30 m*

Nekton distribution had both trend and spatial structure in most data sets. Directional trends (Northing, Easting, or Northing•Easting ) were present in acoustic slope, shelf, and slope-night data layers. Most LIDAR layers also contained trends with direction. Patterns in regression coefficient signs were evident among layers within days (Tables 2 to 4).

Spatial structure remained in all data sets after trend was removed. Variogram results are presented in Tables 4 to 6. Acoustic slope and shelf regions had similar theoretical variogram range, sill, and nugget values in 6-30 m depth bins. LIDAR ranges were similar to acoustic ranges, but LIDAR layers frequently had higher sill and nugget values.

Cluster analyses suggested that patterns in spatial structure (sill, range, nugget) were more obvious among days and depth layers in the shelf region than in the slope (Figure 4). Ten of sixteen shelf day/depth data points strongly clustered (Figure 4). Only LIDAR shelf data sets with linear variograms or high sill values were not in the primary cluster.

*Vertical distribution of backscatter*

In depths common to acoustics and LIDAR (6-30 m), LIDAR backscatter vertical distribution varied among surveys. In the shelf region, LIDAR backscatter vertical distribution was consistently different from acoustic vertical distribution. In the slope region, acoustic vertical distribution was more similar to LIDAR results before the acoustic survey.

Within the 6-30 m depth range, patterns in both LIDAR and acoustic vertical distribution are evident. The highest LIDAR backscatter was consistently in the 6-12 m bin (average 73%) and the lowest was in the 24-30 m bin (average 4%). In the slope-night data, LIDAR backscatter was distributed throughout the water column (average 25%). Acoustic backscatter was evenly distributed (average 25%) throughout the 6-30 m range in all data sets.

Of the acoustic backscatter detected between 6-30 m, 6%-30% can be attributed to large nekton using acoustic thresholds. An average of 60% of acoustic backscatter was found below the 30 m vertical detection range of LIDAR. Of backscatter between 30 m-bottom, an average of 74% would be classified as large nekton. A high amount of LIDAR backscatter (average 58%) was found in the 2-6 m depth range, above the vertical detection range for acoustics.

***Characterizing aggregations***

Twenty aggregations were identified on the echosounder and sampled with both the midwater trawl and the MultiNet. Seven MW trawls and five MN casts were completed in the shelf region. The remaining thirteen MW and ten MN casts were performed in the slope region.

More than 30 species of fishes were captured with the MW (Appendix 1) and 20 zooplankton taxa were identified from MN samples (Appendix 2).

In the shelf region, we primarily sampled pelagic layer and scattered nekton assemblage types (Figure 5 for examples). These aggregations had low Sv_mean (-68 to -61 dB), were spread >1000 m horizontally, and were vertically compressed (20-50 m). Pelagic layers contained walleye pollock during the day but were dominated by Pacific herring in our single night sample (ID 1, 2, 5, Figure 6). Walleye pollock also dominated the scattered nekton and were found in association with flatfish (*Atherestes stomias* and *Lepidopsetta polyxystra*), sturgeon poacher (*Agonus acipenserinus*), and Pacific herring (ID 4, 6, 7, Figure 6). Zooplankton samples in pelagic layers and scattered nekton assemblages were dominated by copepods and euphausiids (ID 1, 2, 5-7, Figure 6). ID 6 had the greatest zooplankton density, driven by high abundances of copepods, euphausiids, and pteropods (Figure 6). The single shelf school (ID 3, Figure 6) had a high Sv_mean value and contained walleye pollock, Pacific herring, Pacific cod (*Gadus macrocephalus*), and flatfish (ID 3, Figure 6).

Slope aggregations were primarily pelagic layers and schools. Shallow pelagic layers contained few targets (ID 8-11, Figure 7) or were dominated by walleye pollock. Zooplankton in pelagic layers were primarily copepods and euphausiids (ID 8-11, Figure 7). Like shelf aggregations, shallow pelagic layers were >1000 m wide horizontally, 10-30 m high vertically, and had low Sv_mean. Deep pelagic layers sampled at night were also > 1000 m horizontal, but were vertically > 100 m and had high Sv_mean. Bathylagids, myctophids, copepods, and euphausiids dominated deep pelagic layers (ID 17-20, Figure 7). Slope schools were dominated by walleye pollock and had high Sv_mean (ID 12, 13, 15, Figure 7). All schools contained copepods and euphausiids (Figure 7). The single scattered aggregation in the slope region

contained only walleye pollock and had a low Sv_mean (ID 14, Figure 7). The only demersal layer sampled contained Pacific ocean perch and squid, had vertical and horizontal extents similar to observed pelagic layers, but a higher Sv_mean (ID 16, Figure 7). Six slope trawls confirmed the presence of jellyfish, but it was not appropriate to count individual animals.

## Discussion

Information on forage species is critical for the application of ecosystem management approaches. In previously unstudied species or groups, the evaluation of survey design strategies is a necessary first step. This study presents an example of species and/or group characterizations in support of survey development. Using both direct and indirect sampling technologies, we evaluated nekton distribution, feasibility of gear types, and necessary next steps.

### *Distribution of nekton*

Variogram and kriging results suggest that shelf and slope regions have different nekton distributions. Shallow layers (6-100 m, shelf and slope-shallow) can be characterized by dispersed backscatter (low sill, low nugget). The slope-shallow layer had lower within-aggregation variation in backscatter and approximately half the areal backscatter of the shelf region. Results for slope-middle layer (100-300 m) suggest that backscatter was concentrated in a small area. This result was expected as the shelf break (~200 m contour) typically contained compact schools associated with the bottom during the day. Distribution within the slope-deep layer (300 m-bottom) was similar to the shallow layers, but the higher sill value suggests greater variation in backscatter within dispersed aggregations. As few discrete schools were observed in this depth layer, deep aggregations of myctophids and bathylagids were the most likely scatterers

(Balanov and Il'inskii 1992, Nagasawa et al. 1997). The full extent of these deepwater aggregations could not be determined due to high vessel noise. Increasing noise at depth caused many acoustic targets to be masked by vessel noise. Our measures of backscatter within the slope-deep layer underestimate the contribution of groups such as myctophids and bathylagids.

***Acoustic and optic spatiotemporal characterization of backscatter***

Repeated LIDAR observations of shelf and slope regions indicated that backscatter distribution was dynamic at the scale of days. Differences in horizontal and vertical distribution were expected given time lags associated with LIDAR sampling. We also recognize the tidal influence in bathymetric regions and the expected heterogeneity of backscatter distribution. In the Akutan region, Ladd et al. (2005) identified diel patterns in seabird horizontal distribution that were related to prey associations with tidal fronts.

Although differences in nekton distribution were expected, our results suggest that some differences in backscatter distribution that may be related to gear. Most 6-30 m slope and shelf data sets had similar ranges, low sills, and low nugget values. These areas are characterized as having dispersed rather than highly aggregated backscatter. However, of the thirteen data sets outside of the primary clusters for shelf and slope, twelve were from LIDAR. Theoretical variogram parameters from these data sets often had high ranges (suggesting large scale spatial patterns) or high sills/nugget values (suggesting aggregations in smaller areas of our study regions). Vertical distribution of backscatter also suggested differences between technologies. Within common depths (6-30 m), LIDAR backscatter was highest in shallow waters and decreased with depth. The 2-6 m depth range had even higher LIDAR backscatter than within 6-12 m. Conversely, acoustic backscatter was more evenly distributed throughout the 6-30 m range.

Apparent differences between acoustic and LIDAR characterizations of nekton distribution are probably due to a combination of factors: 1. Survey timing or vessel effects. It is possible, but unlikely, that nekton distribution varied significantly among days and that acoustic sampling was conducted on anomalous days. Avoidance of the acoustic vessel could affect backscatter distribution, but avoidance cannot explain differences in area-wide spatial distribution; 2. Differences may be artifacts of data processing. The time-varied-gain (TVG) correction applied to LIDAR data may affect the depth distribution. The assumption that the attenuation is uniform in the upper water column can lead to a bias if, in fact, the attenuation depends on depth. Detection capabilities of LIDAR may also cause different distribution results. LIDAR backscatter may be attenuated in surface waters, leaving less energy to penetrate to deeper scatterers; 3. LIDAR may detect more phytoplankton and zooplankton in surface waters than acoustics. Diatoms, copepods and euphausiids are abundant in surface waters in this area (Vlietstra et al. 2005). Previous work by Churnside and Thorne (2005) demonstrated that LIDAR can detect zooplankton assemblages within a phytoplankton bloom, but separation of the phytoplankton and zooplankton components requires thresholding the enhanced backscatter signal.

Both LIDAR and acoustics are constrained to portions of the water column. The importance of these missed segments depends on survey objectives. In this study, LIDAR effectively sampled between 2 m and 30 m. The echosounder could not obtain data between 2 m and 6 m. By setting the acoustic data as a baseline, we calculated the vertical distribution of large nekton in acoustic analyses. Our results suggest that if waters above the acoustic detection range (2-6 m) are similar to next deepest layer (6-12 m), acoustics will miss 1% of total water column large nekton in the slope and 3% in the shelf. Depending on the survey species of

interest, this constraint may introduce bias into abundance estimates. Conversely, our analyses suggest that by sampling to only 30 m, LIDAR will miss 25-63% of the large nekton in the water columns of the shelf and slope (day and night) regions.

***Characterizing aggregations***

Shelf and slope regions contained similar acoustic aggregation structures, but the composition of these structures differed. Walleye pollock and herring dominated both day and night aggregations on the shelf. On the slope, daytime aggregations were dominated by Pacific ocean perch, squid, and walleye pollock. Aggregations sampled on the slope at night were dominated by bathylagids and myctophids.

Given patterns in aggregation species composition, our acoustic results suggest that assemblage structure could be used in directed surveys. Specific candidates include slope myctophids and bathylagids, slope walleye pollock, shelf break squid and Pacific ocean perch, and shelf herring and walleye pollock. Deepwater myctophids and bathylagids were detected and captured in layers at depths >150 m at night. Due to vessel noise, we were unable to acoustically detect bathylagids and myctophids at depth during the day, but expect that scattering layers were present at depths >500 m (Balanov and Il'inskii 1992). On the shelf break, tight schools were consistently observed during the day. Trawling on this aggregation identified the constituents as squid and Pacific ocean perch. In the shelf region, herring and walleye pollock dominated shallow scattered or pelagic layer aggregations during the night. Walleye pollock was also consistently captured in shallow slope scattered or pelagic layer aggregations during the day.

***Recommendations***

Population abundance assessment of mesopelagic species in the Bering Sea is important from an ecosystem and resource management perspective. Previous studies, such as Sinclair and Stabeno

(2002), provide a limited picture of nekton distribution due to the use of single trawl hauls. By combining acoustics, LIDAR, and direct sampling, our June 2005 survey highlight aspects of nekton distribution that will assist in the development of assessment strategies and quantitative abundance estimates for Bering Sea mesopelagic nekton species.

1. Shelf and slope regions should be surveyed separately. Nekton horizontal and vertical distribution differed between the two regions, making it necessary to design region-specific surveys.
2. LIDAR should be restricted to assessment of near-surface forage species. LIDAR may also be appropriate to evaluate species that vertically migrate into surface waters at night.
3. Acoustics remain the most effective and efficient tool for assessing the distribution and abundance of pelagic species.
4. At this time, acoustics and LIDAR do not match and cannot be combined to provide a full water column numeric/biomass estimate.
5. Surveys of Bering Sea mesopelagic species must include direct sampling for target identification and specimen collection.
6. Several potential candidate species/groups for population abundance estimates were identified: deepwater myctophids and bathylagids, shelf break squid and Pacific ocean perch, shelf herring and walleye pollock, and slope pelagic walleye pollock.
7. Dedicated species- or group-specific pilot surveys are necessary to obtain accurate target strength estimates for separating: myctophids versus bathylagids, herring versus walleye pollock, and squid versus Pacific ocean perch.
8. Target species or groups should be observed at different times -daylight, crepuscular, and dark - as the effect of vertical or horizontal migration on assessment results cannot be

determined at this time. Predictable diel movements could also provide additional ways to characterize the mesopelagic community composition.

9. Appropriate transect spacing must be determined for target species or groups. Ranges observed during our spatiotemporal analyses (2.4 – 5.6 km) suggest that 1 nmi transect spacing was too large to capture backscatter spatial structure in some depth layers.
10. Specific surveys should be undertaken to evaluate the contribution of jellyfish to the mesopelagic community. Midwater trawl catches frequently included jellyfish, but our gear did not effectively sample these organisms.

***Summary***

Assessing mesopelagic nekton species in the slope and shelf regions of the Bering Sea is essential for both ecological understanding and effective resource management. Our results suggest that these regions differ in their species composition and nekton distribution over time and space. We identified several potential candidate species/groups for population abundance estimates with acoustics and direct sampling. Other potential, near-surface species/groups could be surveyed with LIDAR and direct sampling. Our results suggest that shelf and slope regions should be surveyed separately and that additional work, in the form of species-specific temporal studies should be undertaken to refine survey designs.

## Literature cited

Balanov, A.A., and Il'inskii, E.N. 1992. Species composition and biomass of mesopelagic fishes in the Sea of Okhotsk and the Bering Sea. Journal of Ichthyology, 32: 85-93.

Bertrand, A., Le Borgne, R., and Josse, E. 1999. Acoustic characterization of micronekton distribution in the French Polynesia. Marine Ecology Progress Series, 191: 127-140.

Brodeur, R.D., Wilson, M.T., Walters, G.E., and Melnikov, E.V. 1999. Forage fishes in the Bering Sea: distribution, species associations and biomass trends. In: Loughlin, T.R. and

Ohtani, K. (Eds.). Dynamics of the Bering Sea. University of Alaska Sea Grant, Fairbanks, pp. 509-536.

Chen, C.T. and Millero, F.J. 1977. Speed of sound in seawater at high pressures. Journal of the Acoustical Society of America, 62: 1129-1135.

Churnside, J.H., Demer, D.A., and Mahmoudi, B. 2003. A comparison of lidar and echosounder measurements of fish schools in the Gulf of Mexico," ICES Journal of Marine Science, 60: 147–154.

Churnside J.H.and Thorne, R.E. 2005. Comparison of airborne lidar measurements with 420 kHz echo-sounder measurements of zooplankton. Applied Optics, 44: 5504-5511.

Churnside, J.H., Wilson, J.J., and Tatarskii, V.V. 2005. Airborne lidar for lisheries applications. Optical Engineering, 40: 406-414.

Cianelli, L., Robson, B.W., Francis, R.C., Aydin, K., and Brodeur, R.D. 2004. Boundaries of open marine ecosystems: an application to the Pribilof Archipelago, southeast Bering Sea. Ecological Applications, 14: 942-953.

Cressie, N and Hawkins, D.M. 1980. Robust estimations of the variogram: I., Mathematical Geology, 12: 115-125.

Cressie, N.A.C. 1993. Statistics for Spatial Data. Wiley-Interscience, New York, 928 pp.

Foote, K.G., Knudsen, H.P., Vestnes, D.N., MacLennan, D.N., and Simmonds, E.J. 1987. Calibration of acoustic instruments for fish density estimation: a practical guide. International Council for the Exploration of the Sea Cooperative Research Report, 144: 1-69.

Francois, R.E. and Garrison, G.R. 1982. Sound absorption based on measurements. Part II: Boric acid contribution and equation for total absorption. Journal of the Acoustical Society of America, 72: 1879-90.

Hunt Jr., G.L., Decker, M.B., and Kitaysky, A.S. 1996. Fluctuations in the Bering Sea ecosystem as reflected in the reproductive ecology and diets of kittiwakes on the Pribilof Islands, 1975 to 1990. In: Greenstreets, S. and Tasker, M. (Eds.). Aquatic predators and their prey. Blackwell, London, pp. 142-153.

Insightful Corporation. 2002. S-Plus 6.1 for Windows. Insightful Corporation, Seattle, WA.

Ladd, C., Jahncke, J., Hunt, G.L., Coyle, K.O., and Stabeno, P.J. 2005. Hydrographic features and seabird foraging in Aleutian Passes. Fisheries Oceanography 14(Suppl. 1): 178-195.

Matheron, G. 1963. Principles of Geostatistics. Economic Geology, 58: 1246-1266.

McClatchie, S. and Dunford, A. 2003. Estimated biomass of vertically migrating mesopelagic fish off New Zealand. Deep Sea Research I, 50: 1263-1281.

Mello, L.G.S. and Rose, G.A. 2005. Using geostatistics to quantify seasonal distribution and aggregation patterns of fishers: an example of Atlantic cod (Gadus morhua). Canadian Journal of Fisheries and Aquatic Sciences, 62: 659-670.

Nagasawa, K., Nishimura, A., Asanuma, T., and Marubayashi, T. 1997. Myctophids in the Bering Sea: distribution, abundance, and significance as food for salmonids. In: Forage fishes in marine ecosystems: proceedings of the International Symposium on the Role of Forage Fishes in Marine Ecosystems, Anchorage Alaska. Lowell Wakefield Symposium 14, University of Alaska Sea Grant College Program Report no 97-01, pp. 337-349.

Ohizumi, H, Kuramochi, T., Kubodera, T., Yoshioka, M., and Miyazaki, N. 2003. Feeding habit of Dall's porpoises (Phocoenoides dalli) in the subarctic North Pacific and the Bering Sea basin and the impact of predation on mesopelagic micronekton. Deep-Sea Research I, 50: 593-610.

Orlov, A.M. 1998. The diets and feeding habits of some deep-water benthic skates (Rajidae) in the Pacific waters off the Northern Kuril Islands and Southeastern Kamchatka. Alaska Fishery Research Bulletin, 5: 1-17.

Ream, R. 2005. Presentations. http://nmml.afsc.noaa.gov/AlaskaEcosystems/nfshome/nfs.htm

Reid, D., Scalabrin, C., Petitgas, P., Masse, J., Aukland, R., Carrera, P., and Georgakarakos, S. 2000. Standard protocols for the analysis of school based data from echo sounder surveys. Fisheries Research, 47: 125-136.

Rivoirard, J., Simmonds, J., Foote, K.G., Fernandes, P., and Bez, N. 2000. Geostatistics for estimating fish abundance. Blackwell Science Limited, London, 206 pp.

Sinclair E.H. and Stabeno, P.J. 2002. Mesopelagic nekton and associated physics of the southeastern Bering Sea. Deep Sea Research II, 49: 6127-6145.

Sinclair, E.H. and T.K. Zeppelin. 2002. Seasonal and spatial differences in diet in the western stock of Steller sea lions (Eumetopias jubatus). Journal of Mammology, 83: 973-990.

Sinclair, E., Loughlin, T., and Pearcy, W. 1993. Prey selection by northern fur seals (Callorhinus ursinus) in the eastern Bering Sea. Fishery Bulletin, 92: 144-156.

Simmonds, J. and D. MacLennan. 2005. Fisheries acoustics: theory and practice. Blackwell Science Publishers, Oxford.

SonarData. 2005. Echoview 3.30. SonarData Pty Ltd., Tasmania, Australia.

Sterling, J.T. and Ream, R.R. 2004. At-sea behavior of juvenile male northern fur seals (Callorhinus ursinus). Canadian Journal of Zoology, 82: 1621-1637.

Vlietstra, L.S, Coyle, K.O., Kachel, N.B., and Hunt, G.L. 2005. Tidal front affects the size of prey used by a top marine predator, the short-tailed shearwater (Puffinus tenuirostris). Fisheries Oceanography, 14(Suppl. 1): 196-211.

Watanabe, H., Masatoshi, M., Kawaguchi, K., Ishimaru, K., and Ohno, A. 1999. Diel vertical migration of myctophid fishes (Family Myctophidae) in the transitional waters of the western North Pacific. Fisheries Oceanography, 8: 115-127.

Zorn, H.M. Churnside, J.H., and Oliver, C.W. 2000. Laser safety thresholds for cetaceans and pinnipeds. Marine Mammal Science, 16: 186-200.

Table 1. Variogram and forward stepping regression parameters for shelf and slope 38 kHz acoustics. Acoustic data are based on mean.Sv (dB). Empirical variograms were classical or robust and fit with exponential models using weighted least squares (Cressie 1993). *Range* is effective range. All stepwise regressions contained an intercept term. *N* is number of 250 m horizontal bins. *Northing*, *Easting*, and *Northing•Easting* are signs of the associated regression coefficients.

| Area | Depth (m) | *N* | Northing | Easting | Northing• Easting | Range (km) | Sill | Nugget |
|---|---|---|---|---|---|---|---|---|
| Shelf-water column | 6 m-bottom | 880 | - | - | + | 3.6 | 11.15 | 1.24 |
| Slope-water column | 6 m-bottom | 612 | + | + | + | 3.2 | 11.28 | 2.01 |
| Slope-shallow | 6-100 m | 612 | - | + | | 4.4 | 6.94 | 0.73 |
| Slope-middle | 100-300 m | 588 | - | + | | 4.5 | 48.99 | 9.36 |
| Slope-deep | 300 m-bottom | 446 | | - | | 3.3 | 19.90 | 1.12 |

Table 2. Forward stepping regression results for slope acoustic and LIDAR observations. Acoustic data are based on lnABC and LIDAR data are based on untransformed backscatter. All stepwise regressions contained an intercept term. *N* is number of 250 m horizontal bins. *Northing*, *Easting*, and *N•E* (Northing•Easting) are signs of the associated regression coefficients.

| | 38 kHz 6/10-6/12 | | | | Lidar 6/8 | | | | Lidar 6/11 | | | | Lidar 6/14 | | | |
|---|---|---|---|---|---|---|---|---|---|---|---|---|---|---|---|---|
| Depth (m) | *N* | Northing | Easting | N•E | *N* | Northing | Easting | N•E | *N* | Northing | Easting | N•E | *N* | Northing | Easting | N•E |
| 2-6 | | | | | 564 | - | - | + | 537 | - | - | + | 530 | + | + | + |
| 6-12 | 611 | + | + | + | 564 | - | - | + | 537 | - | - | + | 530 | + | + | + |
| 12-18 | 611 | + | + | + | 564 | - | - | | 537 | + | | | 528 | - | | |
| 18-24 | 611 | + | | | 564 | | + | | 532 | + | + | + | 529 | | | |
| 24-30 | 611 | - | - | + | 564 | | + | | 519 | + | + | + | 362 | | | |

Table 3. Forward stepping regression parameters for shelf acoustic and LIDAR observations. Acoustic data are based on lnABC and LIDAR data are based on untransformed backscatter. All stepwise regressions contained an intercept term. *N* is number of 250 m horizontal bins. *Northing*, *Easting*, and *N•E* (Northing•Easting) are signs of the associated regression coefficients.

| | 38 kHz 6/14-6/18 | | | | Lidar 6/13 | | | | Lidar 6/18 | | | | Lidar 6/19 | | | |
|---|---|---|---|---|---|---|---|---|---|---|---|---|---|---|---|---|
| Depth (m) | *N* | Northing | Easting | N•E | *N* | Northing | Easting | N•E | *N* | Northing | Easting | N•E | *N* | Northing | Easting | N•E |
| 2-6 | | | | | 642 | - | - | + | 1047 | - | - | + | 943 | + | + | + |
| 6-12 | 885 | | + | | 641 | - | - | + | 1047 | - | - | + | 933 | - | + | |
| 12-18 | 885 | - | - | + | 640 | | + | | 1046 | | | | 930 | + | + | + |
| 18-24 | 885 | - | - | + | 639 | | | | 1030 | + | + | + | 909 | + | + | + |
| 24-30 | 884 | - | - | + | 485 | + | | | 221 | | | | 145 | - | | |

Table 4. Variogram and forward stepping regression parameters for nighttime slope LIDAR. LIDAR data are based on untransformed backscatter. All stepwise regressions contained an intercept term. *N* is number of 250 m horizontal bins. *Northing*, *Easting*, and *N•E* (Northing•Easting) are signs of the associated regression coefficients*. Empirical variograms were robust and fit with exponential models using weighted least squares (Cressie 1993). *Range* is effective range.

| | Lidar 6/13 night | | | | | | |
|---|---|---|---|---|---|---|---|
| Depth (m) | *N* | Northing | Easting | N•E | Range (km) | Sill | Nugget |
| 2-6 | 843 | - | - | + | 1.9 | 12.04 | 3.15 |
| 6-12 | 843 | + | + | + | 1.4 | 0.48 | 0.15 |
| 12-18 | 843 | | | | 1.4 | 22.78 | 4.53 |
| 18-24 | 843 | | | | 2.1 | 247.91 | 206.97 |
| 24-30 | 843 | | | | 3.5 | 185.93 | 84.48 |
| 30-bottom | | | | | | | |

Table 5. Variogram parameters for slope acoustic and LIDAR observations. Acoustic data are based on lnABC and LIDAR data are based on untransformed backscatter. Empirical variograms were classical or robust and fit with exponential or spherical models using weighted least squares (Cressie 1993). *N* is number of 250 m horizontal bins. *Range* for exponential model is effective range. All variograms included a nugget. Unbounded (linear) variograms have "inf" ranges and sills.

| | 38 kHz 6/10-6/12 | | | | Lidar 6/8 | | | | Lidar 6/11 | | | | Lidar 6/14 | | | |
|---|---|---|---|---|---|---|---|---|---|---|---|---|---|---|---|---|
| Depth (m) | *N* | Range (km) | Sill | Nugget | *N* | Range (km) | Sill | Nugget | *N* | Range (km) | Sill | Nugget | *N* | Range (km) | Sill | Nugget |
| 2-6 | | | | | 564 | 11.0 | 7.75 | 0.03 | 537 | 5.2 | 0.21 | 0.07 | 530 | 6.1 | 0.36 | 0.32 |
| 6-12 | 611 | 5.6 | 0.50 | 0.08 | 564 | 6.6 | 0.33 | 0.04 | 537 | 7.1 | 0.05 | 0.04 | 530 | 11.8 | 0.33 | 0.12 |
| 12-18 | 611 | 2.6 | 0.49 | 0.65 | 564 | 2.6 | 2.68 | 0.65 | 537 | 1.6 | 0.76 | 0.00 | 528 | 3.0 | 0.02 | 0.01 |
| 18-24 | 611 | 2.5 | 0.53 | 0.00 | 564 | 2.3 | 9.58 | 1.36 | 532 | 27.0 | 0.07 | 0.02 | 529 | 3.7 | 0.01 | 0.00 |
| 24-30 | 611 | 2.4 | 0.55 | 0.01 | 564 | 2.3 | 13.62 | 2.28 | 519 | 56.8 | 0.03 | 0.00 | 362 | 4.0 | 0.1 | 0.05 |

Table 6. Variogram parameters for shelf acoustic and LIDAR observations. Acoustic data are based on lnABC and LIDAR data are based on untransformed backscatter. Empirical variograms were classical or robust and fit with exponential or spherical models using weighted least squares (Cressie 1993). *N* is number of 250 m horizontal bins. *Range* for exponential model is effective range. Unbounded (linear) variograms have "inf" ranges and sills.

| | 38 kHz 6/14-6/18 | | | | Lidar 6/13 | | | | Lidar 6/18 | | | | Lidar 6/19 | | | |
|---|---|---|---|---|---|---|---|---|---|---|---|---|---|---|---|---|
| Depth (m) | *N* | Range (km) | Sill | Nugget | *N* | Range (km) | Sill | Nugget | *N* | Range (km) | Sill | Nugget | *N* | Range (km) | Sill | Nugget |
| 2-6 | | | | | 642 | 6.5 | 1.60 | 0.19 | 1047 | 3.9 | 6.16 | 0.71 | 943 | 10.7 | 51.82 | 24.51 |
| 6-12 | 885 | 4.0 | 0.83 | 0.08 | 641 | 14.3 | 0.60 | 0.58 | 1047 | 3.1 | 2.56 | 0.44 | 933 | 3.9 | 3.00 | 0.50 |
| 12-18 | 885 | 3.9 | 0.54 | 0.00 | 640 | 9.3 | 0.20 | 0.19 | 1046 | 3.5 | 0.30 | 0.47 | 930 | inf | inf | 16.54 |
| 18-24 | 885 | 3.2 | 0.43 | 0.02 | 639 | inf | 19.31 | 0.00 | 1030 | 2.3 | 16.44 | 8.36 | 909 | 10.6 | 39.56 | 20.42 |
| 24-30 | 884 | 2.7 | 0.45 | 0.01 | 485 | inf | 265.81 | 0.03 | 221 | 1.5 | 5.51 | 0.44 | 145 | inf | inf | 55.51 |

Appendix 1. Midwater trawl results for aggregation characterization.

| *Scientific Name* | *Common Name* | 1 | 2 | 3 | 4 | 5 | 6 | 7 | 8 | 9 | 10 | 11 | 12 | 13 | 14 | 15 | 16 | 17 | 18 | 19 | 20 |
|---|---|---|---|---|---|---|---|---|---|---|---|---|---|---|---|---|---|---|---|---|---|
| Agonus acipenserinus | Sturgeon poacher | | | | 1 | | 1 | 2 | | | | | | | | | | 1 | | | |
| Alepisaurus ferox | Longnose lancetfish | | | | 1 | | | | | | | | | | | | | | | | 1 |
| Atherestes stomias | Arrowtooth flounder | 1 | | 1 | 1 | | 4 | 1 | | | | | | | | | | | | | |
| Bathylagus pacificus | Slender blacksmelt | | | | | | | | | | | | | | | | | | | 664 | |
| Chauliodus macouni | Pacific viperfish | | | | | | | | | | | | | | | | | | | 3 | |
| Clupea harengus pallasi | Pacific herring | 16 | | 4 | 13 | | 1 | 3 | | | | | | | | | | | | | |
| Coryphaeanoides leptolepis | Ghostly grenadier | | | | | | | | | | | | | | | | | | | 1 | |
| Diaphus theta | California headlightfish | | | | | | | | | | | | | | | | | 4 | 268 | 190 | 1550 |
| Gadus macrocephalus | Pacific cod | | | 1 | | | | | | | | | | | | | | | | | |
| Hemitripterus bolini | Bigmouth sculpin | | | | | | 1 | | | | | | | | | | | | | | |
| Lampanyctus jordani | Brokenline lanternfish | | | | | | | | | | | | | | | | | | 4 | 205 | 79 |
| Lepidopsetta polyxystra | Northern rocksole | | | | 1 | | | | | | | | | | | | | | | | |
| Leuroglossus schmidti | Northern smoothtongue | | | | | | | | | | | | | | 2 | | | 2450 | 6082 | 48,930 | 56,699 |
| Lipolagus ochotensis | Eared blacksmelt | | | | | | | | | | | | | | | | | | 8 | 16 | |
| Lumpenus sagitta | Pacific snake prickleback | | | | | | 1 | 1 | | | | | | | | | | | | | |
| Lycodapus c.f. poecilus | Variform eelpout | | | | | | | | | | | | | | | | | 15 | 24 | | |
| Melamphaes lugubris | Highsnout melamphid | | | | | | | | | | | | | | | | | | | 3 | |
| Nannobrachium regale | Pinpoint lanternfish | | | | | | | | | | | | | | | | | | | 1 | |
| Onchorhynchus gorbuscha | Pink salmon | | | | | | | | 4 | | 1 | | | | | | | | | | |
| Onchorhynchus keta | Chum salmon | | | 1 | | | | | | | 1 | 1 | | | | 9 | | | | | |
| Onchorhynchus nerka | Sockeye Salmon | | | | | | | | | | | 1 | | | | | | | | | |
| Petromyzon tridentata | lamprey | | | | | | | | | | | | | | 1 | | | 16 | 2 | | 6 |
| Pleurogrammus monopterygius | Atka mackerel | | | | | | | | 1 | | | | 1 | | | | | | | | |
| Protomyctophys thompsoni | Bigeye lanternfish | | | | | | | | | | | | | | | | | | 80 | 63 | 40 |
| Pseudobathylagus milleri | Stout blacksmelt | | | | | | | | | | | | | | | | | | | 79 | |
| Sebastes alutus | Pacific ocean perch | | | | | | | | | 1 | | | | | | | 81 | | | | |
| Sigmops gracilis | Slender fangjaw | | | | | | | | | | | | | | | | | | | 5 | |
| Stenobrachius leucopsarus | Northern lampfish | | | | | | | | | | | | | | | | | | 793 | 1265 | 4688 |
| Stenobrachius nannochir | Garnet lanternfish | | | | | | | | | | | | | | | | | | | 1027 | |
| Tactostoma macropus | Longnose dragonfish | | | | | | | | | | | | | | | | | | | 3 | |
| Theragra chocogramma | Walleye pollock | | 3 | | 17 | 1 | 47 | 5 | 1 | | 1 | 22 | 7 | 7 | 1142 | 24 | 4 | 286 | 10 | 1 | 7 |
| Triglops metopias | Alaskan sculpin | | | | 1 | | 1 | | | | | | | | | | | | | | |
| Berryteuthis magister | Magistrate armhook squid | | | | | | | | | | | | | | 3 | | 1 | | | | |
| Gonatopsis borealis | Boreopacific armhook squid | | | | | | | | | | | | | | | | 54 | 752 | | | |
| Unidentified squid | Squid | | | | | | | | | | 2 | | | | | | | | | 54 | 477 |
| | Grand Total | 17 | 17 | 7 | 35 | 84 | 63 | 14 | 8 | 1 | 206 | 25 | 8 | 139 | 1148 | 1539 | 140 | 3524 | 7272 | 53,032 | 63,865 |

Appendix 2. Total MultiNet catches by taxonomic groups for aggregation characterization.

| TAXON | 1 | 2 | 5 | 6 | 7 | 8 | 9 | 11 | 12 | 13 | 15 | 16 | 17 | 18 | 20 |
|---|---|---|---|---|---|---|---|---|---|---|---|---|---|---|---|
| Bryozoa | 64 | 640 | 64 | 128 | | 64 | 32 | | 64 | 64 | | 120 | | 128 | 32 |
| Cephalopoda | 1 | 11 | 11 | 3 | 6 | 5 | 8 | 3 | 5 | 8 | 24 | | 6 | 1 | 1 |
| Chaetognatha | 912 | 832 | 1312 | 320 | 1216 | 404 | 536 | 1280 | 256 | 2240 | 1152 | 140 | 2528 | 2528 | 929 |
| Cirripeda | | 576 | 96 | 64 | 264 | 12 | 16 | 256 | 384 | 64 | | 144 | 36 | 320 | 20 |
| Cnidaria | 276 | 56 | 538 | 81 | 97 | 129 | 45 | 360 | 109 | 291 | 221 | 304 | 112 | 92 | 42 |
| Ctenophora | | | 2 | | | | | | | | | | | | |
| Cumacea | | | | | 1 | | | | | | | | | | |
| Decapoda | 5394 | 1935 | 813 | 3881 | 9941 | 97 | 232 | 1144 | 461 | 2031 | 597 | 229 | 239 | 633 | 402 |
| Echinodermata | | | | | | 32 | | | 32 | 64 | | 8 | | | 64 |
| Gammarida | 8 | | | | | | | | | | | | | 1 | 1 |
| Hyperiidea | 448 | 3144 | 1425 | 1280 | 584 | 81 | 589 | 1041 | 388 | 694 | 2140 | 108 | 258 | 1996 | 154 |
| Larvacea | 1600 | 3280 | 2368 | 960 | 2944 | 536 | 112 | 4352 | 2880 | 2880 | 480 | 2120 | 1712 | 2688 | 864 |
| Mollusca | 4480 | 4296 | 1856 | 7132 | 5392 | 1368 | 337 | 7984 | 3292 | 4068 | 2380 | 1364 | 620 | 3880 | 1016 |
| Ostracoda | | | | | | | | | | 16 | | | 464 | 229 | 96 |
| Phoronida | | | | | | | | | | | 128 | | | | |
| Pisces | 82 | 176 | 175 | 72 | 128 | 63 | 39 | 80 | 98 | 78 | 103 | 22 | 29 | 200 | 40 |
| Polychaeta | 1 | 8 | 9 | | 9 | 2 | 1 | 341 | 1 | 20 | 13 | 19 | 127 | 153 | 38 |
| Tunicata | 4 | | 2 | | | | | | 4 | | 6 | 4 | | | |
| Total | 13270 | 14954 | 8671 | 13921 | 20582 | 2793 | 1947 | 16841 | 7974 | 12518 | 7244 | 4582 | 6131 | 12849 | 3699 |

Figure 1. Survey location showing systematic transects.

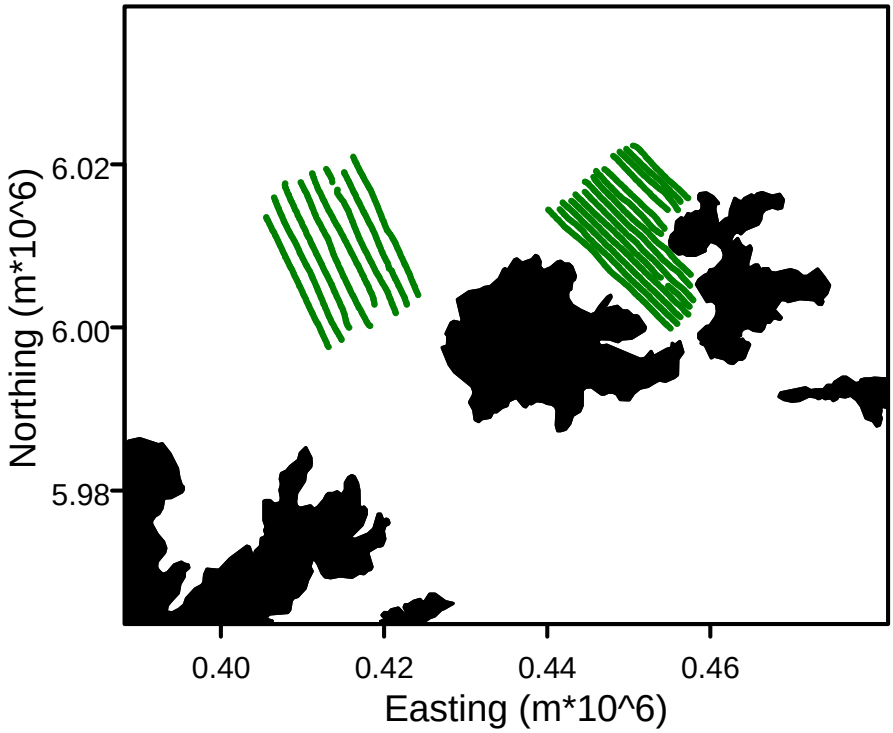

Figure 2. Geostatistical predictions of Sv_mean for shelf and slope-water-column sampling areas.

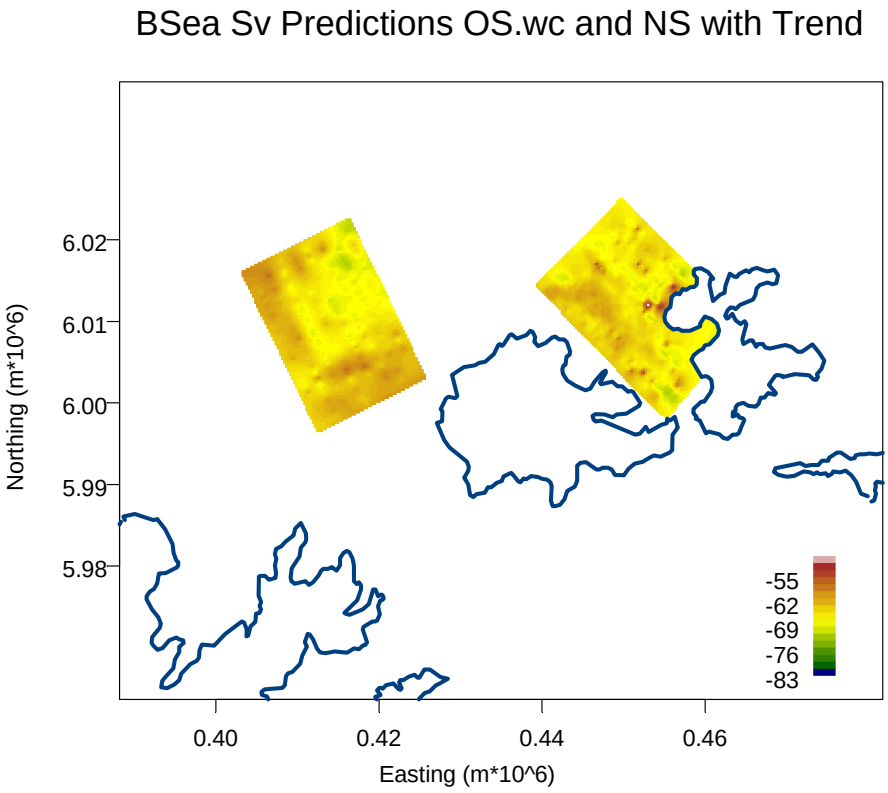

Figure 3. Geostatistical predictions of Sv_mean in slope-shallow (*A*), slope-middle (*B*), and slope-deep (*C*) depth layers.

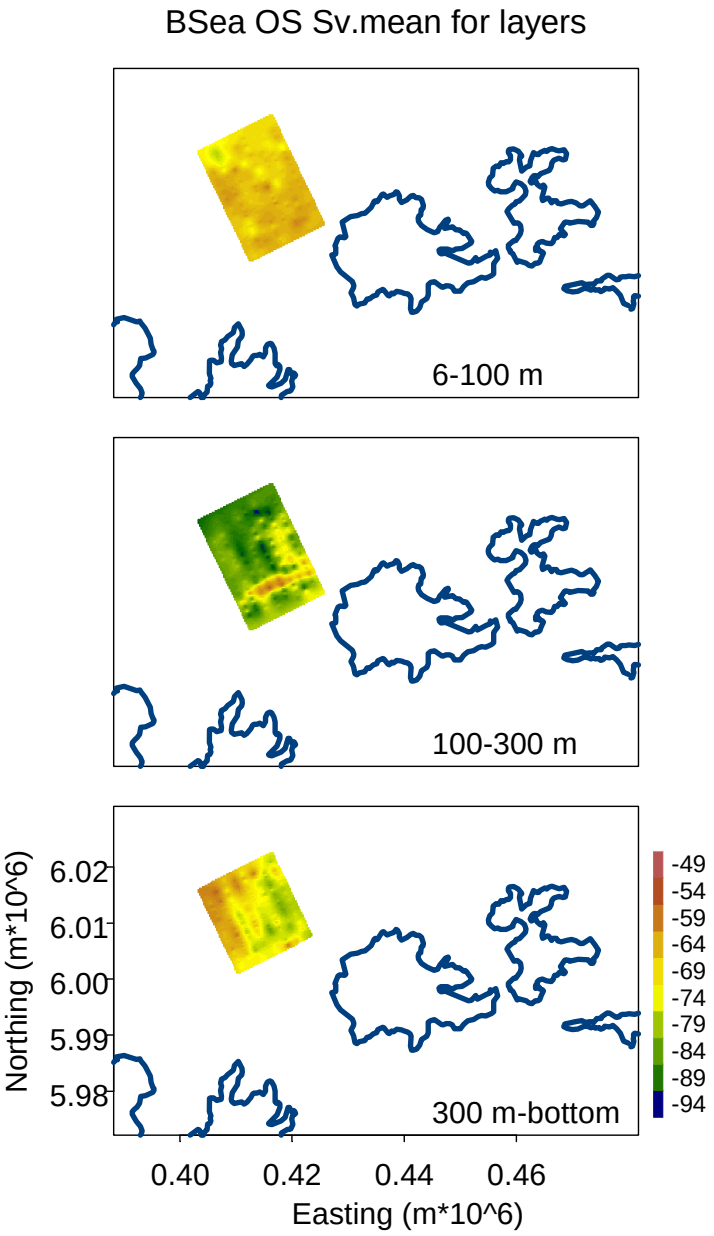

Figure 4. Agglomerative hierarchical cluster analysis results for (*A*) slope and (*B*) shelf regions. Numbers indicate depth layer (1: 6-12 m, 2: 12-18 m, 3: 18-24 m, 4: 24-30 m). In slope, circles are acoustic (10-12 June) and LIDAR are squares (8 June), triangles (11 June), and diamonds (14 June). In shelf, circles are acoustic (14-18 June) and LIDAR are squares (13 June), triangles (18 June), and diamonds (19 June).

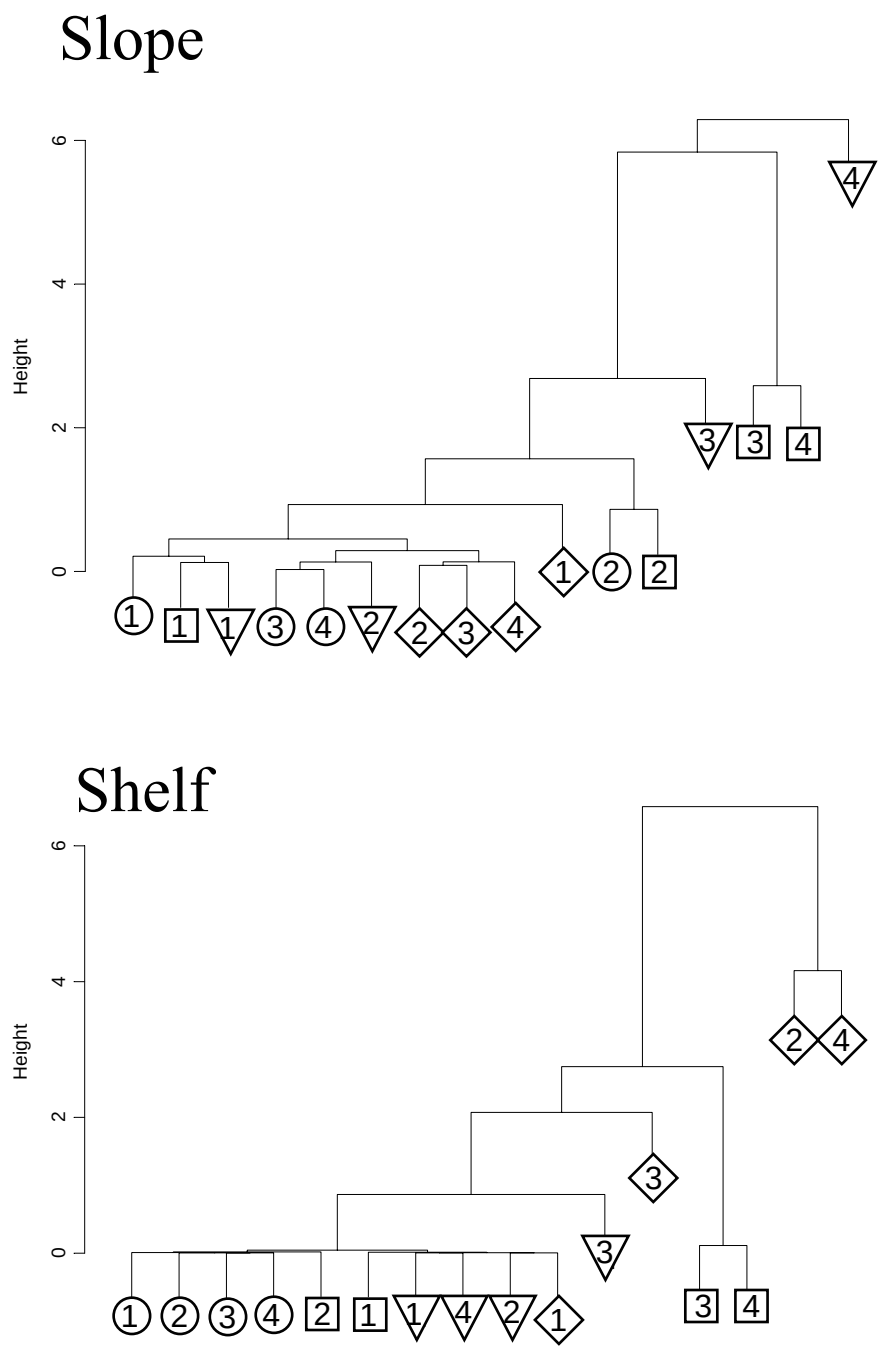

Figure 5. Representative examples of target assemblages observed on the echosounder and sampled with midwater trawl or MultiNet. Pelagic layers (*A*, ID11; *B*, ID 17), demersal school (*C*, ID 16), scattered pelagics (*D*, ID 14), and schools (*E*, ID3; *F*, ID 12).

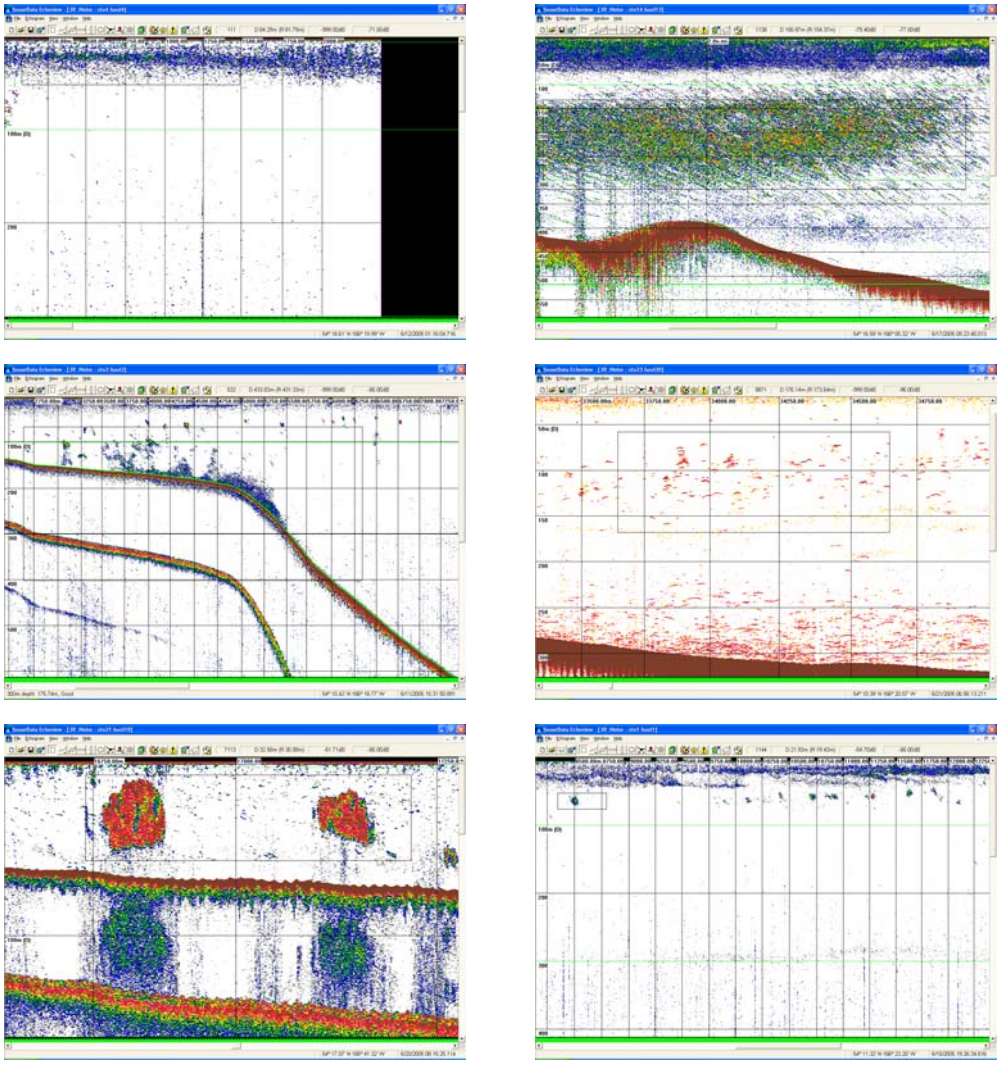

Figure 6. Species distribution within target assemblages in the shelf region from midwater trawl (*A*) and MultiNet (*B*) samples. Equilibrium trawl depth increases from left to right.

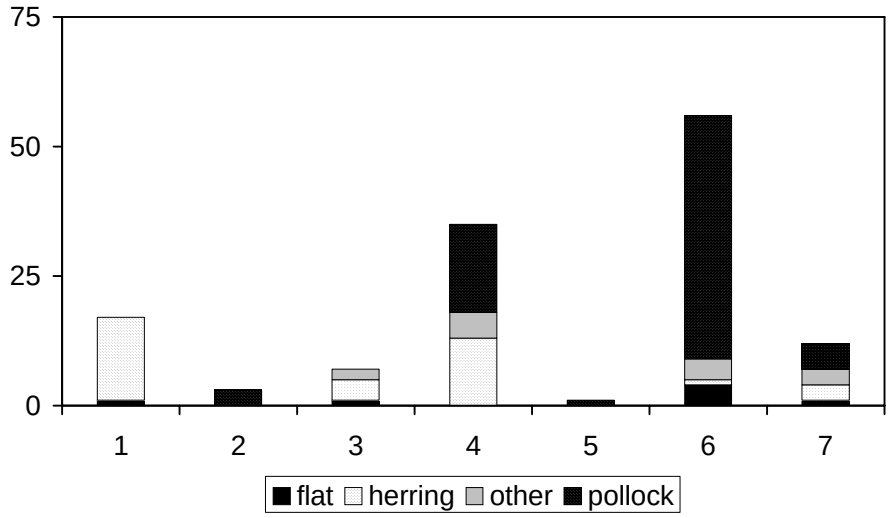


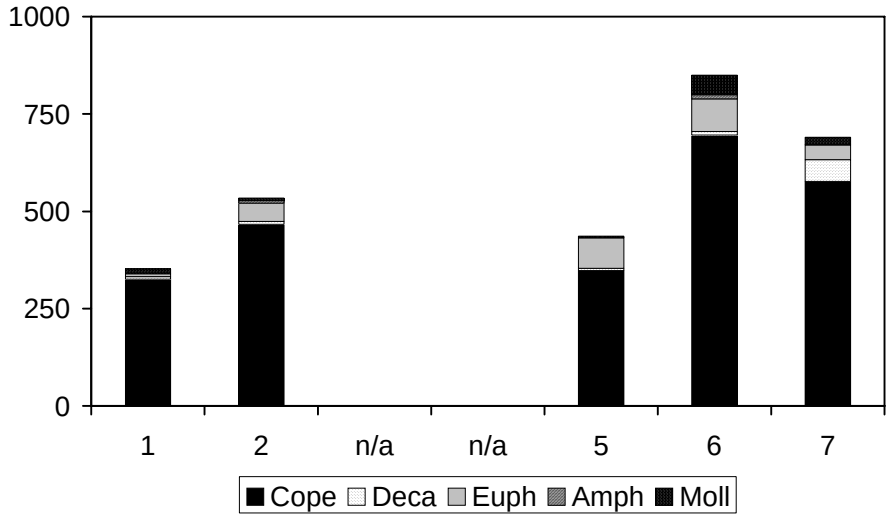

Figure 7. Species distribution within target assemblages in the slope region from midwater trawl (*A*) and MultiNet (*B*) samples. High trawl catches are standardized to 100 individuals. Equilibrium trawl depth increases from left to right.

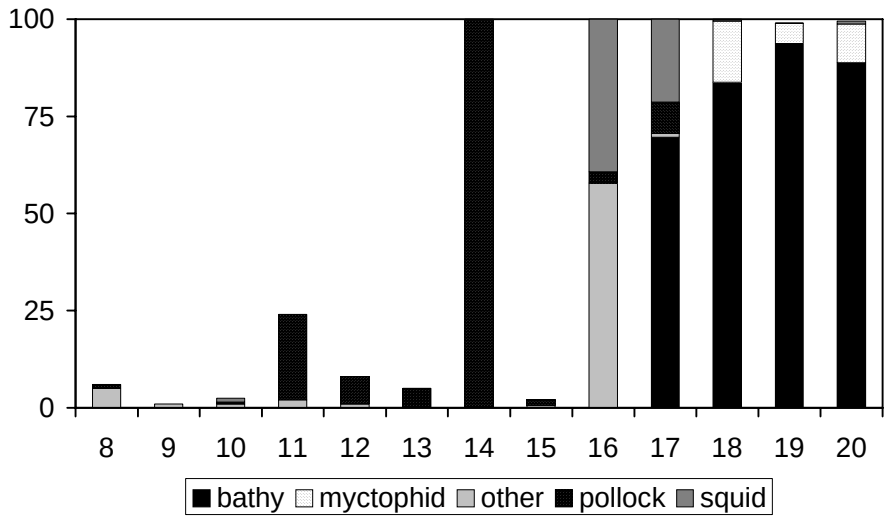


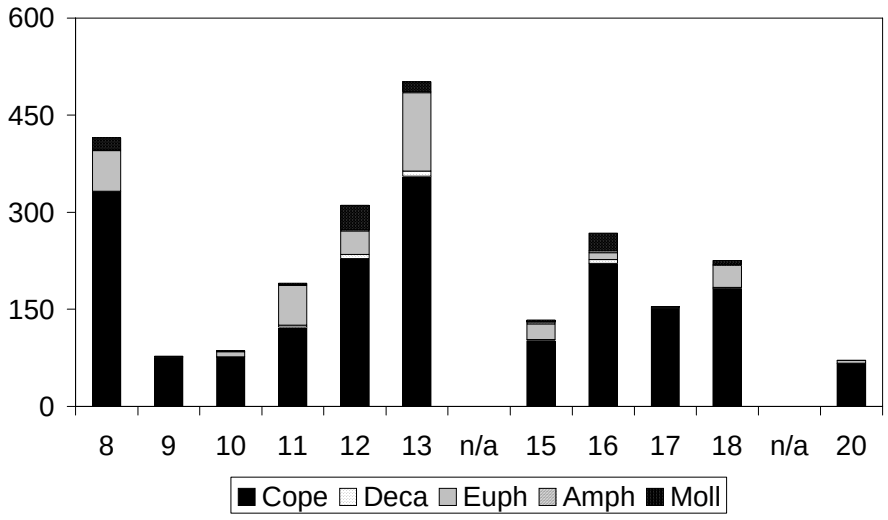

# *Forage Fish in Shallow Nearshore Habitats of the Bering Sea*

John F. Thedinga, Scott W. Johnson, Mandy R. Lindeberg, and A. Darcie Neff
NOAA, Auke Bay Laboratory, Juneau, AK 99801

## Abstract

Nearshore waters of the Bering Sea provide habitat for several forage fish species that are important in the diet of marine mammals, seabirds, and other fishes. Shallow, nearshore waters (<5 m deep, <20 m from shore) of the Bering Sea were sampled with a beach seine to estimate forage fish distribution and relative abundance in June 2005. Three habitat types were sampled: non-vegetated sand substrate, vegetated cobble substrate, and vegetated bedrock substrate. A total of 70 sites were seined on Akutan, Akun, and Unalaska Islands. Total catch was 83,910 fish representing 27 species. Catch per seine haul (all spp.) varied from no fish to over 15,000 fish. Pacific sand lance was the dominant forage fish species captured—approximately 35,000 fish (42% of total catch) occurring in 60% of all seine hauls. Mean size of sand lance captured was 106 mm fork length (FL). Other commonly captured forage fish were young-of-the-year (YOY) Pacific sandfish (mean FL = 36 mm) and YOY gadids (mean FL = 31 mm). Fish were distributed unequally among habitats. Mean catch per seine haul of all species was 1,647 fish in vegetated cobble sites, 1,170 fish in non-vegetated sand sites, and 79 fish in vegetated bedrock sites. Most sand lance (98%) were captured in non-vegetated sand sites, and most sandfish (96%) and gadids (97%) were captured in vegetated cobble substrate sites. Although we captured several forage fish species in shallow, nearshore waters in June, use of the nearshore by forage fish in other seasons and other areas of the Bering Sea is largely unknown. Beach seining is an effective method for sampling forage fish, particularly sand lance, in the nearshore of the Bering Sea.

## Introduction

Forage fish assemblages in the shallow, nearshore waters (<5 m deep, <20 m from shore) of the Bering Sea have been examined in only a few locations. In the western Bering Sea, Isakson et al. (1971) described the nearshore fish community at Amchitka Island. In the southeastern Bering Sea, Houghton (1987) examined nearshore fish assemblages, and Warner and Shafford (1981) surveyed spawning forage fish. In Port Moller, McGurk and Warburton (1992) studied the life history of Pacific sand lance (*Ammodytes hexapterus*). The only studies of nearshore fish within our study area were limited beach seine surveys by Robards (1999) and Robards and Shroeder (2000) in Unalaska Bay and Akutan Bay.

Nearshore areas provide important habitat for many fish species and are vulnerable to human disturbance from oil and other shoreline development. Nearshore habitat is of particular importance to juvenile stages of Pacific cod (*Gadus macrocephalus*), walleye pollock (*Theragra chalcogramma*), and many flatfish and rockfish species, providing young-of-the-year (YOY) fish with essential nursery habitat. Forage fish such as Pacific sand lance, Pacific sandfish (*Trichodon trichodon*), and Pacific herring (*Clupea pallasii*) use nearshore areas for spawning and rearing, but the location, timing, and extent of these activities in the nearshore of the Bering Sea is poorly understood.

The Bering Sea supports the world's largest walleye pollock fishery in addition to important Pacific cod, Pacific halibut (*Hippoglossus stenolepis*), and king crab (*Paralithodes* spp.) fisheries. Additionally, the area supports large populations of marine mammals and seabirds. Forage fish play an important part in the Bering Sea ecosystem because of their role as food for higher trophic level predators. Pacific sandfish occurred in up to 64% of Steller sea lion (*Eumetopias jubatus*) scats in the Aleutian Islands (Sinclair and Zeppelin 2002). Sand lance (*Ammodytes* spp.) are possibly the single most important taxon of forage fish in the northern hemisphere (Springer and Speckman 1997), and are a major prey species for at least 40 species of birds, 12 species of marine mammals, and 45 species of fish (Field 1988; Willson et al. 1999). Our objective was to examine forage fish assemblages in several nearshore habitats in the Bering Sea in the vicinity of Unalaska, Alaska.

## Methods

### *Study locations*

Fishes were sampled with a beach seine in the shallow, nearshore waters (<5 m deep, <20 m from shore) of the Bering Sea from June 10-18, 2005. A total of 70 sites were sampled on Akutan, Akun, and Unalaska Islands (Fig.1). Different habitat types were sampled to account for segregation of some fish species based on habitat preference (Johnson et al. 2003). Habitat types included sand substrate (33 sites) with little or no rooted vegetation, cobble substrate (27 sites) with understory kelps dominated by *Alaria marginata* and *Laminaria longipes*, and steep bedrock walls (10 sites) with understory kelps dominated by *A. marginata* and *Cymathere triplicata*.

### *Fish capture and habitat*

Fish were captured with a 37-m variable-mesh beach seine that tapered from 5 m wide at the center to 1 m wide at the ends. Outer panels were each 10 m of 32-mm stretch mesh, intermediate panels were each 4 m of 6-mm square mesh, and the bunt was 9 m of 3.2-mm square mesh. We set the seine as a "round haul" by holding one end on the beach, backing around in a skiff with the other end to the beach about 18 m from the starting point, and pulling the seine onto shore. The seine had a lead line and a float line so that the bottom contacted the substratum and the top floated on the surface. Sites were sampled during daylight independent of tide height.

Fish captured with the seine were identified to species and enumerated. For large catches, the number of fish was estimated gravimetrically. A random subsample of approximately 500 fish was removed from the total catch, and the remaining fish were collectively weighed to the nearest 0.1 kg. Fish in the subsample were weighed to the nearest gram and counted by species. A mean weight of fish determined from the subsample was used to estimate the number of fish in the total catch. The proportion of each species in the subsample was also used to determine the species composition of the total catch. Fork length (FL) was measured to the nearest millimeter for up to 50 individuals for most species. The number of larvae (≤ 30 mm) in large catches was visually estimated.

Habitat of the areas seined (subtidal) was classified at each site, and the adjacent intertidal areas were classified at about one half of the sites. For the subtidal areas, water temperature and salinity (practical salinity scale; PSS) were measured at a depth of 20 cm with a thermometer and a hand-held refractometer. Substrate composition was visually estimated and

vegetation was identified. For the intertidal areas, *ShoreZone* survey methods were used (Howes and Berry 2001).

***Data analysis***

We used one-way ANOVA to test for significant differences in catch among habitat types and the Tukey test for pairwise tests among habitat types. Kruskal-Wallis ANOVA was used to test for significant differences in the Shannon-Weaver diversity index (H′) among habitat types—pairwise comparisons were tested with Dunn's method.

## Results

***Catch***

A total of 83,910 fish representing 27 species were captured at 70 sites. Catches varied from no fish to more than 15,000 fish per seine haul. Pacific sand lance was the dominant fish species captured—approximately 35,000 were captured, and they occurred in 60% of hauls. Three species, Pacific sand lance, pink salmon (*Oncorhynchus gorbuscha*), and Pacific sandfish, and one family of fishes, Gadidae, comprised 95% of the total catch.

***Habitat***

Fish were distributed unequally among habitats (Table 1). Catch per seine haul for all species was significantly greater (P = 0.001) in cobble sites than bedrock sites and significantly greater (P = 0.040) in sand sites than bedrock sites. Mean catch per seine haul for all species was 1,647 fish in cobble sites, 1,171 fish in sand sites, and 79 fish in bedrock sites. Most Pacific sand lance (98%) were captured in sand sites, whereas most gadids (97%), pink salmon (80%), and Pacific sandfish (96%) were captured in cobble sites. In sand sites, sand lance was the dominant species captured (mean = 1,056 fish per haul), occurring in 94% of sites and comprising 90% of the catch. Young-of-the-year sandfish were the second most abundant forage fish in sand sites (mean = 11 fish per haul), occurring in 24% of sites and comprising 1% of the catch. In cobble sites, YOY gadids were the dominant fish captured (mean = 755 fish per haul), occurring in 74% of sites and comprising 46% of the catch. Sandfish were the second most abundant forage fish in cobble sites (mean = 373 fish per haul), occurring in 48% of sites and comprising 23% of the catch. Sand lance were captured in one third of cobble sites but mean catch was only 22 fish per haul. In bedrock sites, YOY gadids (mean = 34 fish per haul) and pink salmon fry (mean = 34 fish per haul) were the dominant fish captured, occurring in 70% and 30% of hauls, and

comprising a total of 69% of the catch. Few sand lance (mean = 0.2 fish per haul) and sandfish (mean = 3 fish per haul) were captured in bedrock sites.

Species richness varied by habitat. The fewest number of species (16) were captured at bedrock sites, whereas more species were captured at sand (23) and cobble (27) sites. The Shannon-Weaver diversity index (H′) was significantly different (P = 0.007) among the three habitat types. Pairwise comparisons showed significant differences (P<0.05) between bedrock and cobble sites and between bedrock and sand sites. Dominance by Pacific sand lance in sand habitat (90% of catch; Table 1) reduced the diversity index for sand habitat.

***Fish length and age***

Most captured fish were juveniles. Mean FL of all fish ranged from 23 mm to 408 mm. Length frequencies of Pacific sand lance indicated 2 or 3 age groups with modes of 60-69 mm and 120-129 mm (Fig 2). All Pacific sandfish, pink salmon, and gadids were YOY (Table 2).

## Discussion

There has been little research on nearshore forage fish communities in the Bering Sea. Forage fish life histories, except for Pacific herring are poorly understood, primarily because there are no commercial fisheries for most forage fish species. Our study showed that nearshore fish assemblages on Akutan, Akun, and Unalaska Islands were dominated by forage fish, particularly Pacific sand lance. In nearshore waters of other areas of the Bering Sea, Houghton (1987) reported that the most abundant fish in beach seine catches from late June to mid September from False Pass to Ugashik Bay was Pacific sand lance. McGurk and Warburton (1992) found that larvae from sand lance that spawned in Port Moller in the southeastern Bering Sea reared in the same or nearby estuarine habitats. In areas near our sampling sites in Unalaska Bay and Akutan Harbor, however, Robards (1999) and Robards and Schroeder (2000) reported beach seine catches in summer were dominated by pink salmon fry, and captured few sand lance. Mean catch per seine haul by Robards and Robards and Schroeder (653 and 536 fish per haul) were about half of our catch (1,202 fish per haul). We did not capture any Pacific herring, capelin (*Mallotus villosus*) or other smelts (Osmeridae).

Fish catch and species richness varied by habitat. Although we captured Pacific sand lance in all habitats, highest catches were in sand habitat. In most studies in the Bering Sea, catches of forage fish were not separated by habitat type (Houghton1987; Robards 1999;

Robards and Schroeder 2000). Isakson et al. (1971) divided their nearshore sampling areas near Amchitka Island into rock/algae and sand/gravel habitats and found different fish communities in each habitat—Pacific sand lance and Pacific sandfish were prominent species in sand/gravel habitat but not in rock/algae habitat. In our study, 96% of sandfish were captured in cobble habitat, whereas in southeastern Alaska, most sandfish were captured in bedrock habitat (Thedinga et al. in press).

Most of the forage fish we captured were juveniles. In other areas of Alaska, most forage fish captured with beach seines were also juveniles (Abookire et al. 2000; Robards 2000; Johnson et al. 2005; Thedinga et al. in 2006; Thedinga et al. in press; Johnson et al. in prep.). Some adult forage fish spawn in the shallow nearshore (McGurk and Warburton 1992; Warner and Shafford 1981), but timing and habitats used for spawning are poorly understood.

## Conclusions

Shallow, nearshore areas in the Bering Sea provide rearing habitat for several species of forage fish, most importantly Pacific sand lance. How long sand lance and YOY Pacific sandfish and gadids rear in the nearshore is unknown, although Houghton (1987) captured sand lance throughout summer in the nearshore of the eastern Bering Sea, and McGurk and Warburton (1992) captured sand lance larvae throughout summer in Port Moller. In southeastern Alaska, Sand lance and sandfish were caught throughout summer (Johnson et al., 2003; Johnson and Thedinga, 2005; Thedinga et al. in 2006; Thedinga et al. in prep.), but few were captured in winter (Thedinga et al. in 2006; Thedinga et al. in prep.).

Seasonal studies would help define temporal use of shallow nearshore habitats in the Bering Sea by sand lance and other forage fish species (e.g., Pacific herring, capelin). Pacific herring, capelin, sand lance, and Pacific sandfish spawn in the nearshore (Marliave 1980; Warner and Shafford 1981; McGurk and Warburton 1992), but we do not fully understand their dependence and fidelity to the different habitats types within the nearshore, or which habitats are more important for different life stages. Nearshore waters are some of most productive areas in Alaska and are vulnerable to changing environmental perturbations and increasing stress from shoreline development from oil and other shoreline development. In particular, information is needed on the function and use of nearshore habitats by forage fish because of their importance as a prey resource for higher-level-trophic consumers (e.g., marine mammals, fish). A better

understanding of how the nearshore environment supports ecologically important forage fish species will help managers conserve forage fish populations and protect essential habitats.

## Literature cited

Abookire, A.A., J.F. Piatt, and M.D. Robards. 2000. Nearshore fish distributions in an Alaskan estuary in relation to stratification, temperature and salinity. Est. Coast. Shelf Sci. 51:45-59.

Field, L.J. 1988. Pacific sand lance, *Ammodytes hexapterus*, with notes on related *Ammodytes* species. *In*: Wilimovsky, N. J., Incze, L. S., Westrheim, S. J. (Eds.), Species Synopses, Life Histories of Selected Fish and Shellfish of the Northeast Pacific and Bering Sea. Available from Washington Sea Grant Program, 3716 Brooklyn Ave., NE, Seattle, WA, pp. 15–33.

Houghton, J.P. 1987. Forage fish use of inshore habitats north of the Alaska Peninsula. *In*: Forage fishes of the southeastern Bering Sea Conference proceedings. MMS 87-0017.

Howes, D., and H. Berry. 2001. British Columbia biophysical *Shore-Zone* mapping system. A systematic approach to characterize coastal habitats in the Pacific Northwest. Puget Sound Research Conference, Seattle, Washington, 11 p.

Isakson, J.S., C.A. Simenstad, and R.L. Burgner. 1971. Fish communities and food chains in the Amchitka area. BioScience 21:666–670.

Johnson, S.W., M.L. Murphy, D.J. Csepp, P.M. Harris, and J.F. Thedinga. 2003. A survey of fish assemblages in eelgrass and kelp habitats of southeastern Alaska. U.S. Dep. Commer., NOAA Tech. Memo. NMFS-AFSC-139, 39 p.

Johnson, S.W., A.D. Neff, and J.F. Thedinga. 2005. An atlas on the distribution and habitat of common fishes in shallow nearshore waters of southeastern Alaska. U.S. Dep. Commer., NOAA Tech. Memo. NMFS-AFSC-139, 89 p.

Johnson, S.W., J.F. Thedinga, and K.M. Munk. In prep. Habitat, age, and diet of an important forage fish in southeastern Alaska: Pacific sand lance, *Ammodytes hexapterus*.

Marliave, J.B. 1980. Spawn and larvae of the Pacific sandfish, *Trichodon trichodon*. Fish. Bull. 78:959-964.

McGurk, M.D. and H.D. Warburton. 1992. Pacific sand lance of the Port Moller estuary, southeastern Bering Sea: an estuarine-dependent early life history. Fish. Oceanogr. 1:4, 306-320.

Robards, M. 1999. Assessment of nearshore fish around Unalaska using beach seines during July 1999. Final report. USGS Biological Resources Division, Alaska Biological Sciences Center, Anchorage, AK.

Robards, M. and M. Schroeder. 2000. Assessment of nearshore fish around Akutan Harbor using beach seines during March and June 2000. Final report. USGS Biological Resources Division, Alaska Biological Sciences Center, Anchorage, AK.

Sinclair, E.H., and T.K. Zeppelin. 2002. Seasonal and spatial differences in diet in the western stock of Steller sea lions (*Eumetopias jubatus*). J. Mamm. 83:973–990.

Springer, A.M., Speckman, S.G., 1997. A forage fish is what? Summary of the Symposium. *In*: Forage Fishes in Marine Ecosystems. Proceedings of the International Symposium on the Role of Forage Fishes in Marine Ecosystems. Alaska Sea Grant College Program Report No. 97-01. University of Alaska, Fairbanks, AK, pp. 773–805.

Thedinga, J.F., and S.W. Johnson. In press. Habitat, age, and diet of a forage fish in southeastern Alaska: Pacific sandfish (*Trichodon trichodon*). Fisheries Bulletin.

Thedinga, J.F., S.W. Johnson, and D.J. Csepp. 2006. Nearshore fish assemblages in the vicinity of two Steller sea lion haulouts in southeastern Alaska. *In*: Sea Lions of the World. Alaska Sea Grant College Program Report No. AK-SG-06-01. University of Alaska, Fairbanks, AK, pp. 269-284.

Warner, I.M. and P. Shafford. 1981. Forage fish spawning surveys – southern Bering Sea. *In* Environmental assessment of the Alaskan continental shelf, Final report. Vol. 10:64 p.

Willson, M.F., Armstrong, R.H., Robards, M.D., and Piatt, J.F., 1999. Sand lance as cornerstone prey for predator populations. *In*: Robards, M. D., Willson, M. F., Armstrong, R. H., Piatt, J. F. (Eds.), Sand lance: a Review of Biology and Predator Relations and Annotated Bibliography. Research paper PNW-RP-521. U.S. Department of Agriculture, Forest Service, Pacific Northwest Research Station, Portland, OR, pp. 17–44.

Table 1. Catch per haul and frequency of occurrence (%) of fish captured with a beach seine in three habitat types in the Bering Sea, on Akutan, Akun, and Unalaska Islands, Alaska, June 2005. A blank represents the absence of a species from a site. N = 10 hauls in bedrock sites, 27 hauls in cobble sites, and 33 hauls in sand sites.

| | | Bedrock | | Cobble | | Sand | |
|---|---|---|---|---|---|---|---|
| Common name | Scientific name | Catch/haul | % | Catch/haul | % | Catch/haul | % |
| Pacific sand lance | *Ammodytes hexapterus* | 0.2 | 20.0 | 21.8 | 33.3 | 1,056.4 | 93.9 |
| Juvenile gadid | Gadidae | 34.0 | 70.0 | 755.1 | 74.1 | 6.3 | 18.2 |
| Pink salmon | *Oncorhynchus gorbuscha* | 34.1 | 30.0 | 379.1 | 63.0 | 66.4 | 48.5 |
| Pacific sandfish | *Trichodon trichodon* | 3.4 | 30.0 | 373.4 | 48.1 | 11.0 | 24.2 |
| Snake prickleback | *Lumpenus sagitta* | | | 87.0 | 11.1 | 0.8 | 3.0 |
| Juvenile cottid | Cottidae | 1.4 | 30.0 | 12.4 | 81.5 | 12.5 | 30.3 |
| Silverspotted sculpin | *Blepsias cirrhosus* | 2.5 | 50.0 | 6.0 | 66.7 | | |
| Rock sole | *Lepidopsetta* spp. | | | 1.0 | 14.8 | 4.6 | 54.5 |
| Juvenile flatfish | Pleuronectidae | 0.1 | 10.0 | 1.1 | 22.2 | 4.2 | 39.4 |
| Chum salmon | *Oncorhynchus keta* | | | 3.2 | 3.7 | 0.4 | 3.0 |
| Dolly Varden | *Salvelinus malma* | | | 0.3 | 14.8 | 2.8 | 30.3 |
| Rock greenling | *Hexagrammos lagocephalus* | 0.4 | 30.0 | 2.8 | 66.7 | 0.1 | 6.1 |
| Coho salmon | *Oncorhynchus kisutch* | | | 0.3 | 3.7 | 1.7 | 9.1 |
| Frog sculpin | *Myoxocephalus stelleri* | 0.1 | 10.0 | 0.4 | 18.5 | 1.3 | 39.4 |
| Sturgeon poacher | *Podothecus accipenserinus* | | | | | 1.5 | 9.1 |
| Juvenile greenling | Hexagrammidae | | | 0.9 | 29.6 | <0.1 | 3.0 |
| Pacific cod | *Gadus macrocephalus* | | | 0.9 | 3.7 | | |
| Starry flounder | *Platichthys stellatus* | | | <0.1 | 3.7 | 0.7 | 27.3 |
| Juvenile snailfish | Liparidae | 0.1 | 10.0 | 0.7 | 18.5 | | |
| Manacled sculpin | *Synchirus gilli* | 1.9 | 20.0 | | | | |
| Masked greenling | *Hexagrammos octogrammus* | 0.1 | 10.0 | 0.3 | 14.8 | 0.2 | 6.1 |
| Red Irish lord | *Hemilepidotus hemilepidotus* | 0.1 | 10.0 | 0.2 | 14.8 | | |
| Black rockfish | *Sebastes melanops* | | | 0.2 | 14.8 | | |
| Juvenile poacher | Agonidae | | | | | 0.2 | 12.1 |
| Crescent gunnel | *Pholis laeta* | | | 0.1 | 11.1 | | |
| Sockeye salmon | *Oncorhynchus nerka* | | | | | 0.1 | 3.0 |
| Threespine stickleback | *Gasterosteus aculeatus* | 0.1 | 10.0 | <0.1 | 3.7 | | |
| Armorhead sculpin | *Gymnocanthus galeatus* | | | 0.1 | 3.7 | | |
| Great sculpin | *Myoxocephalus polyacanthocephalus* | | | | | 0.1 | 6.1 |
| Kelp greenling | *Hexagrammos decagrammus* | 0.1 | 10.0 | <0.1 | 3.7 | | |
| Alaska plaice | *Pleuronectes quadrituberculatus* | | | | | <0.1 | 3.0 |
| English sole | *Parophrys vetulus* | | | | | <0.1 | 3.0 |
| Dusky rockfish | *Sebastes ciliatus* | | | <0.1 | 3.7 | | |

Table 2. Total catch, mean fork length, and range of fish captured with a beach seine in the Bering Sea, on Akutan, Akun, and Unalaska Islands, Alaska, June 2005. Sample locations are shown in Figure 1.

| Family or Species | Total Catch | Number Measured | Fork length (mm) Mean | Fork length (mm) Range |
|---|---|---|---|---|
| Pacific sand lance | 35,451 | 1,109 | 106 | 35-190 |
| Gadidae | 20,934 | 451 | 23 | 15-31 |
| Pink salmon | 12,770 | 615 | 45 | 30-65 |
| Pacific sandfish | 10,478 | 299 | 36 | 17-56 |
| Snake prickleback | 2,374 | 92 | 122 | 37-320 |
| Cottidae | 761 | 6 | 30 | 16-49 |
| Silverspotted sculpin | 186 | 24 | 76 | 19-144 |
| Rock sole | 179 | 167 | 181 | 32-522 |
| Pleuronectidae | 168 | 36 | 39 | 16-63 |
| Chum salmon | 100 | 22 | 63 | 56-71 |
| Dolly Varden | 99 | 99 | 307 | 130-535 |
| Rock greenling | 81 | 77 | 258 | 120-495 |
| Coho salmon | 64 | 39 | 121 | 35-145 |
| Frog sculpin | 53 | 48 | 384 | 80-485 |
| Sturgeon poacher | 51 | 5 | 55 | 25-97 |
| Hexagrammidae | 24 | 16 | 54 | 48-65 |
| Pacific cod | 23 | 13 | 200 | 178-237 |
| Starry flounder | 23 | 13 | 372 | 300-520 |
| Liparidae | 21 | 14 | 25 | 12-78 |
| Manacled sculpin | 19 | 4 | 36 | 18-55 |
| Masked greenling | 14 | 14 | 288 | 131-480 |
| Red Irish lord | 7 | 6 | 252 | 87-378 |
| Black rockfish | 6 | 6 | 120 | 92-160 |
| Sockeye salmon | 3 | 3 | 66 | 62-73 |
| Threespine stickleback | 2 | 2 | 69 | 65-73 |
| Armorhead sculpin | 2 | 2 | 78 | 70-85 |
| Great sculpin | 2 | 2 | 408 | 400-415 |
| Kelp greenling | 2 | 2 | 373 | 345-400 |
| Alaska plaice | 1 | 1 | 185 | -- |
| Dusky rockfish | 1 | 1 | 90 | -- |
| English sole | 1 | 1 | 116 | -- |
| Other species | 10 | 0 | -- | -- |

Figure 1. Location of nearshore sites sampled with a beach seine in the Bering Sea on Akutan, Akun, and Unalaska Islands, Alaska, June 2005.

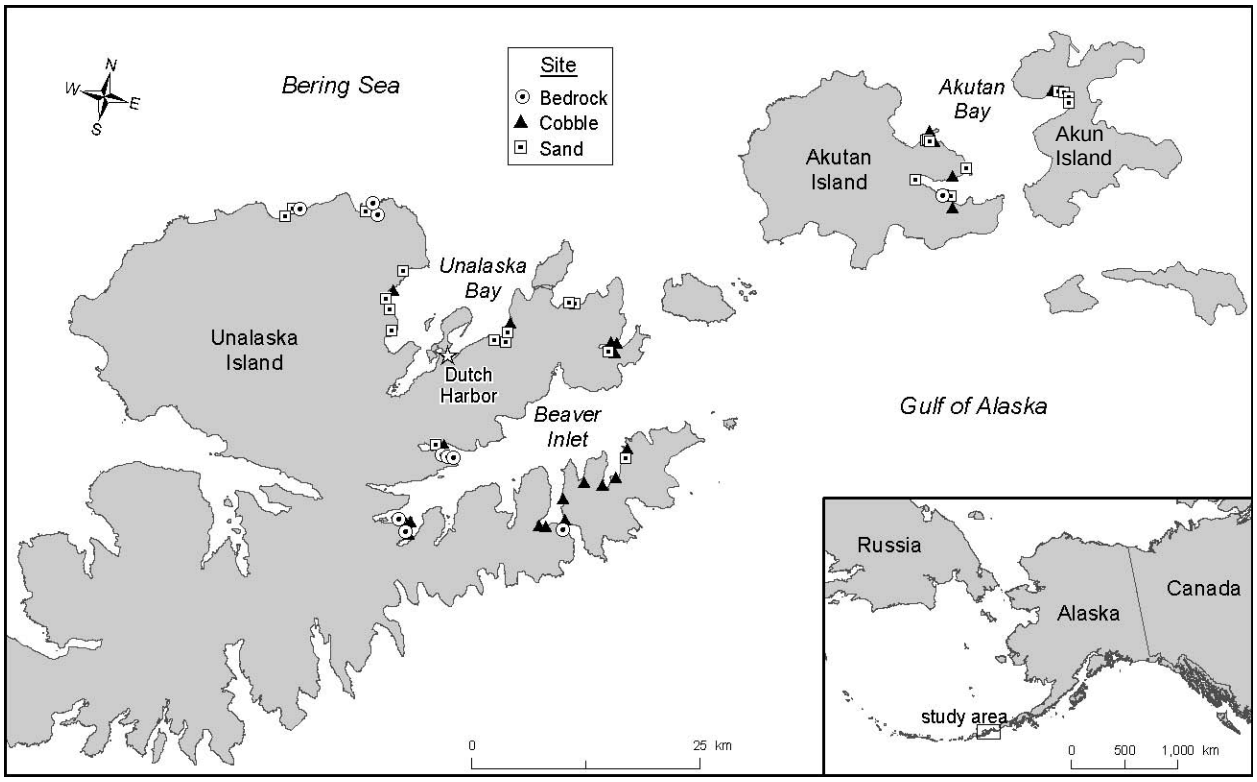

Figure 2. Length frequencies of Pacific sand lance (*Ammodytes hexapterus*) captured with a beach seine in nearshore habitats of the Bering Sea on Akutan, Akun, and Unalaska Islands, Alaska, June 2005.

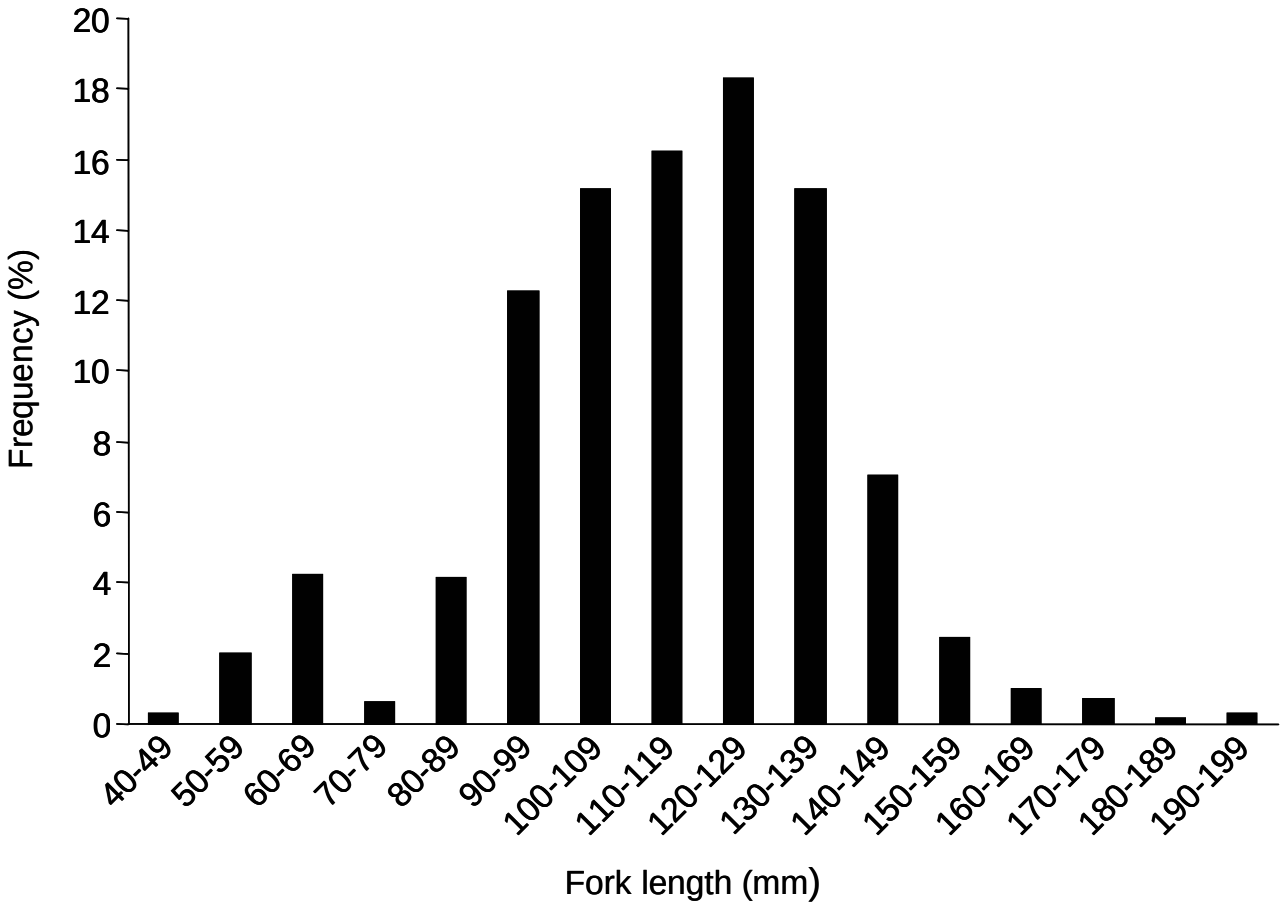

# *Distribution, composition and energy density of zooplankton in the southeastern Bering Sea*

Nicola Hillgruber[1], Johanna J. Vollenweider[2], Wyatt Fournier[2]
[1]School of Fisheries and Ocean Science, University of Alaska Fairbanks, Juneau, AK 99801
[2]NOAA, NMFS, Auke Bay Laboratory, Juneau, AK 99801

## Abstract

The southeastern Bering Sea is a productive area that supports an abundance of economically valuable and ecologically important vertebrate and invertebrate taxa. As part of a survey directed at investigating assessment methods for forage taxa in the southeastern Bering Sea, here we describe the distribution, density, and energy content of zooplankton and micronekton taxa north of Akutan and Akun Island in June 2005. CTD casts and depth-stratified zooplankton sampling were conducted on stations ranging from nearshore areas (< 100 m) to the continental shelf break.

The dominant zooplankton taxa were copepods, followed by euphausiids (*Euphausia pacifica*, *Thyssanoessa inermis*, *T. longipes*, *T. spinifera*, *Tessarabrachion oculatum*), pteropods (*Clione limacina*, *Limacina helicina*), larvaceans (*Oikopleura* sp.), hyperiid amphipods (primarily *Parthemisto pacifica*), and chaetognaths (*Sagitta* sp.). The major copepod taxa were a mixture of oceanic (*Neocalanus* spp., *Eucalanus bungii*, *Metridia pacfica*) and neritic (*Pseudocalanus* spp., *Calanus marshallae*, and *Acartia longiremis*) species. Zooplankton density in the upper 100 m of the water column was significantly higher in the nearshore waters. This difference in density was largely caused by significantly higher densities of copepods, namely *A. longiremis*, *C. marshallae*, and *Pseudocalanus* spp. in the nearshore waters. The oceanic copepod *M. pacifica* appeared to be more abundant in the slope waters. On a relative mass basis (kJ $g^{-1}$ dry mass), the 2 species of pteropods had the most disparate energy contents amongst all the species analyzed, *C. limacina* having the greatest energy content and *L. helicina* having the least. Copepods were relatively high in energy content, followed by chaetognaths, euphausiids and hyperiid amphipods. Though copepods, and secondarily euphausiids, were the most abundant taxa, euphausiids provided the most energy available to predators due to their large size. In addition, chaetognaths were a large energy source, despite low densities.

Our results indicate that the nearshore habitat was more productive than offshore waters as was evidenced by relatively greater zooplankton abundance and total energy content.

## Introduction

The southeastern Bering Sea is a productive area that supports an abundance of economically valuable and ecologically important vertebrate and invertebrate taxa (NRC 1996). In recent years, climate shifts and resultant changes in the meteorological forcing have been implicated in the transformation of the Bering Sea ecosystem (Napp & Hunt 2001, Coyle & Pinchuk 2002, Hunt et al. 2002, Napp et al. 2002). Responses of the Bering Sea and the North Pacific ecosystem to these climatic variations are apparent in changes in species abundance and composition, e.g., declines in the abundance of seabirds, Steller sea lions (*Eumetopias jubatus*) and forage species (Merrick et al. 1997, Anderson & Piatt 1999). It is the latter group of taxa in particular that is currently still difficult to estimate in their abundance due to their generally ephemeral and patchily concentrated distribution. However, it is also these taxa that are of primary importance to the Bering Sea ecosystem, because they effectively link primary and secondary consumers to higher trophic level fishes, seabirds and marine mammal species. Lack of data on forage species abundance, distribution, and life history patterns currently limits our understanding of the role of forage species in the Bering Sea ecosystem. However, it this information that is of exceptional importance to improve our understanding of those processes involved in changing the composition of the Bering Sea ecosystem and to advance predictions about the future of top predators such as sea birds, marine mammals and piscivorous fishes.

Changes in the Bering Sea climate will directly affect all marine taxa through variations in sea temperature. However, climatologic changes can also indirectly impact higher trophic levels through trophic pathways (e.g., Hunt et al. 2002). Thus, not only differences in zooplankton abundance and distribution may be responsible for growth and survival of planktivorous forage species, but also variations in energy density of the given planktonic prey taxa may result in increased or decreased condition as well as survival probability of the consumer (Foy and Norcross 1999).

The zooplankton and micronekton communities consist of very diverse taxa that are likely to react vastly differently to climatic changes. A community-specific reaction to climate forcing has been shown in the western North Pacific (Chiba et al. 2006), where responses of taxa varied based on their seasonal patterns of peak abundance; e.g., spring-summer copepod communities, which were dominated by cold water species, showed a shift in their seasonal peak abundance by one month as a result of an anomalous predominance of fresh, cold surface water

during winter-spring in the 1970 (Chiba et al. 2006). Similar taxa-specific responses have been observed in the Bering Sea (e.g., Brodeur et al. 1999, Napp & Hunt 2001, Napp et al. 2001, Stockwell et al. 2001, Coyle & Pinchuk 2002, Napp et al. 2002). The Oscillating Control Hypothesis (OCH) proposes a mechanism for the pelagic ecosystem of the southeastern Bering Sea to be impacted by either bottom-up or top-down processes depending on climatic patterns (Hunt et al. 2002). During the current warm regime of the Bering Sea, top-down control of piscivorous fishes will not only limit the abundance of forage fishes, but at the same time, by removing the predation pressure on zooplankton, increase the abundance of other planktivores, e.g., jellyfish and chaetognaths. The complexity of these species-specific responses of the pelagic ecosystem to climatic changes makes it apparent that a better knowledge of the southeastern Bering Sea zooplankton and micronekton communities is essential in order to understand and predict changes in this ecosystem.

In addition to measures of zooplankton abundance and distribution, the ability to predict climate change effects on forage fish populations and consequently higher trophic levels is significantly enhanced with the incorporation of quantitative energy pathways. Abundance estimates of multiple trophic levels alone fail to account for discrepancies in energy content amongst prey species. Incorporation of species variation in energy content can reveal significantly different sources of dietary energy than would otherwise be indicated by measures of biomass consumed alone (Vollenweider et al. 2006). Thus, the combination of zooplankton energy content and abundance elucidate energy availability which may influence the structure of energy pathways beyond what is expected from abundance data alone.

Energy availability of from prey influences organism fitness and consequently exerts control on population and food web structure. Juvenile forage fish in particular, are highly susceptible to energy limitation, particularly at high latitudes such as the North Pacific Ocean (Foy and Norcross 1999). Juveniles must balance energy allocation between the demands of 1) growth for predation avoidance, and 2) energy storage to forestall starvation during periods of limited resource. If minimum threshold levels of storage energy are not attained during spring and summer plankton blooms, juveniles suffer predation or starvation mortalities resulting in poor year-class strength (Paul and Paul 1998). Similarly, energy limitations for mature fish can structure forage fish populations by limiting the amount of energy available for gonad provisioning and other reproductive costs (Robards 1999). Despite the importance of

zooplankton energy values which are essentially the foundation of bottom-up structure, little data exists for the North Pacific Ocean (Musayeva and Sokolova 1979).

As part of a study examining different methods for assessment of Bering Sea forage species abundance, we analyzed distribution and abundance of zooplankton and micronekton prey taxa and their energy density. To our knowledge, this is the first study to compare distributional and energetic patterns of selected zooplankton and micronekton taxa from the southeastern Bering Sea. Specifically, our objectives were:

1. Examine zooplankton and micronekton species composition and abundance in the nearshore and offshore waters off Akutan and Akun Island in the southeastern Bering Sea.
2. Analyze and compare energy density major zooplankton and micronekton taxa.
3. Estimate the total energy density of zooplankton and micronekton biomass in our study area.

## Methods

### *Study area*

This study was conducted in the southeastern Bering Sea, north of the Aleutian Islands. The Aleutians, a chain of volcanic islands, form a boundary between the North Pacific Ocean and the Bering Sea. This boundary, however, is interspersed with passes that allow some water transport between the North Pacific Ocean and the Bering Sea (Stabeno et al. 2002). This water exchange is considered to be primarily a one-way influence from the North Pacific to the Bering Sea in the eastern part of the chain, where there are three passes, namely Umnak, Akutan and Unimak Pass, with the latter representing the most important conduit (Ladd et al. 2005).

Sampling for this study focused on the eastern part of the island chain, namely the area north of Akutan and Akun Islands (Figure 1). These islands are bordered in the east by Unimak Pass and in the west by Akutan Pass. These eastern passes of the Aleutian Island chain are generally narrow and shallow (Hunt & Stabeno 2005). On the Bering Sea side of the Aleutian Island chain, the shelf is also narrow, i.e., < 10 km (Hunt & Stabeno 2005). Sampling stations were located north of Akutan Pass, Akutan and Akun Island. Our stations covered the nearshore area in water < 100 m depths and extended into offshore areas (>100 m depth) along the shelf and the continental slope.

***Field sampling***

Sampling was conducted from June 10-20, 2005 off the fishing vessel (F/V) *Great Pacific*. A total of 20 stations were sampled, 5 of them located in nearshore water close to Akutan Island (< 100 m) and 15 above the continental slope in water depths > 100 m (Table 1, Figure 1).

At each station, hydrographic data and zooplankton were collected. Hydrographic data were recorded with a SeaBird SBE-19 Seacat CTD (conductivity, temperature, density) profiler, equipped with a Wetstar fluorometer and a D&A Instruments transmissometer. Zooplankton and ichthyoplankton were sampled with a 0.25 $m^2$ multiple opening/closing MultiNet®, MN (HydroBios) equipped with five 335 µm mesh net bags. Two flow meters, one located inside the net opening and one located outside, were used to monitor the volume of water filtered. The MN was fished in a double oblique manner; plankton was collected over five depth ranges on the up-cast. Upon retrieval, the five nets were carefully rinsed down, cod-ends were detached and samples concentrated in sieves of the appropriate mesh size. Subsamples of major zooplankton taxa were collected and immediately frozen at -20° C for further analyses of energy density. The remainders of the concentrated samples were fixed in 5% formalin seawater solution and returned to the lab for further processing.

***Zooplankton abundance estimation***

In the lab, zooplankton samples for species identification and abundance estimates were rinsed with tap water to remove all traces of formaldehyde. Displacement volume (DV) of the total plankton sample was estimated to the nearest 1.0 ml prior to sorting. Estimates of DV were divided by the volume of water filtered to obtain an estimate of biomass standing stock (ml $m^{-3}$) per sample (Park et al. 2004).

Whole samples were scanned for large organisms, such as jelly fish and cephalopods, which were removed, identified to the lowest feasible taxonomic level and counted. The remaining samples were split with a Folsom plankton splitter until a sample size of approximately 100 specimens of the most abundant taxonomic group was achieved. In this split, all individuals of the abundant taxonomic groups were identified to the lowest level and developmental stage feasible and counted. The larger sub-samples were scanned for the less abundant taxa, which were identified and counted.

*Analysis of energy content*

Zooplankton energy content was analyzed using a Parr 1425 semi-micro bomb calorimeter. Prior to sample analysis, energy equivalent (EE) values were generated from 10 benzoic acid pellets with certified energy content on each of the 2 bomb units. The coefficients of variation of the EE values on the 2 bomb units were 0.50 and 0.60%. The mean EE value for each bomb unit was then applied to the same 10 samples to estimate accuracy of the bomb units as well as variability of benzoic acid standards. Energy content measurements of the benzoic acid standards were within 0.47 and 0.43% of the certified energy content for the 2 bomb units, meeting the minimum criteria of not exceeding 0.5%. Literature values of zooplankton energy content were used to calculate minimum sample masses for analysis, such that analyzed energy content would exceed the variability observed in benzoic acid samples by a minimum of 6 standard deviations.

Frozen zooplankton samples were thawed and organisms were identified and separated. Individuals of major zooplankton taxa were combined across stations and depths into composite samples to provide sample masses large enough for analysis. *Neocalanus flemingeri* and *N. plumchrus* were combined due to difficulties with identification from preservation. Composite samples were dried @ 82$^{o}$C for 22 hours and homogenized using mortar and pestle. Dried zooplankton homogenates were sandwiched in layers of benzoic acid to form small pellets (0.0331-0.0751 g) for calorimetry in order to meet minimum energy required by the instrument. Energy content attributed to zooplankton was calculated by subtracting the energy attributed to benzoic acid from the total energy content of the pellet. Quality control samples run with each batch of samples include 2 benzoic acid pellets and one *Thysanoessa spinifera* sample to provide precision and accuracy estimates. Zooplankton energy contents are reported as kJ $g^{-1}$ dry mass for comparison amongst species.

***Statistics***

Using flowmeter values, the abundance of zooplankton was computed as number per 1.0 $m^3$. Since MN casts were conducted to different maximum depths and varying depth intervals were sampled, number of organisms per 1.0 $m^2$ was calculated by multiplying number per 1.0 $m^3$ with the depth ranged sampled with each net. The total number per $m^2$ was computed by summing the values from each depth stratum.

Energy content (kJ $g^{-1}$) of major zooplankton taxa was compared using 1-way analysis of variance (ANOVA). Two-sample t-tests were used to compare energy content within species by 1) offshore versus nearshore habitat types, and 2) night versus day periods.

The total energy density (kJ $g^{-1}$) of zooplankton biomass in our study area was calculated by multiplying zooplankton density estimates (# $m^{-3}$) by estimates of energy content of individual zooplankton specimens. The major zooplankton taxa subsampled shipboard did not align exactly with those taxa that were enumerated for zooplankton density estimates. Thus, energy content of the 3 taxa of euphausiids was averaged. In addition, all the species of copepods identified during enumeration for density estimates were not subsampled for caloric analysis. Thus, the *Neocalanus flemengeri/plumchrus* group analyzed for energy content was combined with the copepoda density estimates. *Neocalanus* spp. was used as a surrogate species as it was the most abundant copepod by number. Lastly, literature values were used for the energy content of mollusks (Foy and Norcross 1999) and larvaceans (Musayeva and Sokolova 1979).

Hydrographic profiles were plotted for each MN-sampling station. Sea surface temperature (SST) and sea surface salinity (SSS) were determined at 5.0 m water depth for every station; the depth of the pycnocline was calculated as the point of maximum rate of change and mean temperature and salinity above and below the pycnocline were calculated. Before statistical analyses, zooplankton data were log-transformed, $ln(X+1)$, to follow the assumptions of ANOVA. Parametric tests were performed on log-transformed abundance data using Systat 10.2 to examine differences of zooplankton taxa by location and time of day.

## Results

### *Hydrography*

As part of this study, a total of 17 CTD casts were successfully conducted (Table 1). SST and SSS varied only little between sampling stations. SST ranged from 6.00 °C to 6.76 °C and SSS ranged from 32.25 to 32.49 (Figure 2). SST was lowest northwest of Akutan Island, apparently trailing the Akutan Pass and northeast of Akutan Island (Figure 2). Highest SST was observed north of Akutan and Akun Island. SSS varied little throughout our study area. Lowest salinity was observed inside the "horseshoe" area between Akutan and Akun Island. Recorded fluorometry data were not calibrated within the framework of this study. However, fluorometry was significantly higher in the nearshore waters than in the offshore waters ($F=6.227$, $p<0.05$),

indicating highest levels of primary productivity in the waters of the "horseshoe" area (Figure 3). There was an indication, albeit not statistically significant, that mixed layer depth in the nearshore water was also shallower than offshore.

***Species composition and distribution***

The zooplankton was dominated by copepods (Table 2). Other major taxa ordered with decreasing numerical importance were euphausiids (*Euphausia pacifica*, *Thyssanoessa inermis*, *T. longipes*, *T. spinifera*, *Tessarabrachion oculatum*), pteropods (*Clione limacine*, *Limacina helicina*), larvaceans (*Oikopleura* sp.), decapod larval stages, hyperiid amphipods (*Parthemisto pacifica*, *Hyperoche medusarum*, *Primno macropa*), and chaetognaths (primarily *Sagitta* sp.) (Table 2, Appendix 1). All other taxa occurred sporadically only or at an average densities of <2 $m^{-3}$ and were lumped as "Other" (Appendix 1). The major copepod taxa were a mixture of oceanic and neritic, primarily calanoid species. The oceanic species were represented primarily by *Neocalanus* spp. (a mixture of *N. plumchrus* and *N. flemengeri*), *Eucalanus bungii*, and *Metridia pacfica*, while the major shelf species were *Pseudocalanus* spp., *Calanus marshallae*, and *Acartia longiremis*.

Total mean zooplankton density ($m^{-3}$) in the upper 100 m water column varied with location (Table 2), with significantly higher counts of planktonic organisms in the nearshore waters ($F=8.53$, $p=0.011$). This difference in density was largely caused by significantly higher densities of copepods and decapod larvae in the nearshore waters (Figure 4). No significant differences in mean density were detected for other major taxa, namely euphausiids, hyperiid amphipods, larvaceans and pteropods.

Copepod density varied with location and was significantly higher in the nearshore than in the offshore upper 100 m of the water column ($F=15.197$, $p<0.001$) (Figure 5). The difference in copepod density between areas was driven primarily by significantly larger densities of *A. longiremis* ($F=6.903$, $p< 0.05$), *C. marshallae* ($F=12.747$, $p<0.01$), and *Pseudocalanus* spp. ($F=24.261$, $p<0.001$) in the nearshore areas (Table 3). Densities of *M. pacifica* were higher in the offshore waters, however, the difference was not statistically significant. Particularly stations 10 and 14 had very high densities of *M. pacifica*. No significant differences were observed in the species-specific abundance of copepods by time of the day (Figure 6). However, since only the mean abundance in the upper 100 m water depth was considered, these results could change if analyses were extended to samples from deeper depth strata.

Euphausiid adults were identified to species, while immature stages were summarized as juveniles. Our samples from the upper 100 m of the water column were dominated by juvenile euphausiid stages ($F=43.0104$, $p<0.001$). There was no difference in density of juvenile stages of euphausiids with either location (offshore/nearshore) or time of the day (day/night). Considering only the mean density in the upper 100 m of the water column, adult euphausiids were significantly more abundant at night than during daytime ($F=6.95$, $p<0.05$). Large catches of adult euphausiids were limited to offshore waters, however, no significant difference was identified (Figure 7a). Vertical distribution of adult euphausiid at nighttime revealed peak densities of *T. inermis* and *T. spinifera* in the 50-0 m depth interval (Figure 7b) while other euphausiid species were restricted to depths below 200 m (Figure 7c).

Only zoea and megalopa stages of decapods were collected (Appendix 1). Abundance of larval decapods was significantly higher in the nearshore waters ($F=21.129$, $p<0.0001$). Larval decapods densities predominated on the eastern side of the horseshoe area, namely station 22, 12, and 20, between Akutan and Akun Island (Figure 3).

***Energy content and density***

Zooplankton energy content varied significantly amongst species (Figure 8), with some similarities between the hyperiid amphipod species (*P. pacifica*) and several euphausiid species. Though not statistically similar ($p=0.042$), the 2 copepod species (*Neocalanus flemengeri/plumchrus* and *Neocalanus cristatus*) were relatively similar in comparison to all zooplankton species. In contrast, the two pteropod species, *C. limacina* and *L. helicina*, had the most disparate energy densities of all taxa analyzed, *C. limacina* having more than twice the energy density of *L. helicina*.

Sample size limitations only accommodated 2 species for comparisons of differences in energy content between day and night sampling, *Thysanoessa inermis and Thysanoessa spinifera*. *T. spinifera* had significantly greater energy content when sampled during the night compared to the day (20.15 versus 19.54 kJ $g^{-1}$, $p = 0.020$) (Figure 9). In contrast, *T. inermis* sampled during the day had relatively elevated energy content though the difference was not significant (23.20 versus 21.74 kJ $g^{-1}$, $p = 0.079$).

Energy density of zooplankton taxa in the water column revealed a different relative importance of taxa than did zooplankton species densities (Figure 10). Copepods occurred most densely in both offshore and nearshore habitats. Though copepods were also the most energy-

rich taxa evaluated for energy density estimates, euphausiids comprised more energy available to predators due to their greater size. Similar disparities between the two analyses were also observed for chaetognaths, which are relatively energy-rich and relatively large, though they occurred with less frequency than did hyperiids, mollusks and larvaceans. Energy density estimates of chaetognaths indicate that they are more valuable as a prey item than would zooplankton density estimates alone.

Zooplankton-derived energy density in the water column was relatively elevated in nearshore habitats (19.34 kJ $m^{-3}$) compared to offshore habitats (13.45 kJ $m^{-3}$) though not significantly so (ANOVA general linear model; p=0.067). Due to elevated abundance of each species in nearshore habitats, energy content of each taxa were also elevated in nearshore habitats, Copepoda being the only taxa significantly so (2-sample t-test; p=0.016) (Figure 10).

## Conclusions

- The "horseshoe area" between Akutan Island and Akun Island in the southeastern Bering Sea was characterized by decreased surface salinity, reduced mixed layer depth and increased fluorescence, indicating an area of higher primary productivity.
- Zooplankton and micronekton of the southeastern Bering Sea in June 2005 was dominated by copepods, followed by euphausiids, pteropods, larvaceans, hyperiid amphipods and chaetognaths. Other taxa occurred sporadically only or in average densities < 2 $m^{-3}$.
- Densities of zooplankton were significantly higher in the nearshore waters of the "horseshoe area", driven primarily by higher densities of neritic copepod species (*A. longiremis*, *C. marshallae*, and *Pseudocalanus* spp.) and decapod larvae.
- Juvenile euphausiids were more abundant than adult stages. Regarding adults only, densities were higher at night and highest catches were recorded for offshore waters. Vertical distribution of adult euphausiid at night revealed a species-specific depth separation with *T. inermis* and *T. spinifera* occurring at shallower depths than *E. pacifica*, *T. longipes*, and *T. oculatum*.
- Energy content of zooplankton species differed significantly on a relative mass basis (kJ $g^{-1}$ dry mass). The 2 species of pteropods had the most disparate energy contents, with *Clione limacine* being the most energy dense and *Limacina helicana* being the least. Copepods were relatively energy dense, followed by chaetognaths, euphausiids and hyperiid amphipods.

- The relative importance of zooplankton taxa indicated from abundance estimates differed from energy density (kJ $m^{-3}$) estimates. Though copepods and secondarily euphausiids were the most abundant taxa, euphausiids provided more energy in the water column due to their relatively large size. Additionally, chaetognaths were a relatively large energy source, despite low numerical densities.
- Total zooplankton-derived energy density in the water column was relatively elevated in nearshore habitats compared to offshore habitats due to greater overall biomass in nearshore areas. However, Copepoda was the only taxon which had significantly different energy density between the two habitats.

## Acknowledgements

We would like to thank captain and crew of the F/V "Great Pacific" for their invaluable support at sea. We are also grateful to W. Park for the processing and identification of zooplankton samples and to W. Strassburger for pre-processing samples. We also thank R. Heintz for consultation. Funding for this research was supported with a grant from the North Pacific Research Board, project # F0401.

## Literature Cited

Anderson, P. J., and Piatt, J. F. 1999. Community reorganization in the Gulf of Alaska following ocean climate regime shift. Marine Ecology Progress Series 189: 117-123.

Brodeur, R. D., Mills, C. E., Overland, J. E., Walters, G. E., Schumacher, J. D. 1999. Evidence for a substantial increase in gelatinous zooplankton in the Bering Sea, with possible links to climate change. Fisheries Oceanography 8 (4): 296-306.

Chiba, S., Tadokoro, K., Sugisaki, H. and Saino, T. 2006. Effects of decadal climate change on zooplankton over the last 50 years in the western subarctic North Pacific. Global Change Biology 12: 907-920.

Coyle, K. O. 2005. Zooplankton distribution, abundance and biomass relative to water masses in the eastern and central Aleutian Island passes. Fisheries Oceanography 14 (Suppl. 1): 77-92.

Coyle, K.O., and Pinchuk, A. I. 2002. Climate-related differences in zooplankton density and growth on the inner shelf of the southeastern Bering Sea. Progress in Oceanography 55: 177-194.

Coyle, K. O., Weingartner, T. J., and Hunt Jr., G. L. 1998. Distribution of acoustically determined biomass and major zooplankton taxa in the upper mixed layer relative to water masses in the western Aleutian Islands. Marine Ecology Progress Series 165: 95-108.

Foy, R.J., and Norcross, B.L. 1999. Spatial and temporal variability in the diet of juvenile Pacific herring (*Clupea pallasi*) in Prince William Sound, Alaska. Canadian Journal of Zoology, 77: 697-706.

Hunt Jr., G.L., and Megrey, B. A. 2005. Comparison of the biophysical and trophic characteristics of the Bering and Barents Sea. ICES Journal of Marine Science 62: 1245-1255.

Hunt Jr., G. L., and Stabeno, P. J. 2005. Oceanography and ecology of the Aleutian Archipelago: spatial and temporal variation. Fisheries Oceanography 14 (Suppl. 1): 292-306.

Hunt Jr., G. L., Stabeno P., Walters G., Sinclair, E., Brodeur, R. D., Napp, J. M., and Bond, N. A. 2002. Climate change and control of the southeastern Bering Sea pelagic ecosystem. Deep-Sea Research II 49: 5821-5853.

Ladd, C., Jahncke, J., Hunt Jr., G.L., Mordy, C. W., Salo, S. A., and Stabeno, P.J. 2005. Marine environment of the eastern and central Aleutian Islands. Fisheries Oceanography 14 (Suppl. 1): 22-38.

Merrick, R. L., Chumbley, M. K., Byrd, G. V. 1997. A potential relationship between the diet diversity of Steller sea lions (*Eumetopias jubatus*) and their population decline in Alaska. Canadian Journal of Fisheries and Aquatic Science 54: 1342-1348.

Musayeva, E.I., and Sokolova, I.A. 1979. Caloricity (caloric value) of planktonic animals from the Pacific Ocean. Oceanology 19 (1): 90-92.

NRC (National Research Council) 1996. The Bering Sea ecosystem. National Academy Press, Washington, D. C.

Napp, J. M., and Hunt Jr., G. L. 2001. Anomalous conditions in the south-eastern Bering Sea 1997: linkages among climate, weather, ocean and biology. Fisheries Oceanography 10 (1): 61-68.

Napp, J. M., Baier, C. T., Brodeur, R. D., Coyle, K. O., Shiga, N., and Mier, K. 2002. Interannual and decadal variability in zooplankton communities of the southeast Bering Sea shelf. Deep-Sea Research II 49: 5991-6008.

Paul, A.J., and Paul, J.M. 1998. Comparisons of whole-body energy content of captive fasting age-0 Alaskan Pacific herring (*Clupea pallasi* Valenciennes) and cohors over-wintering in nature. Journal of Experimental Marine Biology and Ecology 226: 75-86.

Park, W., Sturdevant, M., Orsi, J., Wertheimer, A., Fergusson, E., Heard, W., and Shirley, T. 2004. Interannual abundance patterns of copepods during an ENSO event in Icy Strait, southeastern Alaska. ICES Journal of Marine Science 61: 464-477.

Robards, M.D., Anthony, J.A., Rose, G.A., Piatt, J.F. 1999. Changes in proximate composition and somatic energy content for Pacific sand lance (*Ammodytes hexapterus*) from Kachemak Bay, Alaska relative to maturity and season. Journal of Experimental Marine Biology and Ecology 242: 245-258.

Stabeno, P. J., Reed, R. K., and Napp, J. M. 2002. Transport through Unimak Pass, Alaska. Deep-Sea Research II 49: 5919-5930.

Stockwell, D. A., Whitledge, T. E., Zeeman, S. I., Coyle, K. O., Napp, J. M., Brodeur, R. D., Pinchuk, A. I., Hunt Jr., G. L. 2001. Anomalous conditions in the south-eastern Bering Sea, 1997: nutrients, phytoplankton and zooplankton. Fisheries Oceanography 10(1): 99-116.

Vollenweider, J.J., Womble, J.N., Heintz, R.A. 2006. Estimation of seasonal energy content of Steller sea lion (*Eumetopias jubatus*) diet. In: Sea Lions of the World. Trites A.W., Atkinson, S.K., DeMaster, D.P., Fritz, L.W., Gelatt, T.S., Rea, L.D. and Wynne, K.M. (eds.) Alaska Sea Grant College Program, University of Alaska Fairbanks. p. 155-176.

**Table 1.** MN station location and characterization, and sampled depth intervals.

| Station | Date | Latitude (°N) | Longitude (°W) | Area | Time | Bottom | Net 1 | Net 2 | Net 3 | Net 4 | Net 5 |
|---|---|---|---|---|---|---|---|---|---|---|---|
| 1 | 6/10 | 54.1873 | 166.3795 | Offshore | Day | 772 | 154-102 | 102-75 | 75-50 | 50-25 | 25-0 |
| 2 | 6/10 | 54.1538 | 166.3518 | Offshore | Day | 144 | 150-100 | 100-75 | 75-50 | 50-25 | 25-0 |
| 3 | 6/11 | 54.1767 | 166.2912 | Offshore | Day | 171 | 150-100 | 100-75 | 75-50 | 50-25 | 25-0 |
| 4 | 6/11 | 54.3000 | 166.3328 | Offshore | Day | 844 | 141-100 | 100-75 | 75-50 | 50-25 | 25-0 |
| 5 | 6/12 | 54.1972 | 166.2148 | Offshore | Day | 233 | 123-100 | 100-75 | 75-50 | 50-25 | 25-0 |
| 6 | 6/12 | 54.2678 | 166.2290 | Offshore | Day | 602 | 190-150 | 150-100 | 100-50 | 50-25 | 25-0 |
| 7 | 6/13 | 54.2790 | 166.2433 | Offshore | Night | 659 | 300-250 | 250-200 | 200-150 | 150-50 | 50-0 |
| 8 | 6/13 | 54.3355 | 165.8523 | Offshore | Day | 130 | N/A | 80-60 | 60-40 | 40-20 | 20-0 |
| 9 | 6/14 | 54.2695 | 165.8952 | Nearshore | Day | 89 | N/A | 75-60 | 60-40 | 40-20 | 20-0 |
| 10 | 6/15 | 54.3340 | 165.9908 | Offshore | Night | 511 | 400-300 | 300-200 | 200-100 | 100-50 | 50-0 |
| 11 | 6/15 | 54.2675 | 165.8373 | Nearshore | Day | 78 | N/A | 64-40 | 40-20 | 20-10 | 10-0 |
| 12 | 6/16 | 54.2472 | 165.7518 | Nearshore | Night | 99 | N/A | 80-60 | 60-40 | 40-20 | 20-0 |
| 13 | 6/16 | 54.2842 | 166.0870 | Offshore | Dusk | 520 | 27-21 | 21-15 | 15-9 | 9-3 | 3-0 |
| 14 | 6/17 | 54.2940 | 166.0723 | Offshore | Night | 660 | 392-300 | 300-200 | 200-100 | 100-50 | 50-0 |
| 15 | 6/17 | 54.2862 | 166.0637 | Offshore | Day | 599 | 50-40 | 40-30 | 30-20 | 20-10 | 10-0 |
| 16 | 6/17 | 54.3645 | 165.7583 | Offshore | Day | 118 | N/A | 80-57 | 57-40 | 40-20 | 20-0 |
| 17.1 | 6/17 | 54.3590 | 165.7812 | Offshore | Day | 116 | 21-16 | N/A | 16-9 | 9-3 | 3-0 |
| 17.2 | 6/18 | 54.3570 | 165.7367 | Offshore | Day | 99 | 27-22 | 22-15 | 15-9 | 9-4 | 4-0 |
| 17.3 | 6/18 | 54.3433 | 165.7568 | Offshore | Day | 97 | 25-20 | 20-15 | 15-11 | 11-5.5 | 5.5-0 |
| 18 | 6/18 | 24.3632 | 165.7905 | Offshore | Night | 143 | N/A | 78-60 | 60-40 | 40-20 | 20-0 |
| 20 | 6/19 | 54.1790 | 165.7387 | Nearshore | Night | 75 | N/A | N/A | 60-40 | 40-20 | 20-0 |
| 22 | 6/20 | 54.2995 | 165.7227 | Nearshore | Night | 79 | N/A | N/A | 60-40 | 40-20 | 20-0 |

**Table 2**. Mean density [# $m^{-3}$] (S.E.) of dominant zooplankton and micronekton species from June 10-20, 2005, in the upper 100 m of the water column in nearshore (n=5) and offshore (n=12) waters and averaged over both habitats south of Akutan and Akun Island, southeastern Bering Sea.

| Zooplankton Taxa | Offshore | | Nearshore | | Total | |
|---|---|---|---|---|---|---|
| Chaetognatha | 2.8 | (0.42) | 3.2 | (0.41) | 2.9 | (0.32) |
| Copepoda | 290.2 | (22.79) | 418.0 | (49.40) | 327.8 | (25.37) |
| Decapoda | 2.58 | (0.50) | 15.94 | (4.55) | 6.51 | (1.99) |
| Euphausiacea | 38.0 | (7.33) | 54.8 | (12.63) | 43.0 | (6.44) |
| Hyperiidea | 2.9 | (0.67) | 5.9 | (2.29) | 3.8 | (0.85) |
| Larvacean | 8.3 | (2.16) | 7.8 | (1.53) | 8.2 | (1.56) |
| Pteropoda | 11.3 | (1.97) | 18.9 | (5.08) | 13.6 | (2.12) |
| Other | 2.3 | (0.54) | 3.4 | (1.47) | 2.6 | (0.57) |
| Total | 358.31 | (26.51) | 528.04 | (67.53) | 408.23 | (32.41) |

**Table 3**. Mean density [# $m^{-3}$] (S.E.) of dominant copepod species from June 10-20, 2005, in the upper 100 m of the water column in nearshore (n=5) and offshore (n=12) waters south of Akutan and Akun Island, southeastern Bering Sea. *Neocalanus* spp. represents a mixture of *N. plumchrus* and *N. flemengeri*.

| Copepod Taxa | Offshore | | Nearshore | |
|---|---|---|---|---|
| *Acartia longiremis* | 7.01 | (1.86) | 16.58 | (4.27) |
| *Calanus marshallae* | 26.58 | (3.77) | 77.78 | (20.18) |
| *Calanus pacificus* | 2.28 | (0.39) | 5.00 | (2.22) |
| *Candacia columbiae* | 0.02 | (0.00) | | |
| *Eucalanus bungii* | 80.66 | (12.02) | 89.82 | (13.30) |
| *Euchaeta elongata* | 0.05 | (0.02) | | |
| *Metridia pacifica* | 38.24 | (17.16) | 24.61 | (6.81) |
| *Neocalanus cristatus* | 0.46 | (0.09) | 0.78 | (0.30) |
| *Neocalanus* spp. | 109.33 | (11.96) | 106.31 | (27.69) |
| *Oithona* sp. | 0.77 | (0.11) | 0.87 | (0.07) |
| *Pseudocalanus* spp. | 31.22 | (2.94) | 102.89 | (23.47) |
| *Scaphocalanus* spp. | 1.82 | (0.19) | 1.09 | |
| Others | 0.13 | (0.11) | 0.34 | (0.17) |
| **Total** | 290.17 | (23.81) | 418.03 | (49.40) |

**Figure 1.** Location of MultiNet (MN) stations sampled in the southeastern Bering Sea. Symbols indicate location of sampling station, numbers indicate the station number, ○ = nearshore, ● = offshore.

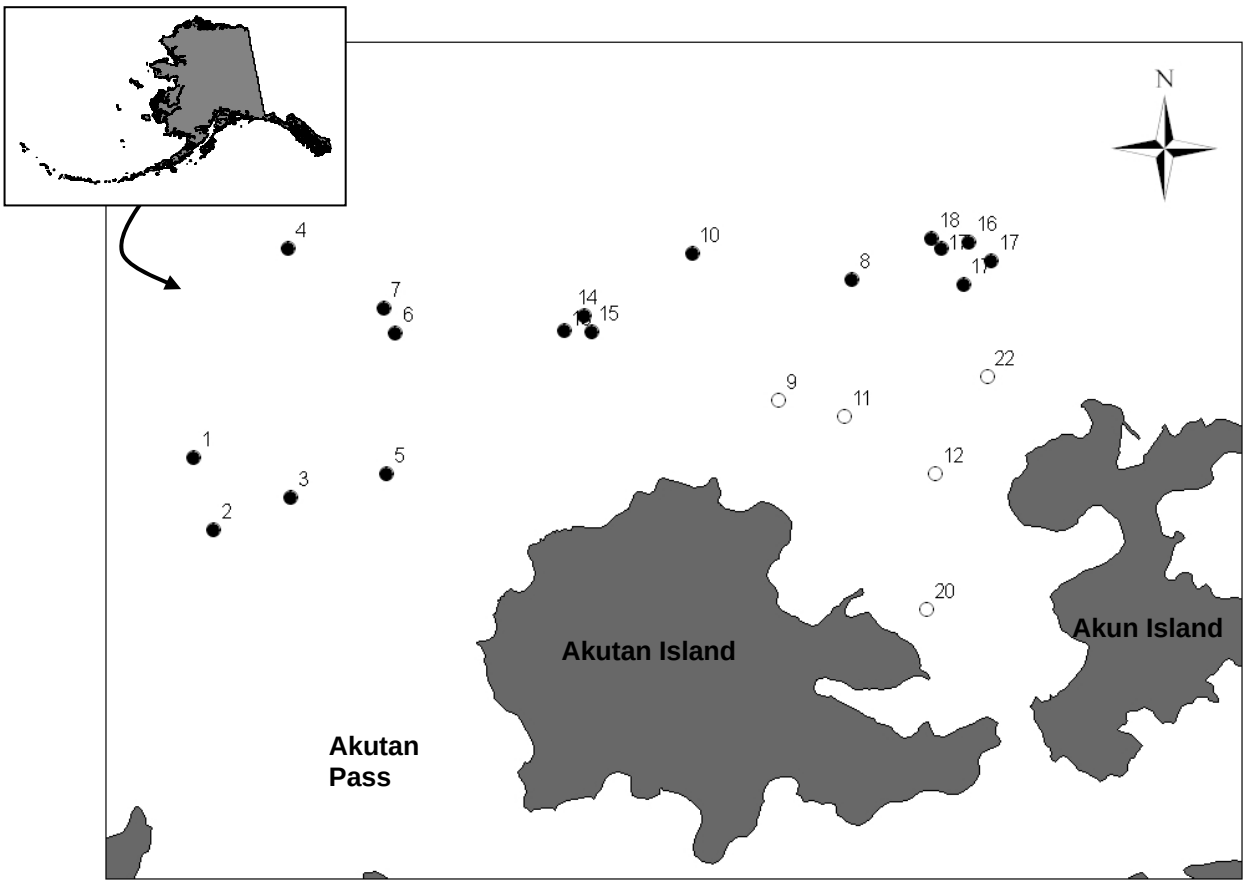

**Figure 2.** Surface plot of mean sea surface temperature (SST) and sea surface salinity (SSS) at 5 m water depth in the southeastern Bering Sea, June 10-20, 2005.

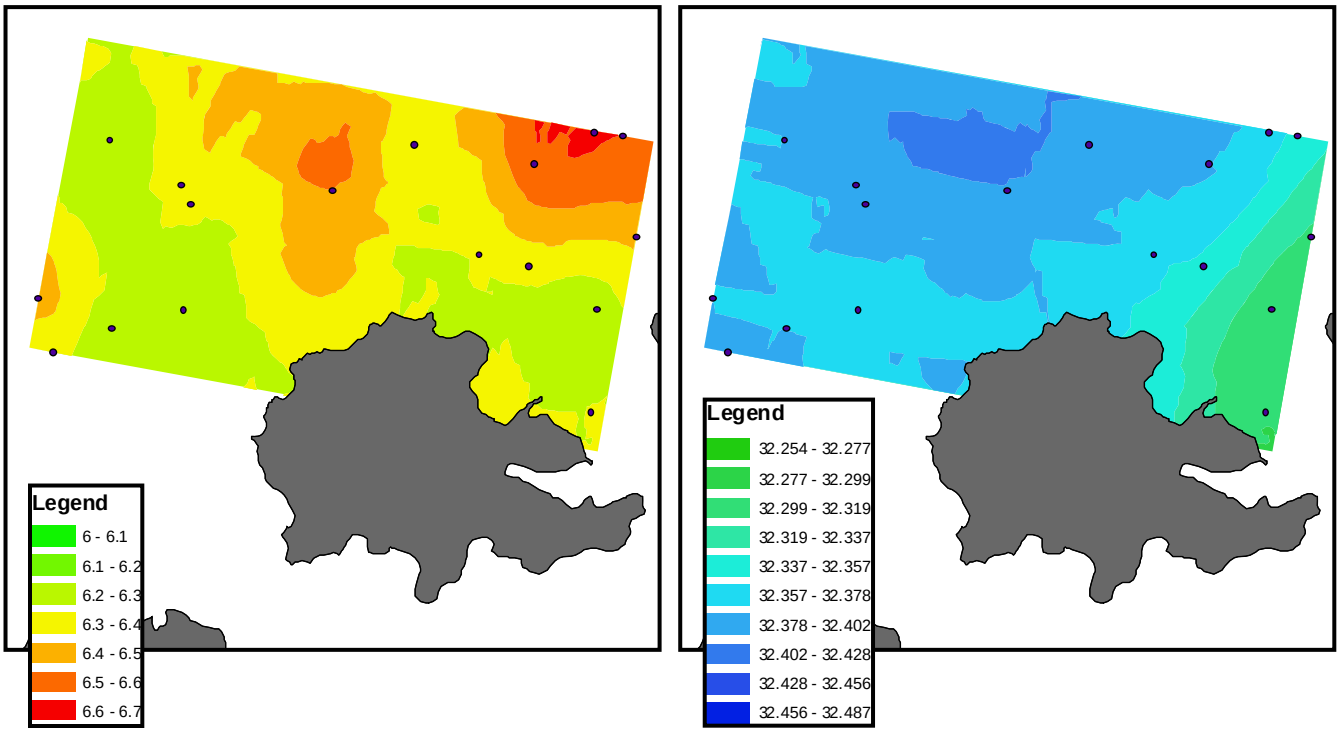

**Figure 3.** Surface fluorometry values at 5 m water depth in the southeastern Bering Sea, June 10-20, 2005.

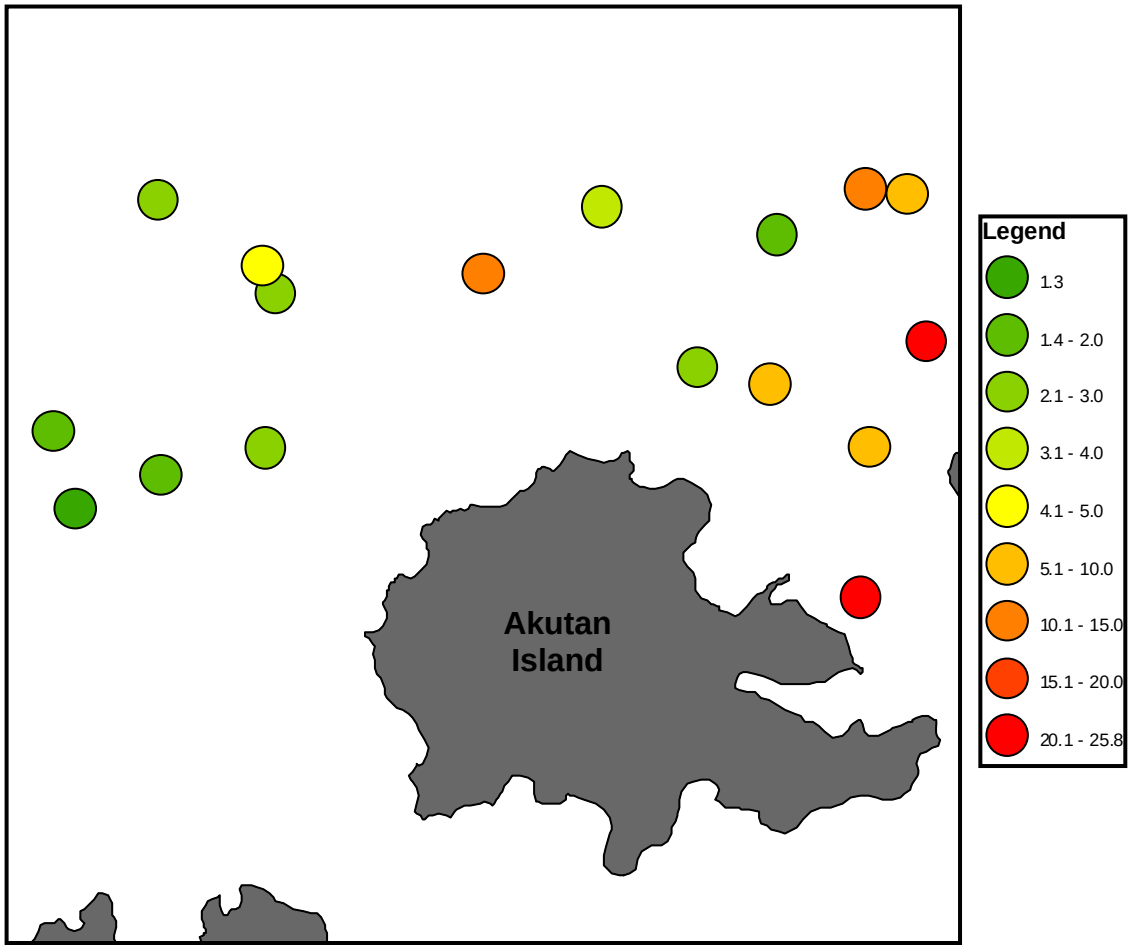

**Figure 4.** Mean density [# $m^{-3}$] of major zooplankton and micronekton taxa in 0-100 m water depth in the southeastern Bering Sea, June 10-20, 2005.

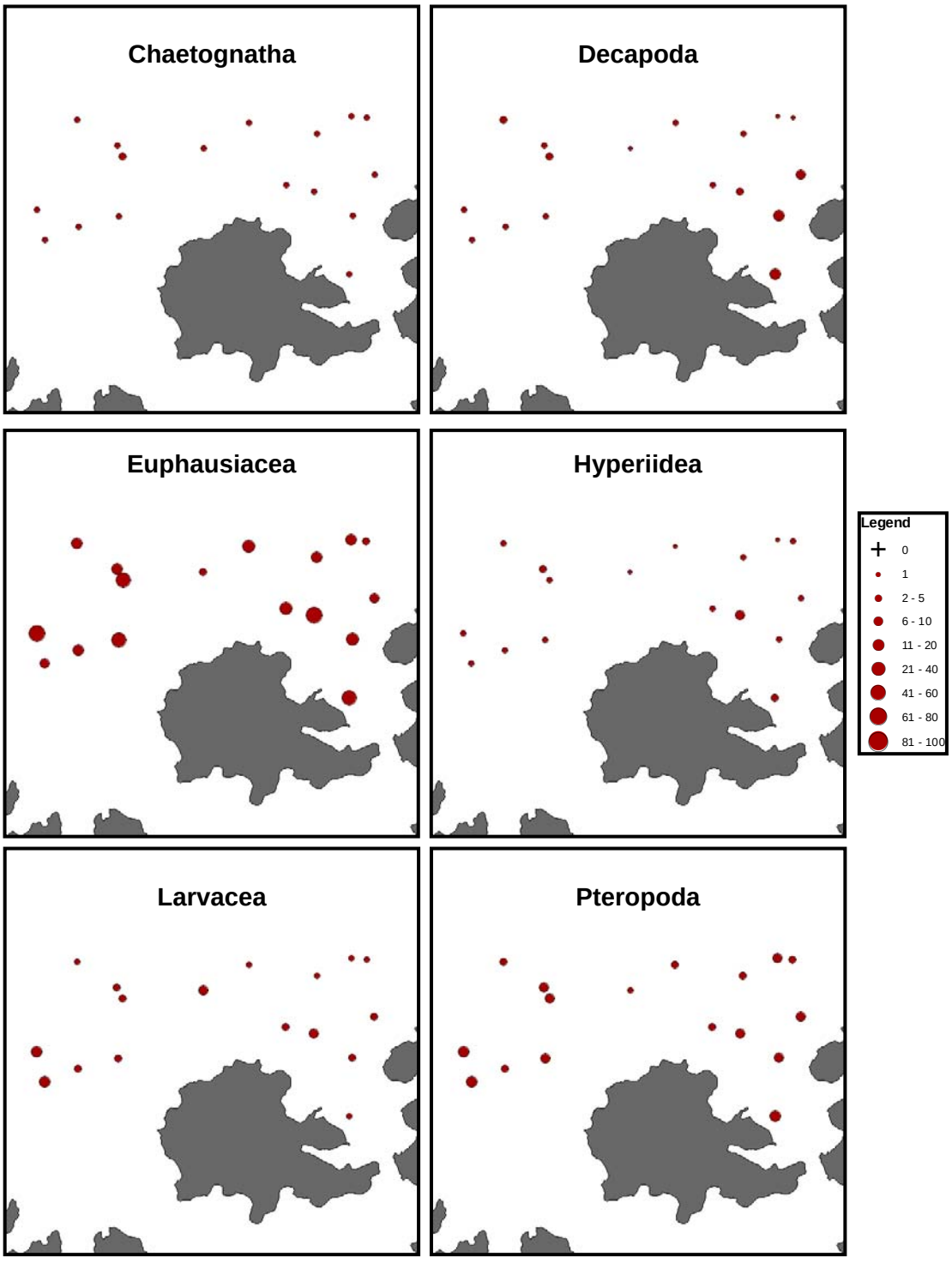

**Figure 5.** Mean density [# $m^{-3}$] of major copepod species in 0-100 m water depth in the southeastern Bering Sea, June 10-20, 2005.

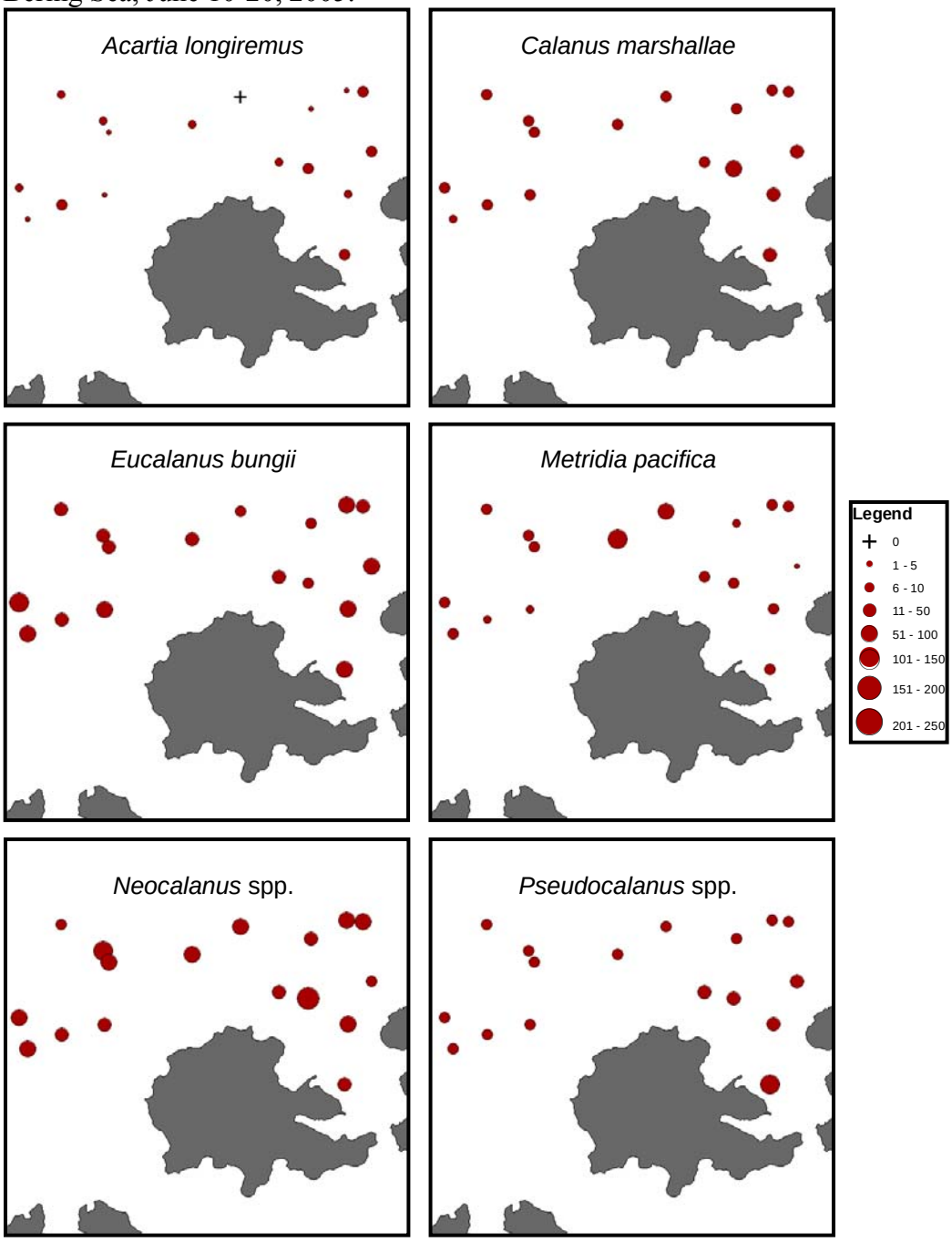

**Figure 6.** Comparison of mean density [# $m^{-3}$] of major copepod species in 0-100 m between nearshore and offshore stations and between day and night.

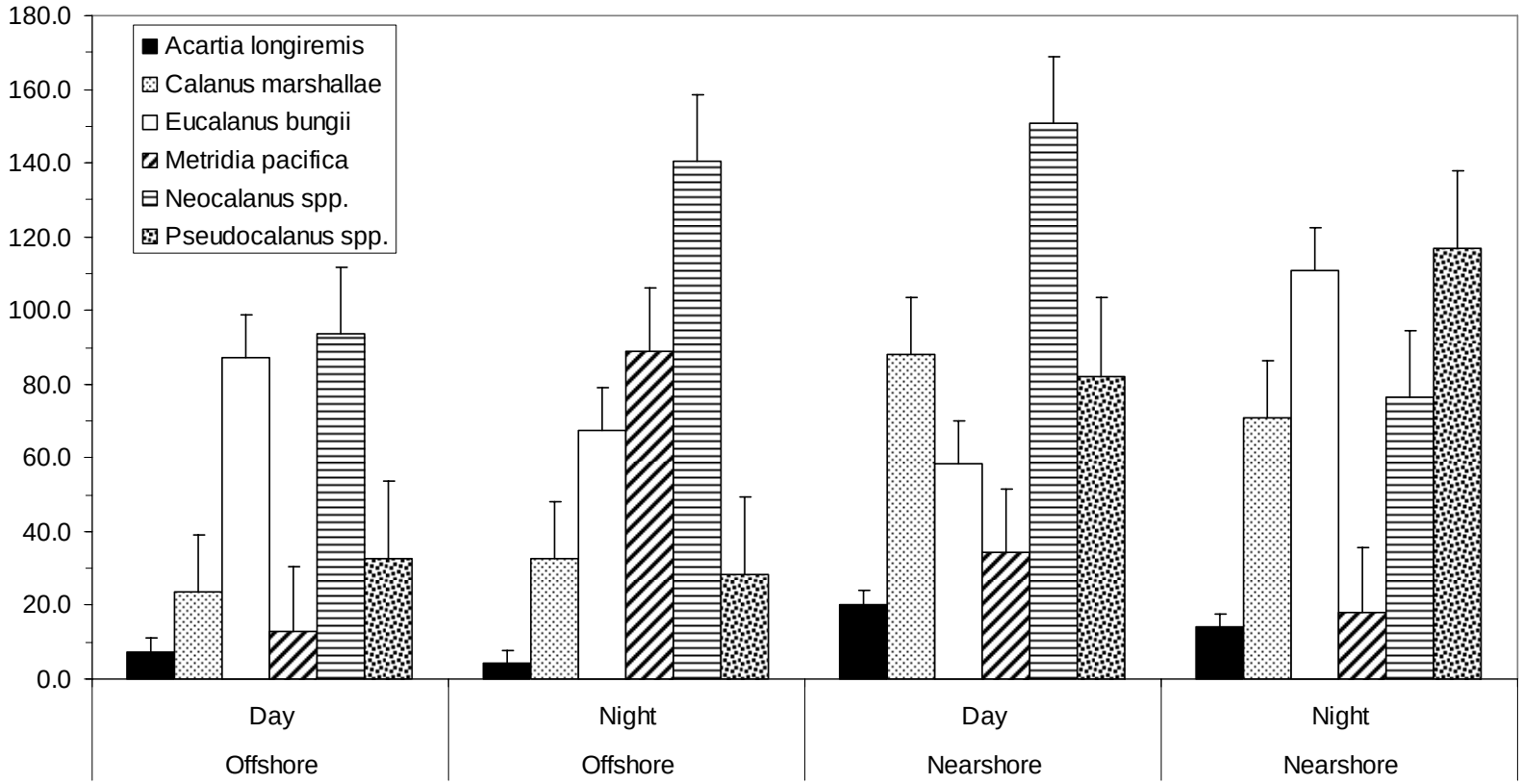

**Figure 7.** Mean density [# $m^{-3}$] of adult euphausiids (A), and depth distribution of euphausiid species on station 10 (B&C).

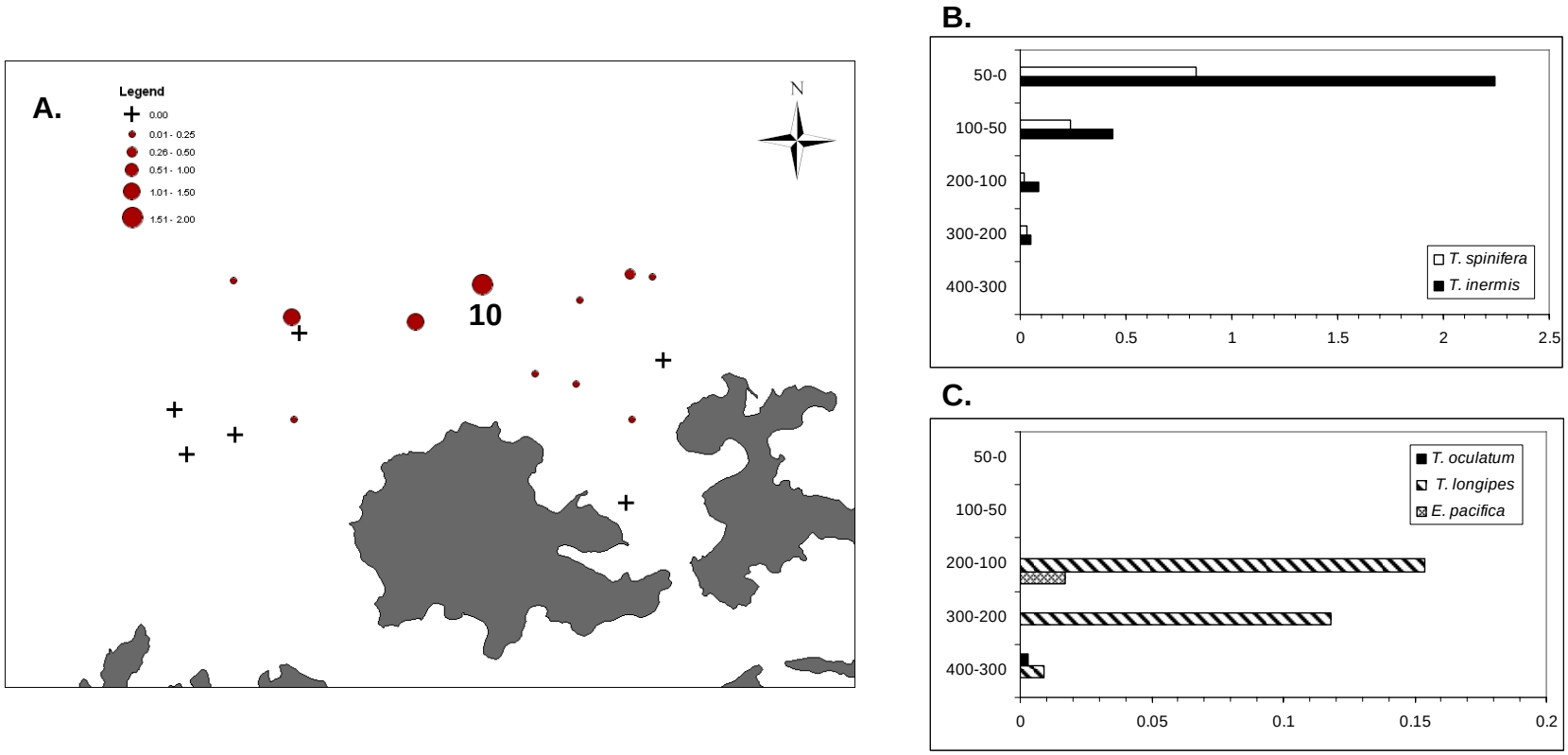

**Figure 8.** Mean energy content of major zooplankton taxa [kJ $g^{-1}$ dry mass +/- 1 S.E.] in the southeastern Bering Sea. Like letters indicate statistically similar groups. Numbers indicate the number of composite samples analyzed.

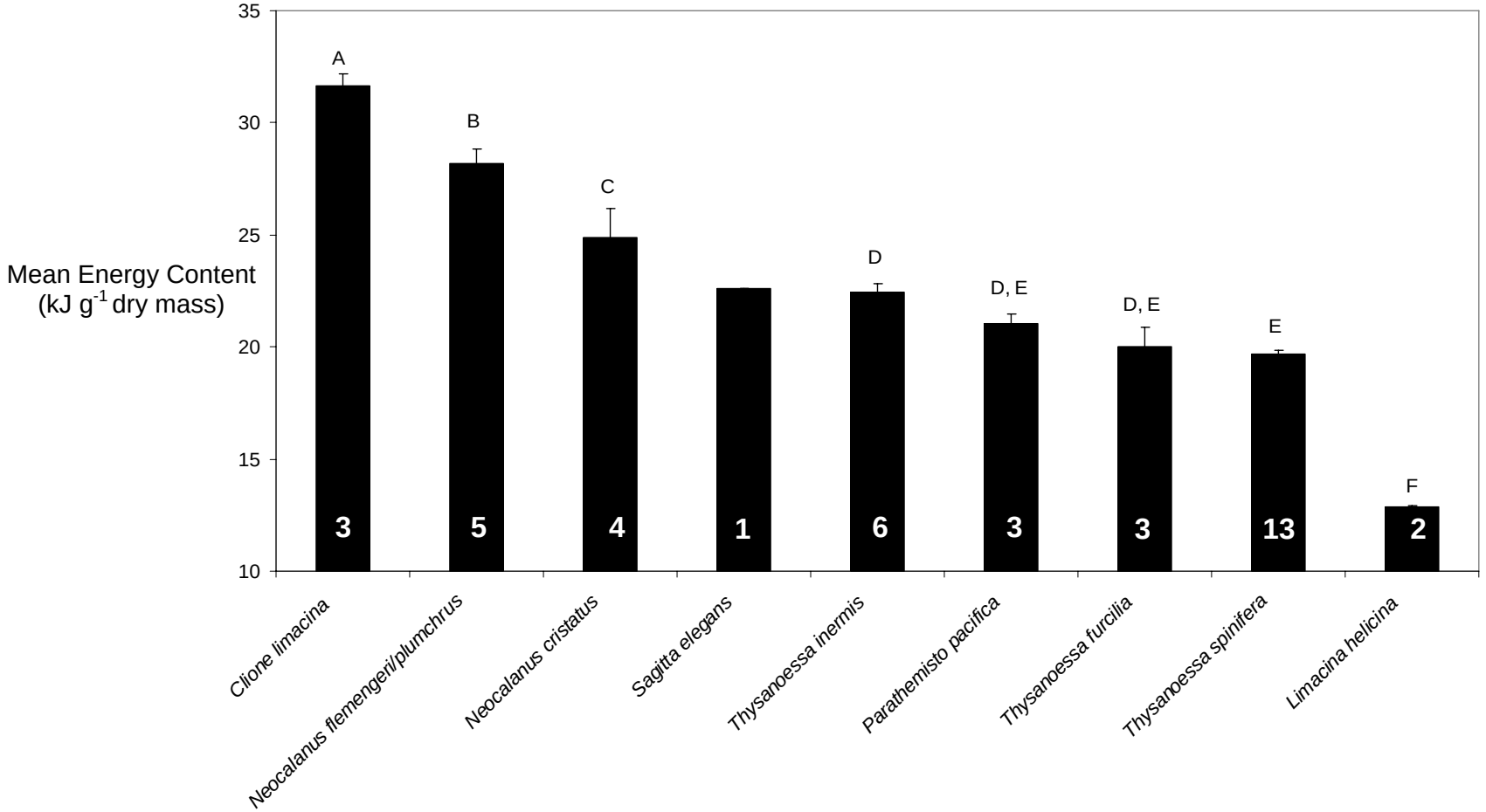

**Figure 9.** Mean energy content [kJ $g^{-1}$ dry mass +/- 1 S.E.] of *Thysanoessa inermis* and *Thysanoessa spinifera* from day and night collections in the southeastern Bering Sea.

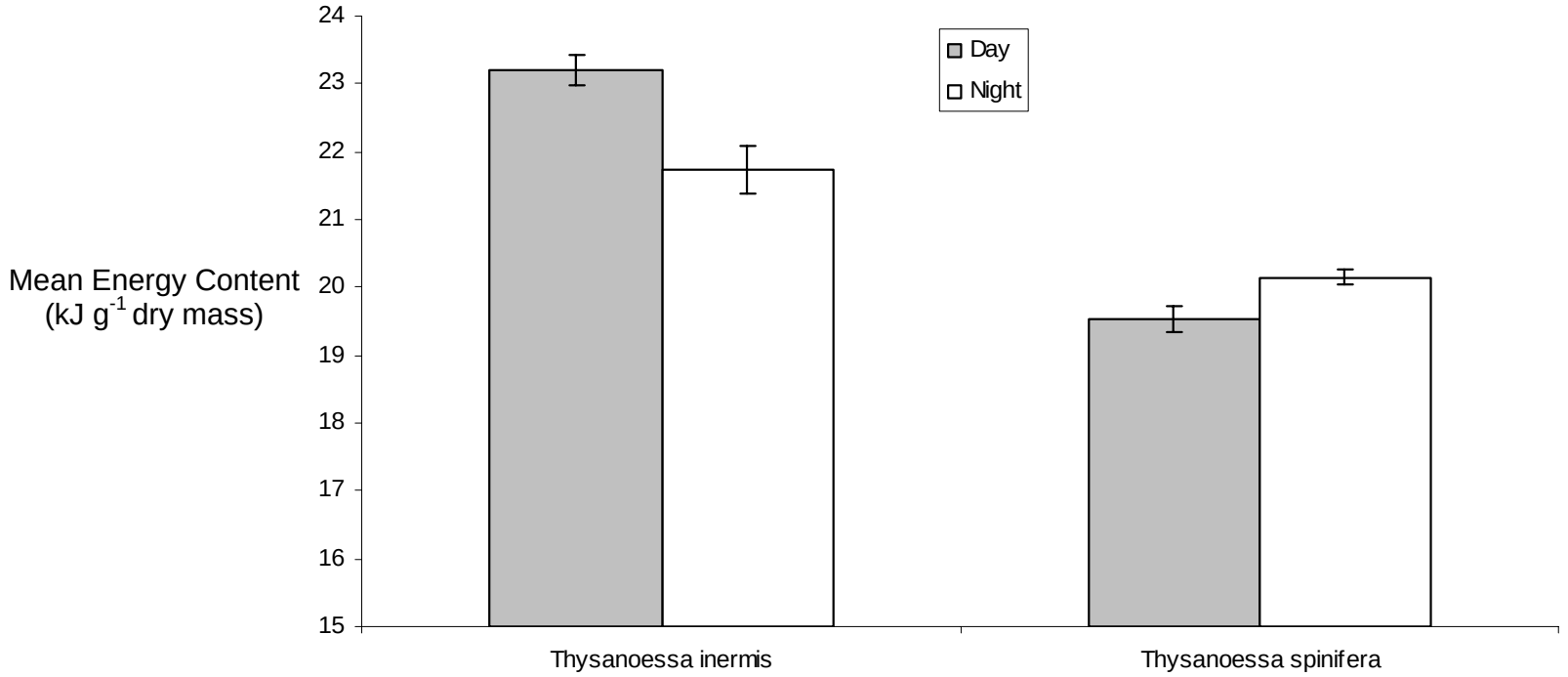

**Figure 10.** Comparison of 1) mean energy density [kJ $m^{-3}$ +/- 1 S.E.] in the water column comprised by zooplankton and 2) zooplankton density [# $m^{-3}$] in 0-100 m water depth in offshore and nearshore habitats.

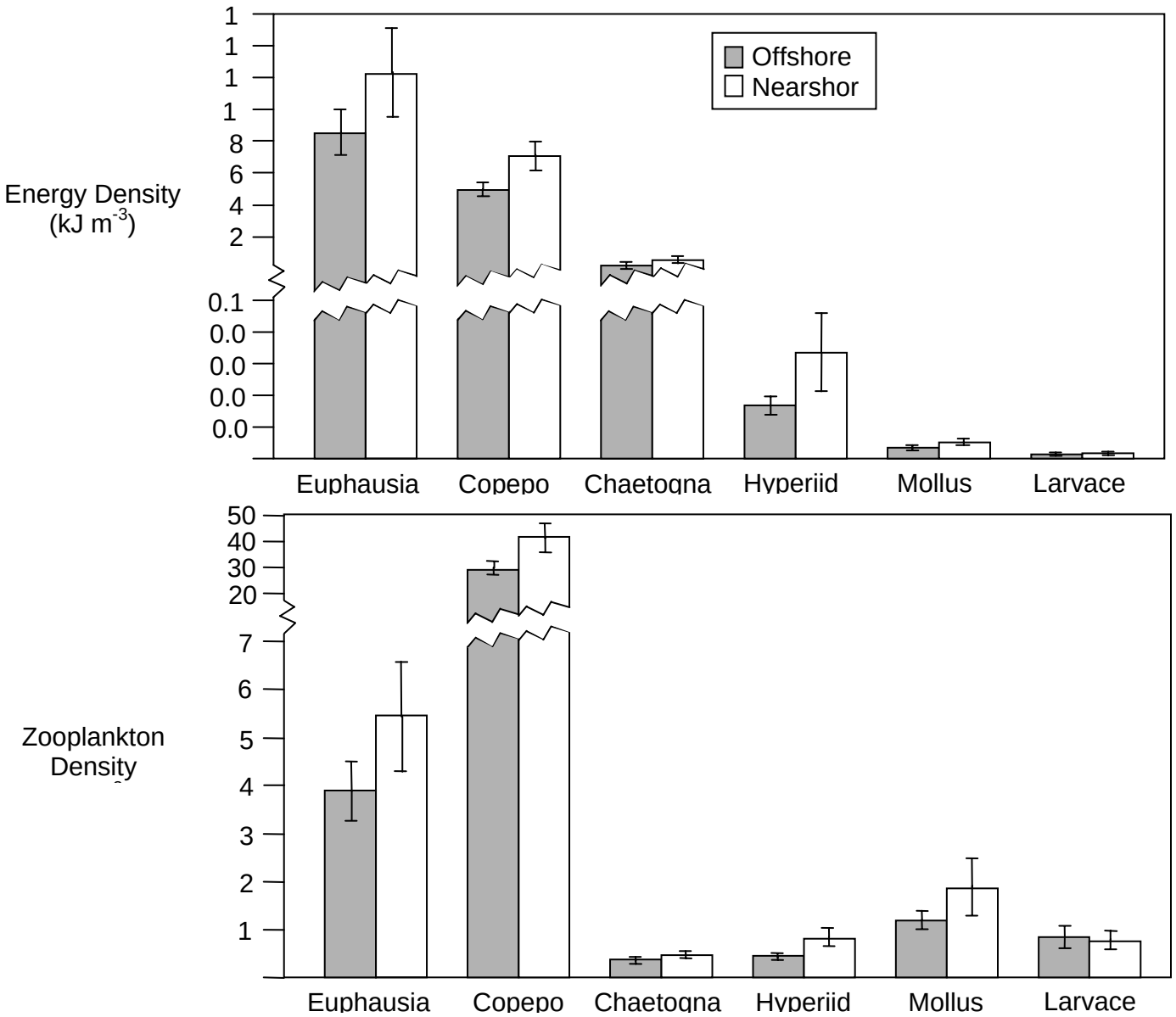

**Appendix 1.** Species composition from MN samples in the southeastern Bering Sea, June 10-20, 2005

| | | |
|---|---|---|
| **Amphipoda** | | *Cyphocaris challengeri* |
| | | *Hyperoche medusarum* |
| | | *Parathemisto pacifica* |
| | | *Primno macropa* |
| **Bryozoa** | | |
| **Cephalopoda** | | |
| **Chaetognatha** | | *Sagitta* sp. |
| **Cirripedia** | | |
| **Cnidaria** | | |
| **Copepoda** | Calanoida | *Acartia longiremis* |
| | | *Calanus marshallae* |
| | | *Calanus pacificus* |
| | | *Candacia columbiae* |
| | | *Centropages abdominalis* |
| | | *Chiridus* sp. |
| | | *Eucalanus bungii* |
| | | *Euchaeta elongata* |
| | | *Gaetanus intermedius* |
| | | *Heterorhabdus* spp. |
| | | *Metridia pacifica* |
| | | *Neocalanus cristatus* |
| | | *Neocalanus* spp. |
| | | *Pleuromamma scutullata* |
| | | *Aetidius* spp. |
| | Cyclopoida | *Oithona* sp. |
| | Harpacticoida | |
| **Ctenophora** | Hydrozoa | |
| | Siphonophora | |
| **Decapoda** | | *Rhinolithodes wosnessenskii* (rhinoceros crab) |
| | | *Paralithodes camtschaticus* (red king crab) |
| | | *Telmessus chaeiragonus* (helmet crab) |
| | | *Acantholithodes hispidus* (spiny lithoid crab) |
| | | *Erimacrus isenbeckii* (hair crab) |
| | | *Cryptolithodes* sp. |
| **Echinodermata** | | |
| **Euphausiacea** | | *Euphausia pacifica* |
| | | *Thysanoessa inermis* |
| | | *Thysanoessa longipes* |
| | | *Thysanoessa spinifera* |
| | | *Tessarabrachion oculatum* |
| **Isopoda** | | |
| **Mollusca** | Gastropoda | *Clione limacina* |
| | | *Limacina helicina* |
| **Pisces** | | |
| **Polychaeta** | | *Tomopteris* spp. |
| **Ostracoda** | | *Conchoecia* sp. |
| **Tunicata** | Larvacea | *Oikopleura* sp. |

# *Aerial remote sensing and ecological hot spots in the southeastern Bering Sea*

Evelyn D. Brown[1] and James H. Churnside[2]
[1]School of Fisheries and Ocean Science, University of Alaska Fairbanks, Fairbanks, AK 99775-7220
[2]NOAA, ETL, 325 Broadway R/E/ET2, Boulder, CO 80305

## Abstract

Ephemeral ecological hot spots comprising thousands of seabirds, marine mammals predating on immense swarms of euphausiids and schooling forage fish were tracked using aerial remote sensing and visual counting methods. These hot spots were large enough to cause a surface effect visible from space using Synthetic Aperature Radar (SAR). These foraging event hot spots may be difficult to locate and track without using measurement techniques that can cover large areas in a short amount of time. These events may be critical in the life history of apex predators, represent the exchange of enormous amounts of trophic energy, and exert strong top-down control on ecologically and economically important forage fish species such as herring or capelin. Over a ten-day period, 7900 km of continental shelf, slope, and nearshore marine habitats were surveyed by aircraft in the southeastern Bering Sea, an ecological productive area. Geolocated data collected included visual observations, quantified subsurface features with airborne lidar (light detecting and ranging), SST via an infrared radiometer, and SAR imagery overlapping the times and locations of the aerial surveys. The hot spots occurred at the shelf slope, were approximately 5 nmi in diameter, and comprised humpback whales, Dall porpoise, and thousands of sooty shearwaters, fulmar, and other pelagic seabirds. Underlying the apex community was a concentration of patchy fish schools and euphausiid swarms ranging in size of 10s to 100s of meters in diameter, averaging 10 m thick, and ranging in the upper 30 m of the water column. Using spatial correlation, fish school locations were significantly ($p < 0.001$) correlated with apex predator counts and bathymetry but not SST. These hot spot events exhibited daily fluctuations in magnitude and location. Documenting and tracking this spatial variation would be difficult with slow moving ships. More studies are needed to determine what physical and biological factors govern their appearances. It is possible grazing pressure on plankton and local weather patterns affect distribution and movements of forage fish and euphausiids (also extremely abundant here) which in turn affects distributions and movements of apex predators. To our knowledge, this is the first attempt to track and describe such events in the Bering Sea using remote sensing.

## Introduction

While the importance of forage species to healthy ecosystem functioning is widely accepted, targeted and comprehensive studies on many of those species are non-existent. In 1999, amendments to Alaskan groundfish management plans created a new forage fish category to allow for specific management actions intended to conserve and manage forage fish resources. However, without critical life history, distribution and abundance information on these species, the effects of targeted management actions will be poorly understood and possibly immeasurable with the current array of assessment tools in place.

Despite the present information gaps, over the past 100 years a multitude of studies have occurred in the Bering Sea region that include information on the listed forage taxa (squid, osmerids or smelt, bathylagids or deepsea smelt, clupeids or herring, ammodytids or sand lance, and myctophids or lanternfishes) and the diverse oceanographic environments that they occupy. All of these species are considered pelagic but some have seasonal affinities to nearshore zones (< 50 m depths) while others spend their entire lives in deepwater regions (> 250 m depths). Some species (e.g. squid) appear to concentrate along the "green belt" (see Figure 1) The diverse life histories, distributions, and population dynamics will likely dictate a similarly diverse array of survey designs and assessment tools needed to for management or protective measures. Much of the information from these studies has been summarized in books, workshop or symposium proceedings and some data is available on line or obtainable from former investigators (Table 1).

From a preliminary overview of the literature, key species and their associated habitats can be defined (Table 2). Habitat ranges are listed by domain or regions in the Bering Sea defined by bathymetric contours (Figure 1): coastal domain (50 m or shallower), middle domain (between 50 and 100 m), outer domain (between 100 and 200 m) and oceanic domain or basin (over 200 m). Future studies may reveal other key species that are important but poorly understood in terms of ecological importance. For example, stomiidae (dragonfish) and notosudidae (waryfishes), although not on the proposal request list of taxa, were listed as the third and fourth most abundant mesopelagic fish in the western Bering Sea following myctophidae and bathylagidae (Sobolevsky et al. 1996). Other unlisted fish, Pacific sandfish (*Trichodon trichodon*) and juvenile salmon (*Onchorhynchus* spp.) may be important regionally based on abundance in the nearshore (Livingston 2002; Farley et al. 2000). In addition, juvenile walleye pollock (*Theragra chalcogramma*), euphausiids (e.g. *Thysanoessa* spp.), and gelatinous macrozooplankton (jellyfish) may need to be included in ecosystem modeling or assessment

of targeted forage taxa because of the sheer abundance and ecological importance to other forage taxa as well as the apex community (see Coyle and Pinchuk, Brodeur et al., Hunt et al., and Stabeno et al. 2002, Deep-Sea Research II 49). Some of the listed species (e.g. Pacific herring, capelin, and squid) are better understood than others because they are abundant and are or were targeted in fisheries. However, none of the species in the list (Table 2) have been the focus of ecosystem-based studies and therefore trophic relationships and top-down or bottom-up forcing processes are poorly understood.

Given the gap in understanding of most aspects concerning forage species in the Bering Sea, a pilot study with multiple investigators was initiated with the goal of assessing distribution, species composition, and the ecological role of forage species within the nearshore, continental shelf, and continental slope habitats as well as the technologies and techniques used to collect them. As part of this ambitious study, our role was to assess the utility of aerial remote sensing in the study of forage species. Our rationale was that many of the forage species are planktivorous, are therefore associated with surface, plankton-rich waters, and are often accompanied by a host of surface-dwelling or associated apex predators. These species are good candidates for remote sensing from the air.

The patchy and contiguous distribution of schooling fish, such as capelin (*Mallotus villosus*) requires large numbers of sampling units or transects to achieve statistical validity of assessments if a priori information is not available (Cram and Hampton, 1976; Fiedler, 1978; Barange and Hampton, 1997). Ship survey methods are slow and therefore costly, and generally sample narrow swaths of water. When fish schools are near the surface, acoustic biomass estimates can be unrealistically low (Vilhjálmsson, 1994). Ship and net avoidance can confound biological assessments of fish and ecological research on the relationships between predators and their fish prey (Aglen and Misund, 1990; Olsen, 1990; Logerwell and Hargreaves, 1996).

Water penetrating instrumentation, such as LIght Detecting and Ranging (LIDAR), are being used with increasing frequency from aircraft as the technology is developing. Blue-green light propagates to depths up to 100 m (Squire and Krumboltz, 1981) and green lasers have been applied in the form of lidar (light detection and ranging), where photon backscatter is collected from light reflecting off biological targets in the water column. Although numerical algorithms for lidar detection of fish were established more than 20 years ago (Murphree et al., 1974), modelling of signal-to-noise ratio, estimation of fish abundance, and statistical treatment of lidar data is a continuing area of research (Krekova et al., 1994; Mitra and Churnside, 1999; Lo et al., 2000). Target strength is a function of green-light reflectivity and has been measured on frozen samples of several fish species

(Churnside and McGillivary, 1991), and live sardines in a tank experiment (Churnside et al., 1997). Airborne lidar has also been used to detect subsurface oceanic scattering layers (Hoge et al., 1986]). In the early 1990s, the Fish Lidar Oceanic Experimental (FLOE) system was constructed from off-the-shelf components, and improvements were made to signal-processing techniques used to discriminate fish returns from small particles in the water (Churnside et al., 1998, 2001a). The FLOE system penetrates depths up to 50 m, and has been used off the coast of California to survey anchovy and sardine (Churnside et al., 1997; Hunter and Churnside, 1995; Lo et al., 2000), and has more recently been used to measure plankton, squid, and marine mammals (Churnside et al., 2001a). The FLOE system was first used in Alaska and used to document large schools of capelin and map variations in plankton distribution in the Gulf of Alaska (Brown et al. 2002). Comparisons of LIDAR with acoustic data have been very encouraging, and these methods can produce similar results (Churnside et al., 2001b). Spain is developing a program for sardine assessment that incorporates LIDAR and Norway is undertaking commercially available fish LIDAR instrumentation.

## Methods

This study was conducted in the southeastern Bering Sea along the northern coasts of Unalaska, Akutan and Akun Islands (Figure 2). Oceanographic descriptions of this location are covered in Chapters 1 and 3 of this report. Aerial surveys were designed to bracket a coordinated ship survey (see Chapters 1-3) extending and tripling the area transected by the vessel in order to provide a broadscale view of the area and to address how well the ship regions represented distributions for near-surface schools and surface predators. The ship surveyed two regions, one nearshore and one offshore covering shelf and slope habitat. In addition, ship survey tracks were repeatedly measured (5 times during the day and twice at night) in order to gain a better understanding of short term variation of biological features observed. Aerial surveys were flown from June 8 through June 19, 2006.

Instrumentation mounted on the aircraft consisted of the LIDAR, and infrared radiometer used to measure sea surface temperature, and an RGB high resolution camera. The LIDAR system was used and is described in detail by Churnside et al. (2001). It is a non-scanning, radiometric LIDAR with three major components: (1) the laser and beam-control optics, (2) the receiver optics and detector, and (3) the data collection and display computer. The laser is linearly polarized and the beam diverged, using a lens in front of the laser, to meet eye-safety standards established for marine mammals (Zorn et al., 2000). During the day, a narrower divergence filter is used than at night, when it is three times

wider. The narrow filter minimizes the amount of background light entering the receiver, but effectively limits the penetration depth of laser light (Gordon, 1982). A polarizer in front of the telescope selects the cross-polarized component of the reflected light, thus maximizing contrast between fish and smaller light-scattering particles (Churnside et al., 1997; Lewis et al., 1999). The telescope collects the light onto an interference filter to reject background light. As with the divergence filter, a narrow interference filter is used by day and a wider one at night. An aperture at the focus of the primary lens also limits background light by limiting the field of view of the telescope to match the divergence of the transmitted laser beam. The resulting light is incident on a photomultiplier tube, which converts the light into an electrical current. For the night-time receiver, the active area of the photomultiplier tube is the field-stop aperture. By day, a separate aperture is used, and the light is transferred to the photomultiplier tube by a second lens. The combination of divergence lens size, field-of-view setting, interference filter width, and altitude flown in 2000 determined the spot diameter or sampling swath at 5 m by day and 15 m by night. The photomultiplier tube output is passed through a logarithmic amplifier to increase the dynamic range of the signal. A 50-Ω load resistor converts the current in a voltage, which can be digitized in the computer.

LIDAR signal was processed according to the protocols established earlier (Churnside et al. 1997) with the main goal of removing the background signal attributable to water. Signal above background was sorted by applying thresholds to sort out the plankton scattering contribution versus fish with a multi-scale expansion to aid in target identification. The multi-scale expansion was based on the Multiresolution Median Transform (MMT) (Starck et al, 1998). Preliminary results produced a correlation of $R2 = 0.97$ between LIDAR return strength, integrated over depth, and the catch of sardines when a median filter of 150 m along the flight track was applied. When the filter length was doubled to 300 m using the same data, the correlation was reduced to $R2 = 0.35$. This suggests that the horizontal scale of the LIDAR return can be an important clue to target identification.

Processed signal was sorted into two main categories, weak scattering layers representing plankton and strong discriminate signal aggregations representing fish schools. In addition, the penetration depth (point at which laser light attenuates) is recorded from data processing is a function of water clarity and phytoplankton content (Brown et al. 2002). Within the context of this report, we describe only the fish signal in relation to the apex predator community.

Visual counts were obtained on seabird and mammals following protocols established during previous similar surveys (Brown et al. 2002). Counts were geocoded by measuring the time of the observation and linking that time to the geocoded flight track recorded by the instrument GPS units.

SAR data was obtained and processed from imagery and software available at the Alaska SAR Facility at the University of Alaska. Images were selected based on temporal overlap with the survey period. SAR images basically show changes in sea surface roughness and internal waves. Bright spots in the images are produced by large metal objects (e.g. ships) and other large surface formations such as the hot spot observed. The resolution of the images obtained was 12.5 m (pixel resolution) at the surface.

In order to test the relationship between physical variables and fish distribution and between fish distribution and apex predators, spatial linear models were derived in the form of generalized least squares regression. The model form and process is described by Kaluzny et al. 1998 and the statistical program SPlus was used to analyze the data.

## Results

In total, we flew the LIDAR just under 7900 km (Figure 2). Of these, about 11% were within the offshore box (shelf and slope habitat) surveyed by the vessel and 16% within the nearshore box. Most of the fish schools detected by the LIDAR were outside of these regions. Of 830 schools, only 20 were within the offshore box and 30 within the nearshore box. The resulting density of schools was 0.023 ± 0.005 schools / km within the offshore box, 0.024 ± 0.004 schools / km within the nearshore box, and 0.105 ± 0.004 schools / km for all flights. The average school length was 87.5 m. Average depth of the schools was 6.2, 5.4, and 5.2 m for the offshore, nearshore, and all schools, respectively. The probability density function of depth shows that the nearshore schools have a secondary peak in the 12-18 m depth bin (Figure 3).

Describing observations sequentially within the ship survey regions, in the offshore area:

June 8: We covered the entire box and detected no schools within.

June 9: We covered the entire box and detected 2 schools in the SE corner at about 2300 UTC. There was also a strong layer in about the top 2 m. This layer was not always at the surface, and seemed to go deeper to avoid surface predation.

June 11: We covered the entire box and detected no schools within.

June 12: We covered the entire box and detected no schools. Later, we covered the north and east parts of the box, and saw several schools along the north edge. The first coverage of the northern part of the box was between about 10:20 UTC and 11:20 UTC. The schools were observed a little less than 2 hours later at about 13:15 UTC.

June 14: We covered the entire box, although not as densely as on previous days. Two schools were detected in the SE corner of the box at about 19:49 UTC.

June 17: We only covered the southern part of the box, but detected more schools than previously. The time was between about 22:45 and 22:50 UTC. More schools were also detected just south of the box.

In the nearshore area:

June 8: We covered 3 lines on the western side of the box and detected 1 school near the southern edge at 21:23 UTC.

June 9: We covered the western part of the box and detected 2 schools near the NW corner at about 21:20 and 1 near the center in the southern part at about 22:00.

June 13: We covered most of the box with 2 schools detected in the northern part at 1:25 and 1:52 UTC. More schools were detected just to the north of the box. At about the same time, a number of schools were detected very close to shore off the point the north of Lost Harbor.

June 17: We covered the eastern part of the box, and detected several schools near the southern edge in shallow water.

June 18: We covered the entire box and detected the most schools of any flight over this region. Three were in the same shallow-water region as on the 17th, and the rest were spread through the center of the bay.

June 19. Three widely spaced schools were detected in another fairly complete coverage of the box. Generally, the school density was too sparse to interpolate.

Given the results of the observations within the ship survey area, we decided to evaluate the region as a whole within the confines of the aerial flight paths and were able to describe the formation of the hot spots. The hot spots occurred at the shelf slope, were approximately 5 nmi in diameter, and comprised humpback whales, Dall porpoise, and thousands of sooty shearwaters, fulmar, and other pelagic seabirds. Underlying the apex community was a concentration of patchy fish schools and euphausiid swarms ranging in size of 10s to 100s of meters in diameter, averaging 10 m thick, and ranging in the upper 30 m of the water column. On the first survey day, June 8, we observed a

concentration of seabirds north of Akutan Island (Figure 4). By July 9th, fish schools and whales began to accumulate in the same area (Figure 5). On June 11th, large numbers of seabirds began to accumulate in the region resulting in a feature that could be discerned from space using SAR imagery (Figures 6 and 7). One can only appreciate the size of this feature by observation from the surface (Figure 8). By June 13th, the feature was enormous (Figure 9). On June 16, fish schools dissipated at the surface along with the seabirds and marine mammals (Figure 10). The original hot spot reformed on June 17th along with a secondary one between Unalaska and Akutan Islands (Figure 11). By June 18th only the original hot spot remained (Figure 12). On the last day of survey (June 19), the main hot spot appeared to have shifted westward along the shelf moving in the same direction as the residual current in the area (see Chapter 3 for description of currents). The seabirds as well as the schools were observed with the LIDAR in addition to the visual counts (Figure 14). The association of the two features was clear from those results.

Spatial regression analysis indicated a significant ($p < 0.001$) correlation between seabird and fish school distribution as well as between fish school and bathymetry (bottom depth) with surface fish schools concentrated on the shelf. There was not a significant correlation between fish schools and SST detected by the infrared radiometer.

## Conclusions

- Fish school density was lower in the originally designated study area than in the surrounding area. Therefore, pre-selecting transects or survey regions, as opposed to adaptively selecting and/or tracking features, is not a good way to assess surface forage species and ephemeral bouts of foraging and energy exchange
- Using aircraft allowed coverage over a large region and repeat measurements, we were able to map and measure temporal variability within the hot spots.
- Given the enormous numbers of apex predators and fish schools surveyed within the hot spots, they probably represent a significant portion of trophic energy exchange occurring within the region among these species.
- Fish schools were probably aggregating on the shelf due to the high concentrations of copepods and euphausiids there (see Chapter 3).
- The large numbers of seabirds changed the surface roughness of the ocean to a degree that the hot spot was visible with SAR imagery.

- Aerial remote sensing should be developed to assess surface schooling or aggregating features (e.g. capelin, herring, sand lance, euphausiids, and plankton) where features are patchy and where they exhibit a large degree of temporal variability, such as we observed.
- An adaptive survey design, using a moving grid, to track and sample these features with directed ship sampling would result in an improved assessment of the surface forage species and foraging events.

## Acknowledgements

We would like to thank Commander Northwest and our attentive pilot Marco for providing a mechanically reliable aircraft and for protecting our safety. We would like to thank Mike Sigler for organizing and overseeing this project. We would like to thank James Wilson for assistance with equipment engineering, installation, and operation. We would like to thank Christopher Kenaley for the use of his photograph. Funding for this research was supported with a grant from the North Pacific Research Board, project # F0401.

## Literature Cited

Aglen, A. and Misund, O. A. 1990. Swimming behaviour of fish schools in the North Sea during acoustic surveying and pelagic sampling trawling. ICES CM 1990/B: 38.

Barange, M., and Hampton, I. 1997. Spatial structure of co-occurring anchovy and sardine populations from acoustic data: implications for survey design. Fisheries Oceanography, 6: 94–108.

Brodeur, R.D., M.T. Wilson, L. Ciannelli, M. Doyle, and J.M. Napp. 2002. Interannual and regional variability in distribution and ecology of juvenile pollock and their prey in frontal structures of the Bering Sea. Deep-Sea Res. II. 49: 6051-6067.

Brown, E.D., Churnside, J.H., Collins, R.L., Veenstra, T., Wilson, J.J., and Abnett, K. 2002. Remote sensing of capelin and other biological features in the North Pacific using lidar and video technology. ICES Journal of Marine Science, 59: 1120-30.

Churnside, J. H., and McGillivary, P. A. 1991. Optical properties of several Pacific fishes. Applied Optics, 30: 2925–2927.

Churnside, J.H., Wilson, J.J., and Tatarskii, V.V. 1997. Lidar profiles of fish schools. Applied Optics, 36: 6011–6020.

Churnside, J.H., Wilson, J.J., and Tatarskii, V.V. 2001. An airborne lidar for fisheries applications. Optical Engineering, 40: 406–414.

Churnside, J. H., Sawada, K., and Okumura, T. 2001b. A comparison of airborne lidar and echo sounder performance in fisheries. Journal of the Marine Acoustical Society of Japan, 28: 49–61.

Churnside, J.H., D.A. Demer, and B. Mahmoudi. 2003. A comparison of lidar and echosounder measurements of fish schools in the Gulf of Mexico. ICES Journal of Marine Science 60: 147-154.

Coyle, K.O. and A.I. Pinchuk. 2002. The abundance and distribution of euphausiids and zero-age pollock on the inner shelf of the southeast Bering Sea near the Inner Front in 1997-1999. Deep-Sea Research II 49: 6009-6030.

Craig, J.F., M. J. Kenley and J.F. Talling. 1978. Comparative estimations of the energy content of fish tissue from bomb calorimetry, wet oxidation and proximate analysis. Freshwater Biology 8:585-590.

Craig, P. 1987. Forage fishes in the shallow waters of the North Aleutian shelf. Pages 49-54 in Forage Fishes of the Southeastern Bering Sea Conference Proceedings, U.S. Dept. of the Interior, Minerals Management Service Report July 1987.

Cram, D. L., and Hampton, I. 1976. A proposed aerial/acoustic strategy for pelagic fish stock assessment. Journal du Conseil International pour L'Exploration de la Mer, 37: 91–97.

Farley, E.V., Jr., R.E. Haight, C.M. Guthrie, and J.E. Pohl. 2000. Eastern Bering Sea (Bristol Bay) coastal research on juvenile salmon, August 2000. (NPAFC Doc. 499) Auke Bay Laboratory,

Alaska Fisheries Science Center, NMFS, NOAA, 11305 Glacier Highway, Juneau, AK 99801-8626. 18 p.

Fiedler, P. C. 1978. The precision of simulated transect surveys of northern anchovy, Engraulis mordax, school groups. Fishery Bulletin U.S., 76: 679–685

Gordon, H. R. 1982. Interpretation of airborne oceanic lidar: effects of multiple scattering. Applied Optics, 21: 2996–3001.

Hoge, F. E., Berry, R. E., and Swift, R. N. 1986. Active–passive airborne ocean color measurement. 1. Instrumentation. Applied Optics, 25: 39–47.

Houghton, J.P. 1987. Forage fish use of inshore habitats north of the Alaska Peninsula. Pages 39-48 in Forage Fishes of the Southeastern Bering Sea Conference Proceedings, U.S. Dept. of the Interior, Minerals Management Service Report July 1987.

Hunt Jr., G.L., C. Baduini, J. Jahncke. 2002. Diets of short-tailed shearwaters in the southeastern Bering Sea. Deep-Sea Research II 49: 6147-6156.

Hunter, J. R., and Churnside, J. M. 1995. Airborne fishery assessment technology: a NOAA workshop report. NOAA Southwest Fisheries Science Center Administrative Report, La Jolla, California, LJ–95–02. 71 pp.

Kaluzny, S.R., S.C. Vega, T.P. Cardoso, and A.A. Shelly. 1997. S+ spatial stats. Springer, New York.

Lewis, G. D., Jordan, D. L., and Roberts, P. J. 1999. Backscattering target detection in a turbid medium by polarization discrimination. Applied Optics, 38: 3937–3944.

Livingston, P. (ed.) 2002. Ecosystem considerations for 2003. Available http://www.fakr.noaa.gov/npfmc/safes/safe.htm.

Livingston, P., K. Aydin, J. Boldt, S. Gaichas, J. Ianelli, J. Jurado-Molina, and I. Ortiz. 2003. Ecosystem Assessment of the Bering Sea/Aleutian Islands and Gulf of Alaska Management Regions. Available Alaska Fisheries Science Center.

Lo, N. C. H., Hunter, J. R., and Churnside, J. H.. 2000. Modeling statistical performance of an airborne lidar survey system for anchovy. Fishery Bulletin U.S., 98: 264–282.

Logerwell, E. A., and Hargreaves, N. B. 1996. The distribution of sea birds relative to their fish prey off Vancouver Island: opposing results at large and small spatial scales. Fisheries Oceanography, 5: 163–175.

Mecklenberg, C. W., T. A. Mecklenburg, and L. K. Thorsteinson. 2002. Fishes of Alaska. American Fisheries Society. Bethesda, Maryland. 1037 p.

Mitra, K., and Churnside, J. H. 1999. Transient radiative transfer equation applied to oceanographic lidar, Applied Optics, 38: 889–895.

Murphree, D. L., Taylor, C. D., and McClendon, R. W. 1974. Mathematical modeling for the detection of fish by an airborne laser. Journal of the American Institute of Aeronautics and Astronautics, 12: 1686–1692.

Naumenko, E. A. 1996. Distribution, biological condition and abundance of capelin (*Mallotus villosus*) in the Bering Sea. In: Ecology of the Bering Sea: A review of Russian Literature, p. 237-256. Ed. O. A. Mathisen and K. O. Coyle, Ecology of the Bering Sea, Univ. Alaska Sea Grant College Program. Rpt. 97/01. 306 p.

Olsen, K. 1990. Fish behaviour and acoustic sampling. Rapports et Procès-Verbaux des Réunions du Conseil International pour l' Exploration de la Mer, 189: 147–158.

Orlov, A.M. 1997. Mesopelagic fishes as prey of Atka mackerel (*Pleurogrammus monopterygius*, Hexagrammidae, Scorpaeniformes) off the northern Kuril Islands. Pages 323-335 in Forage

Fishes in Marine Ecosystems, University of Alaska Sea Grant College Program Report No. 97-01.

Pahlke, K. A. 1985. Preliminary study of capelin (*Mallotus villosus*) in Alaskan waters. ADFG Info. Lflt. 250. 64 p.

Robards, M. and M. Schroeder. 2000. Assessment of nearshore fish around Akutan Harbor using beach seines during March and July 2000. USGS Biological Resources Division, Alaska, Biological Sciences Center, 1011 E. Tudor Road, Anchorage, AK 99503.

Sinclair, E.H. and P.J. Stabeno. 2002. Mesopelagic nekton and associated physics in the southeastern Bering Sea. Deep-Sea Research II 49: 6127-6146.

Sobolevsky, Y.I., T.G. Sokolovaskaya, A.A. Balanov, and I.A. Senchenko. 1996. Distribution and trophic relationship of abundant mesopelagic fishes of the Bering Sea. Pages 159-168 in Mathisen, O.A. and K.O. Coyle, editors, Ecology of the Bering Sea, University of Alaska Sea Grant College Program, Report No. 96-01.

Squire, J.L. Jr. and H. Krumboltz, "Profiling pelagic fish schools using airborne optical lasers and other remote sensing techniques," Mar. Tech. Soc. J. 15, 27-31 (1981).

Starck, J-L, F. Murtagh, and A. Biuaoui (1998), Image Processing and Data Analysis (Cambridge University Press, Cambridge).

Stabeno, P.J. and G.L. Hunt, Jr. 2002. Overview of the Inner Front and southeast Bering Sea carrying capacity programs. Deep-Sea Research II 49: 6157-6168.

Tsarin, S.A. 1997. Myctophids of the sound scattering layer and their place in pelagic food webs. Pages 271-275 in Forage Fishes in Marine Ecosystems. University of Alaska Sea Grant College Program Report No. 97-01.

Viihjálmsson, H. 1994. The Icelandic capelin stock. Rit Fiskideildar, 13: 281 pp.

Watanabe, H., M. Masatoshi, K. Kawaguchi, K. Ishimaru, and A. Ohno. 1999. Diel vertical migration of myctophid fishes (Family Myctophidae) in the transitional waters of the western North Pacific. Fisheries Oceanography 8(2): 115-127.

Wespestad, V. G. 1991. Pacific herring population dynamics, early life history, and recruitment variation relative to eastern Bering Sea oceanographic factors. Doctoral dissertation, University of Washington, Seattle.

Wilson, J.R. and A.H. Gorham. 1982. Alaska underutilized species Volume 1: Squid. Alaska Sea Grant Report 82-01.

Zorn, H.M., Churnside, J.H., and Oliver, C.W. 2000. Laser safety thresholds for cetaceans and pinnipeds. Marine Mammal Science, 16: 186–200.

**Table 1.** A partial list of research programs and published proceedings or books containing information on forage taxa in the Bering Sea.

| Type | Mo/Yr | Resource or Citation |
|---|---|---|
| Government Report | May 1978 | Resources of Non-Salmonid Pelagic Fishes of the Gulf of Alaska and Eastern Bering Sea. Macy et al. NOAA NMFS Report (no report no.) |
| Sea Grant Report | 1982 | Alaska Underutilized Species Volume 1: Squid. Wilson and Gorham, July 1982. Alaska Sea Grant Report 82-1. |
| NMFS Trawl Survey Results | 1982-present | Forage fish bycatch in stock assessment trawls surveys; Livingston 2003 and other report from NMFS AFSC, Kodiak and Seattle labs |
| Japanese Research Cruises and Commercial Fishing Catches | 1970s to present | Data from the Japanese Fisheries Agency and its research vessels, i.e. the Oshoro Maru, have recently been made available. This data set includes net samples of gillnets, trawls, longlines and jigging equipment. |
| OCSEAP & PROBES | mid-1970s-late 1980s | resource assessments from the Outer Continental Shelf Environmental Assessment Program and research results from the Processes and Resources of the Bering Sea study |
| Workshop Proceedings | Oct. 1983 | Proceedings of the workshop on biological interactions among marine mammals and commercial fisheries in the southeastern Bering Sea. Alaska Sea Grant Report 84-1. UAF. April 1984 |
| Conference Proceedings | July 1987 | Forage Fishes of the Southeastern Bering Sea, USDI MMS, Alaska OCS Region |
| Workshop Summary | March 1991 | Is It Food? Addressing Marine Mammal and Seabird Declines. Alaska Sea Grant Report 93-01. UAF, 1993. |
| Bering Sea FOCI | 1991-1997 | A coordinated series of federally funded studies with NMFS AFSC as the lead agency and conducted by researchers from the NMFS AFSC, NOAA PMEL, UAF and other universities. |
| Book | 1996 | Ecology of the Bering Sea: A Review of Russian Literature. Mathisen and Coyle. University of Alaska Sea Grant College Program Report No. 96-01. |
| Symposium Proceedings | Nov. 1996 | Forage Fishes in Marine Ecosystems. Proceedings of the International Symposium on the Role of Forage Fishes in Marine Ecosystems. University of Alaska Sea Grant College Program Report No. 97-01. |
| SMMOCI | 1995-1997 | A coordinated series of federally funded studies with NMFS NMML as the lead agency and conducted by researchers from NMFS AFSC & NMML, NOAA PMEL, University of Alaska Fairbanks and others. |
| SEBSCC & IFP | 1995-2000 | A series of coordinated studies funded by the NSF Office of Polar Programs and conducted by researchers from UAF, NOAA PMEL, NNFS NMML and NMFS AFSC and other academic organizations. The dedicated volume below shows results from these studies. |
| Dedicated Journal Volume | 2002 | Ecology of the Southeastern Bering Sea. Deep-Sea Research Part II, Volume 49, No. 26. Milliman, editor. |
| BASIS & SEBSOCC | 1999-present | A coordinated series of studies with NMFS as the lead agency and with international participants with a goal of understanding the marine phase of Pacific salmon. |

**Table 2.** A list of key forage fish species and the main habitat ranges observed within the Bering Sea.

| Family/Species | Common Name | Habitat | Reference |
|---|---|---|---|
| ***Gonatidae*** | squid | outer domain, shelf break; exhibit extreme vertical migrations | Wilson and Gorham 1982; Sinclar and Stabeno 2002 |
| *Berryteuthis magister*<br>*Gonatopsis borealis*<br>*Onychoteuthis banskii borealis* | | | |
| ***Osmeridae*** | smelt | | |
| *Mallotus villosus* | capelin | seasonal migrations through coastal, middle and outer domains; surface to 200 m depths | Paulke 1985; Craig 1987; Houghton 1987; Naumenko 1996; Livingston 2002; NMFS AFSC trawl data |
| *Hypomesus olidus* | pond or silver smelt | some are anadromous; mainly occupy river estuaries and coastal domain | Houghton 1987; Naumenko 1996; |
| *Hypomesus pretiosus* | surf smelt | limited range in coastal domain around western end of Alaska Peninsula | Houghton 1987; Robards and Schroeder 2000; Mecklenburg et al. 2002 |
| *Osmerus mordax* | rainbow or Arctic smelt | anadromous with seasonal migrations through coastal, middle and outer domains; surface to 150 m | Craig 1987; Naumenko 1996; Mecklenburg et al. 2002 |
| *Thaleichthys pacificus* | eulachon | anadromous with seasonal migrations through coastal, middle and outer domains apparently restricted to eastern shelf; surface to 300m | Houghton 1987; Mecklenburg et al. 2002; Livingston 2002; NMFS AFSC trawl data |
| ***Bathylagidae*** | deepsea smelt | | |
| *Leuroglossus schmidti* | northern smooth-tongue | in deepwater from the outer domain and shelf break throughout basin; extreme vertical migrations between surface and 1800 m | Orlov 1997; Sinclair and Stabeno 2002; Mecklenburg et al. 2003 |
| *Bathylagus pacificus* | slender blacksmelt | in deepwater from the shelf break and over the basin; no vertical migration; found in depths of 150 to 7700 m | Sinclair and Stabeno 2002; Mecklenburg et al. 2003 |
| *Bathylagus ochotensis* | eared blacksmelt | in deepwater from the shelf break and over the basin; extreme vertical migration between the surface and 6,100 m | Sinclair and Stabeno 2002; Mecklenburg et al. 2003 |
| *Pseudobathylagus milleri* | stout blacksmelt | in deepwater from the shelf break and over the basin; extreme vertical migration between the 60 and 6,000 m | Sinclair and Stabeno 2002; Mecklenburg et al. 2003 |
| ***Clupeidae*** | herring | | |
| *Clupea pallasi* | Pacific herring | seasonal migrations through coastal, middle, and outer domains; vertically migrate from surface to 100 m | Wespestad 1991 and many others (best known species in list) |
| ***Ammodytidae*** | sand lance | | |
| *Ammodytes hexapterus* | Pacific sand lance | seasonal migrations through coastal and middle domains; surface to 100 m depths; bury themselves in sand when not schooling | Craig 1987; Farley et al. 2000; Robards and Schroeder 2000; Livingston 2002; Mecklenburg et al. 2003 |
| ***Myctophidae*** | lanternfish | | Tsarin 1997 |
| *Stenobrachius leucopsarus* | northern lampfish | in deepwater over the basin; extreme vertical migrations between 30 m and 1000 m | Watanabe et al. 1999; Sinclair and Stabeno 2002; Mecklenburg et al. 2003 |
| *Stenobrachius nannochir* | garnet lampfish | in deepwater over the basin; does not vertically migrate; found between 500 m and 1000 m | Watanabe et al. 1999; Sinclair and Stabeno 2002; Mecklenburg et al. 2003 |
| *Lampanyctus jordoni* | brokenline lanternfish | in deepwater over the basin; extreme vertical migrations between 200 m and 1400 m | Watanabe et al. 1999; Sinclair and Stabeno 2002; Mecklenburg et al. 2003 |
| *Nannobrachium regale* (also as *Lampanyctus regalis*) | pinpoint lanternfish | in deepwater over the outer domain through the basin; extreme vertical migrations between the surface & 1500m | Watanabe et al. 1999; Sinclair and Stabeno 2002; Mecklenburg et al. 2003 |
| *Diaphus theta* | California headlight-fish | S. Bering Sea only along the shelf break from the Alaska Peninsula through the Aleutian Chain; extreme vertical migrations between the surface and 800 m | Watanabe et al. 1999; Sinclair and Stabeno 2002; Mecklenburg et al. 2003 |

**Figure 1.** Domains and habitats of the eastern Bering Sea: 1a and 1b) SE and NW outer shelf, 2a and 2b) SE and NW middle shelf, 3) Pribilof Islands, 4) Unimak Island, 5) shelf break The "green belt" is the area encompassed by the white oval http://www.pmel.noaa.gov/sebscc/concept). The study area for this project is outlined by the yellow rectangle that encompasses the "horseshoe", a fold in the bathemetry that allowed study of multiple habitats (slope, shelf, and nearshore) within a relatively small area.

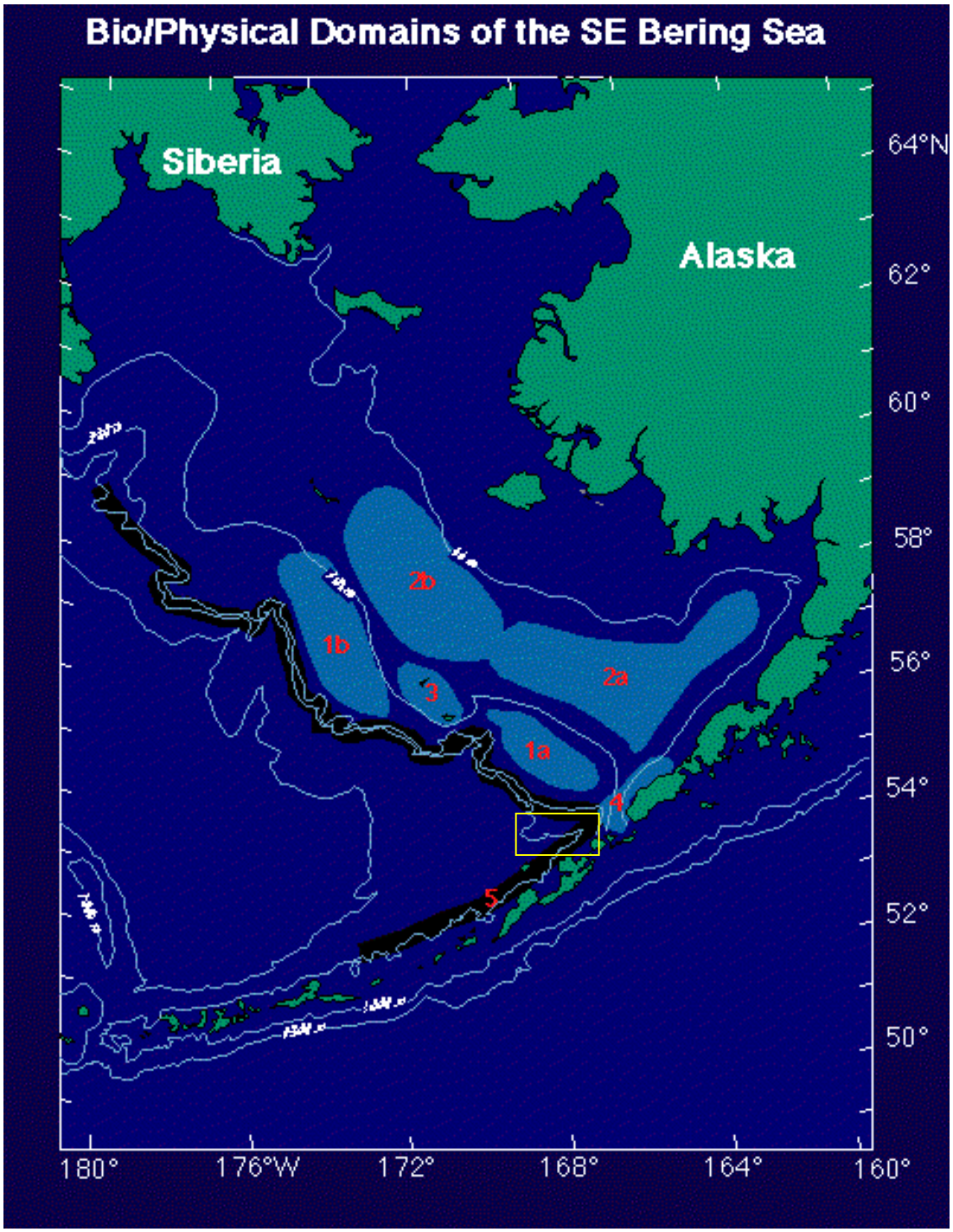

**Figure 2.** The cumulative aerial survey flight path (gray lines) or sampled transects from June 8 to June 19, 2006.

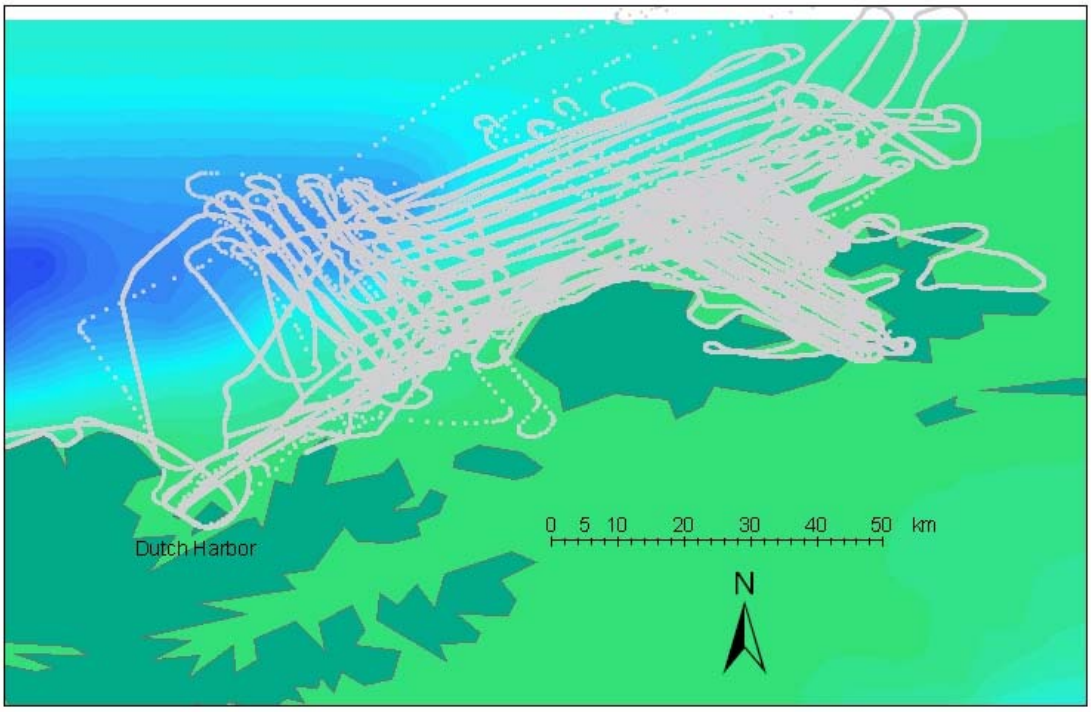

**Figure 3.** The probability density function of depth of schools detected by LIDAR.

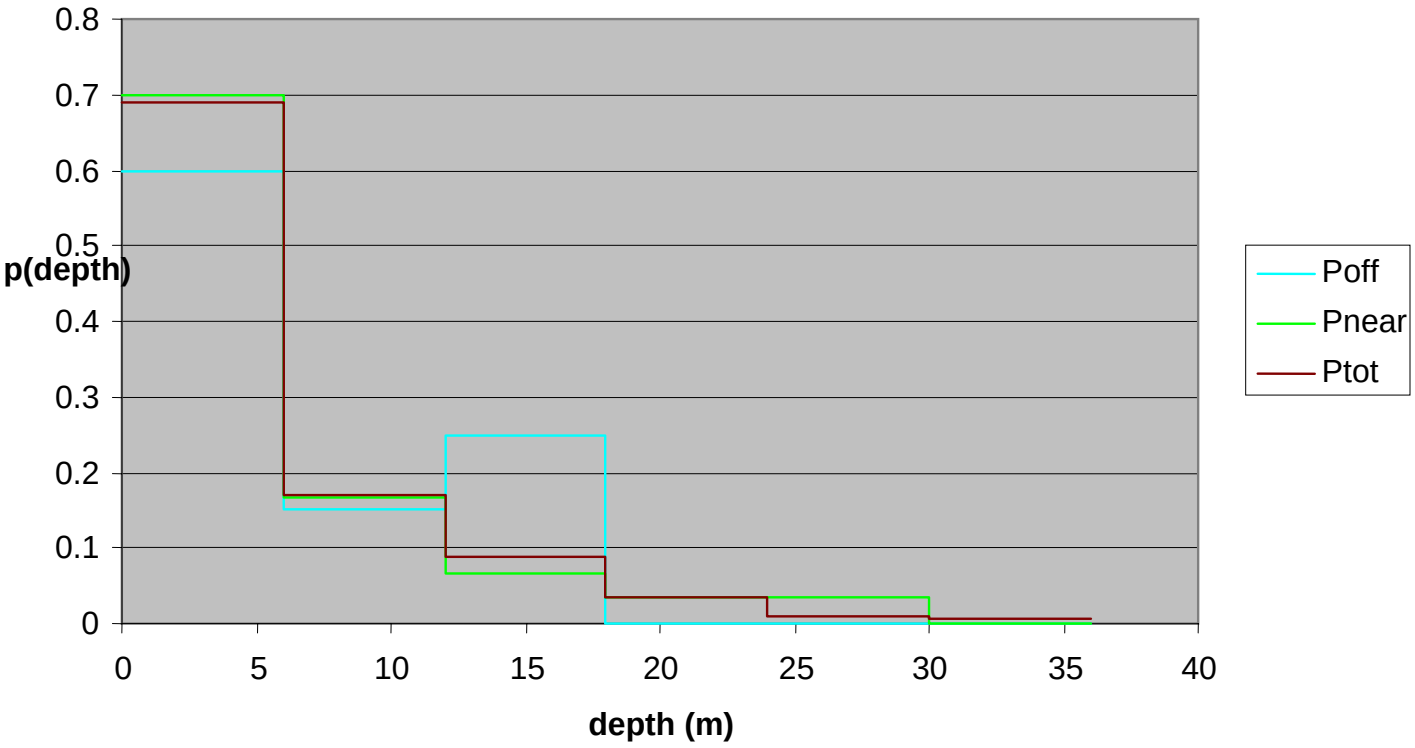

**Figure 4.** The first identification of the hot spot on June 8 mainly indicating the presence of large numbers of seabirds.

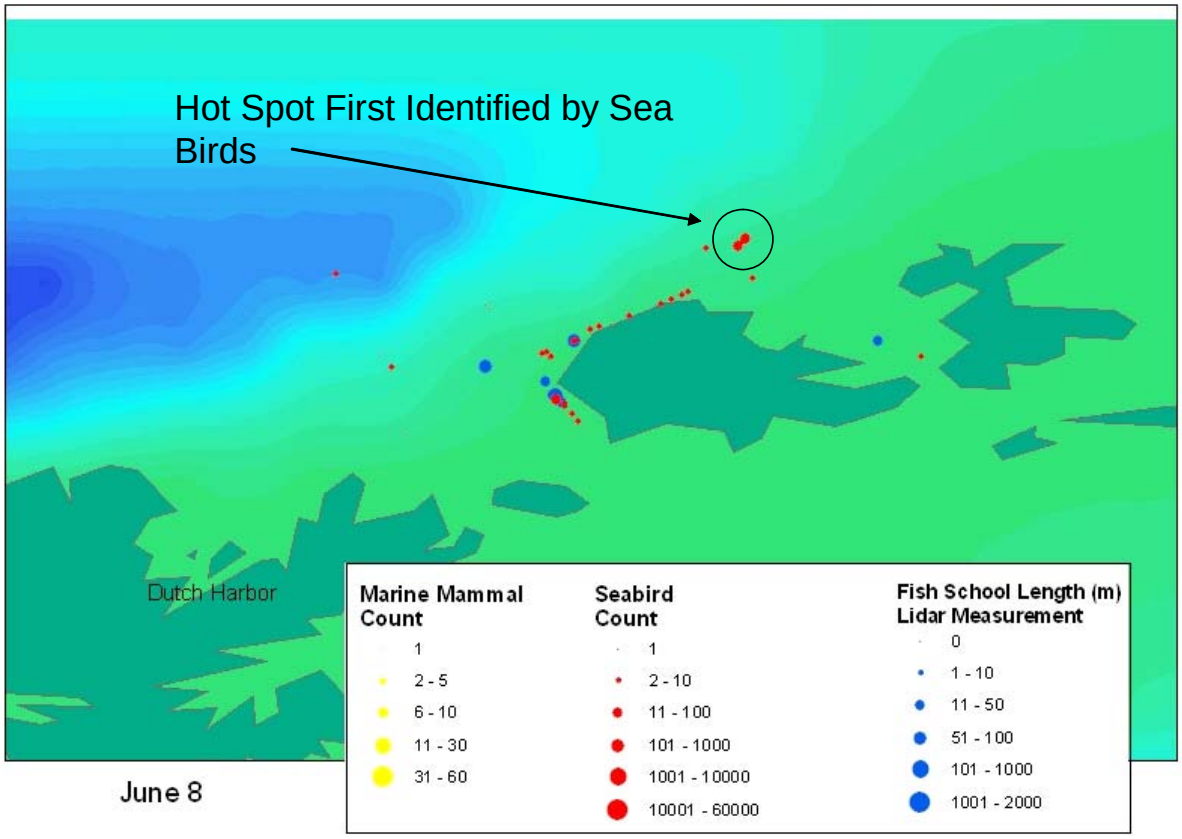

**Figure 5.** Evolution of the hot spot continued June 9 with the appearance of baleen whales and fish schools.

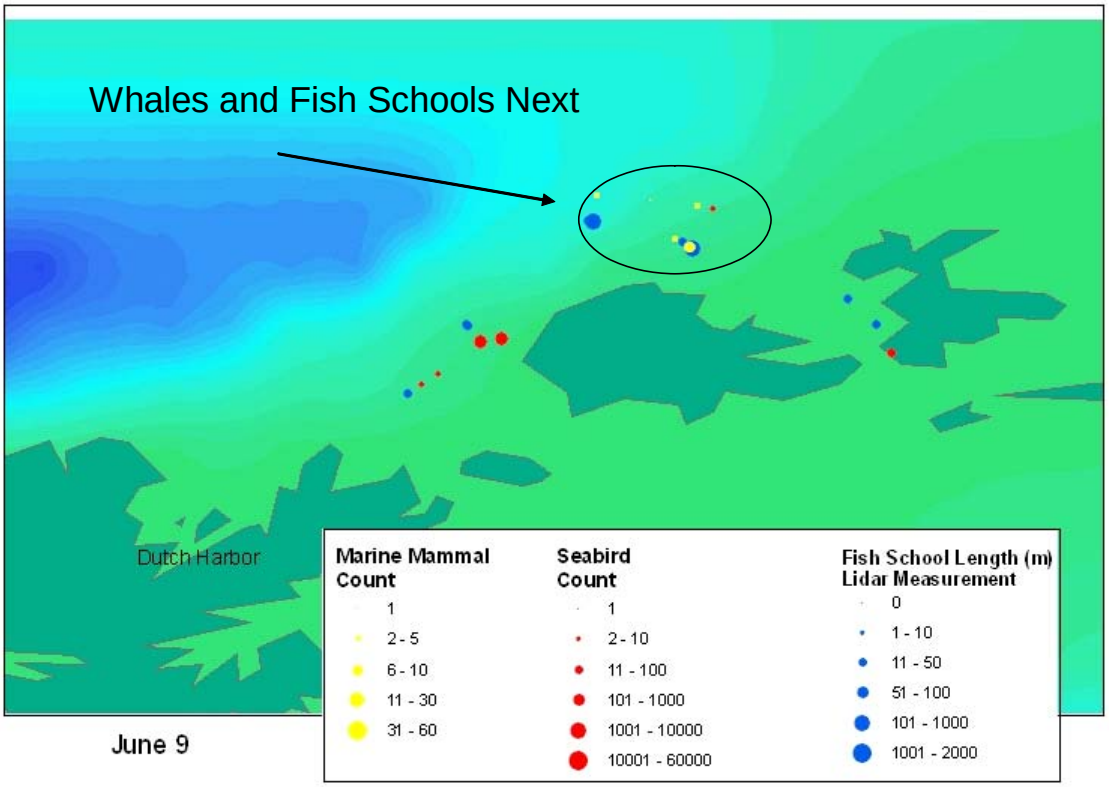

**Figure 6.** The build up of seabird numbers continues on June 11.

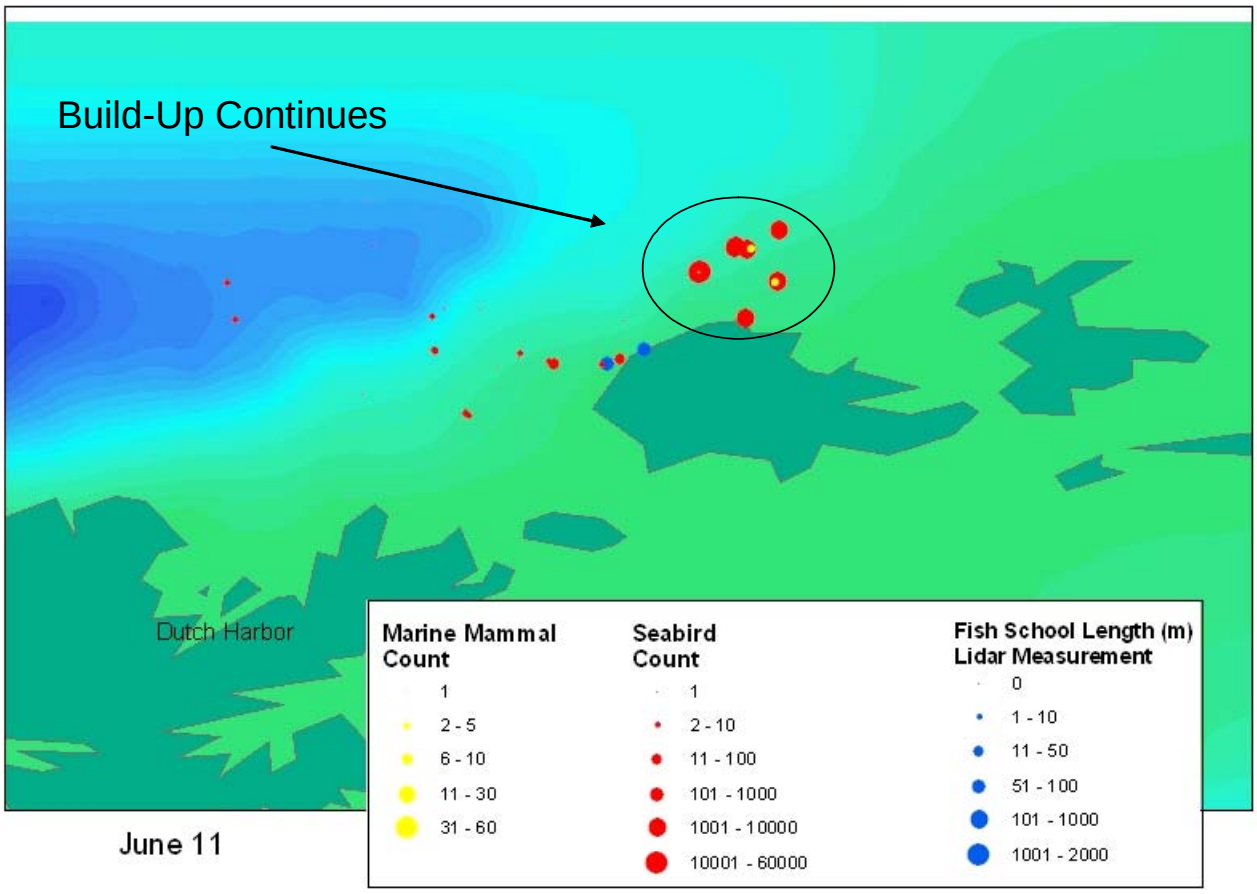

**Figure 7.** SAR image where the large numbers of seabirds and marine mammals create a surface disturbance that can be observed from space.

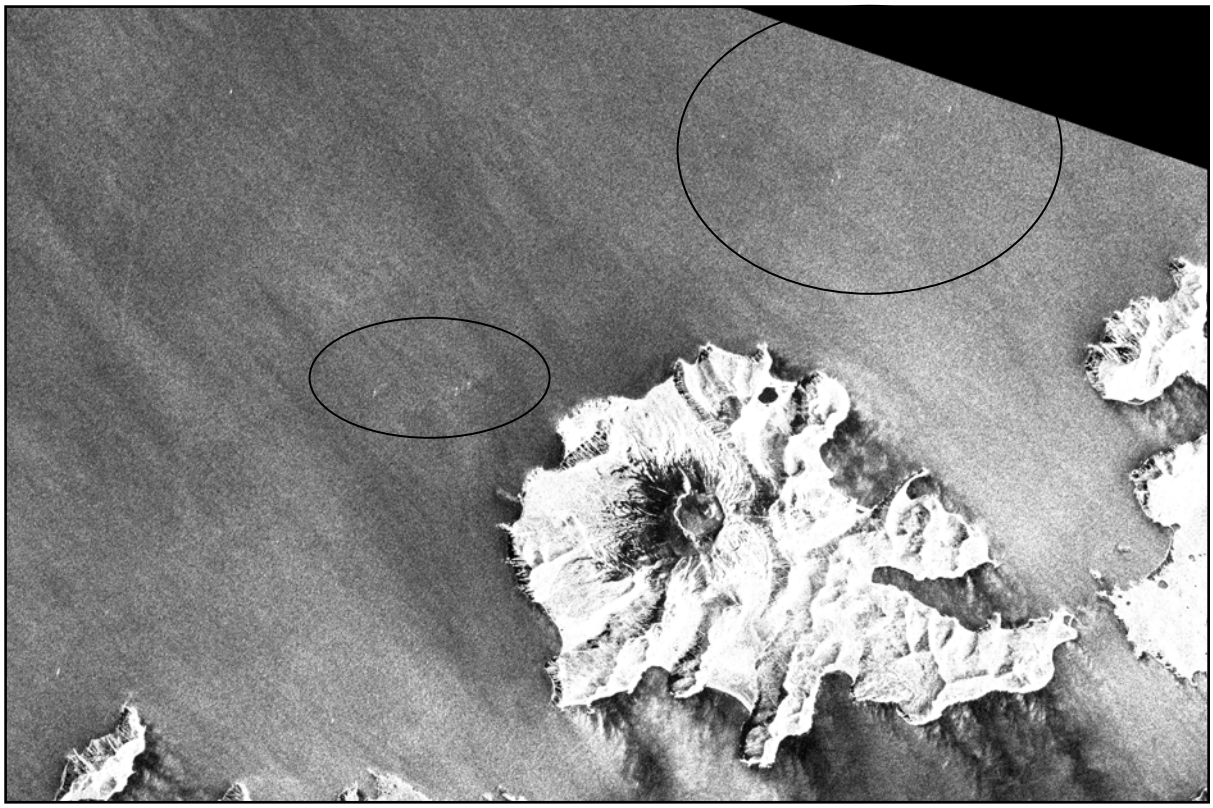

**Figure 8.** Photograph of the hot spot with the large concentrations of seabirds and marine mammals. Photo courtesy Christopher Kenaley.

**Figure 9.** By June 13, the hot spot feature is immense.

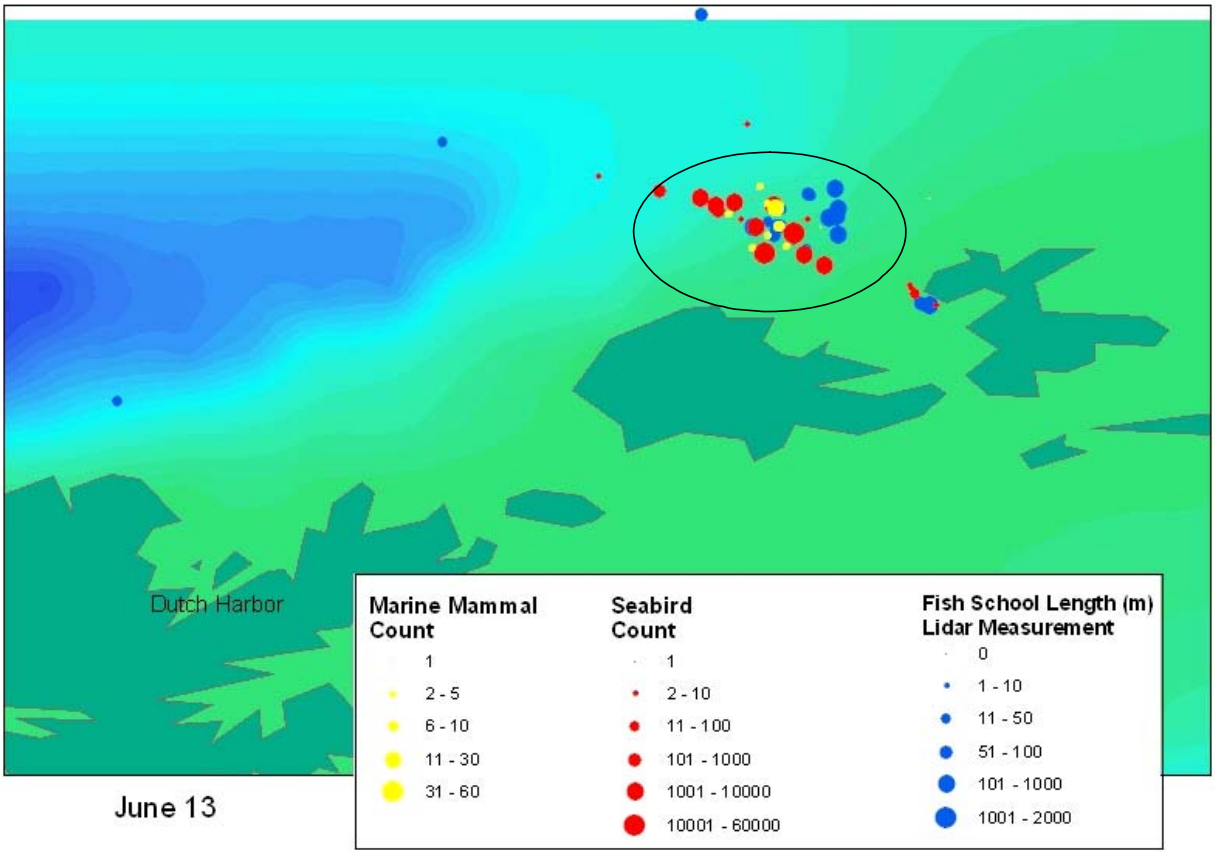

**Figure 10.** On June 16th, fish schools were no longer observed and the seabirds and marine mammals disapated.

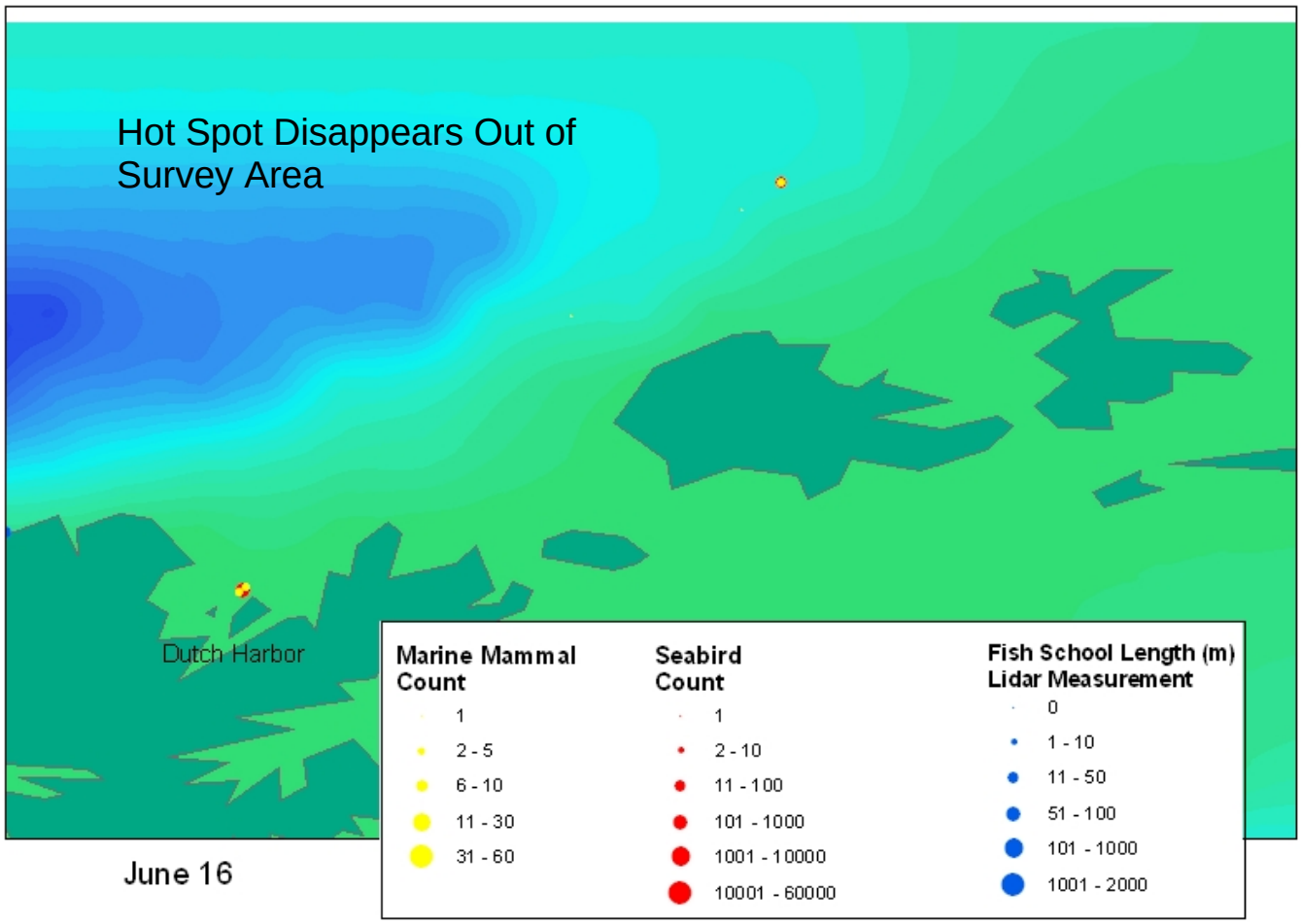

**Figure 11.** On June 17th, fish schools reappear and reform the hot spot as well as a secondary hot spot between Unalaska and Akutan Islands.

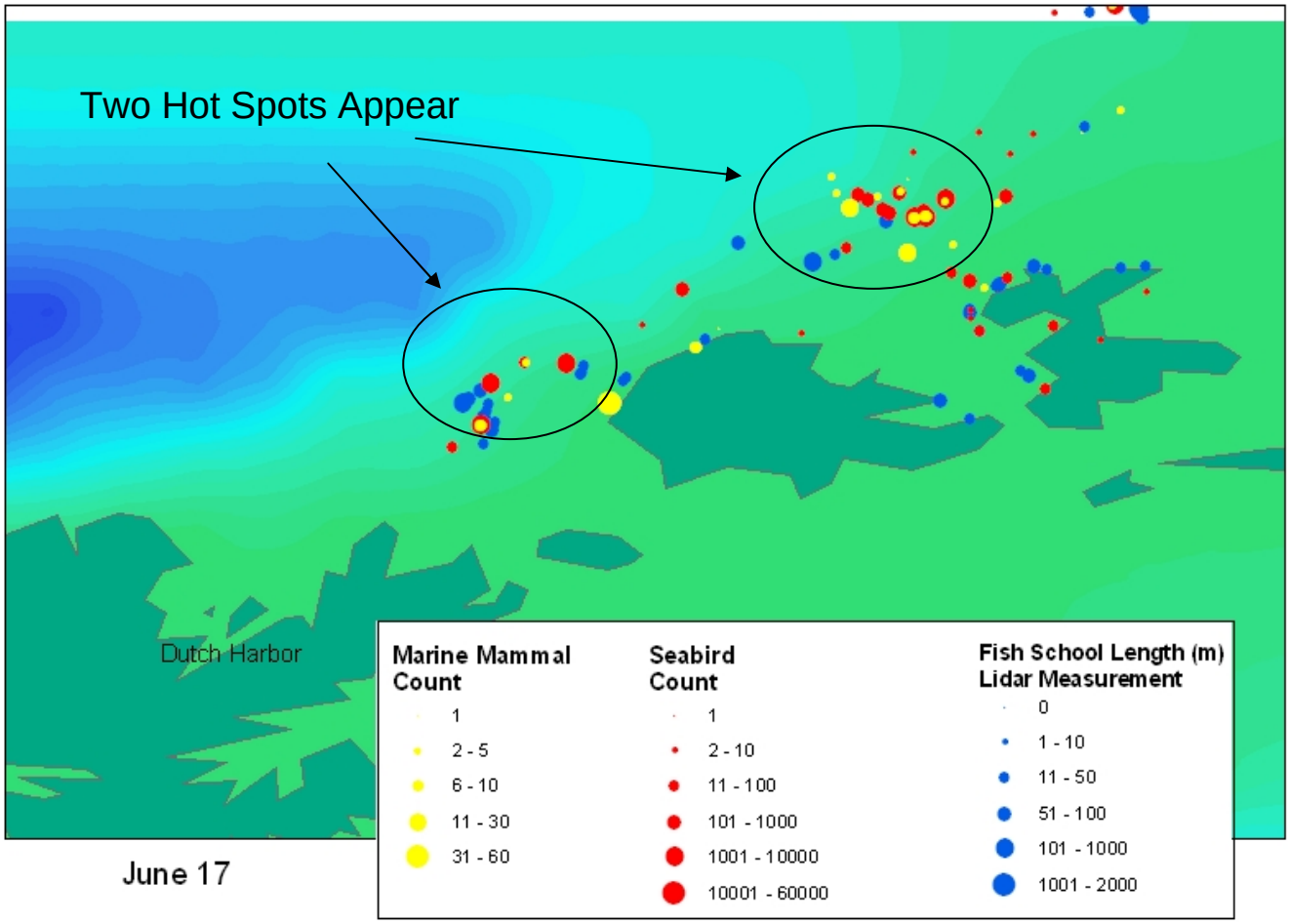

**Figure 12.** By June 18th, the original hot spot remains and the secondary one disappeared.

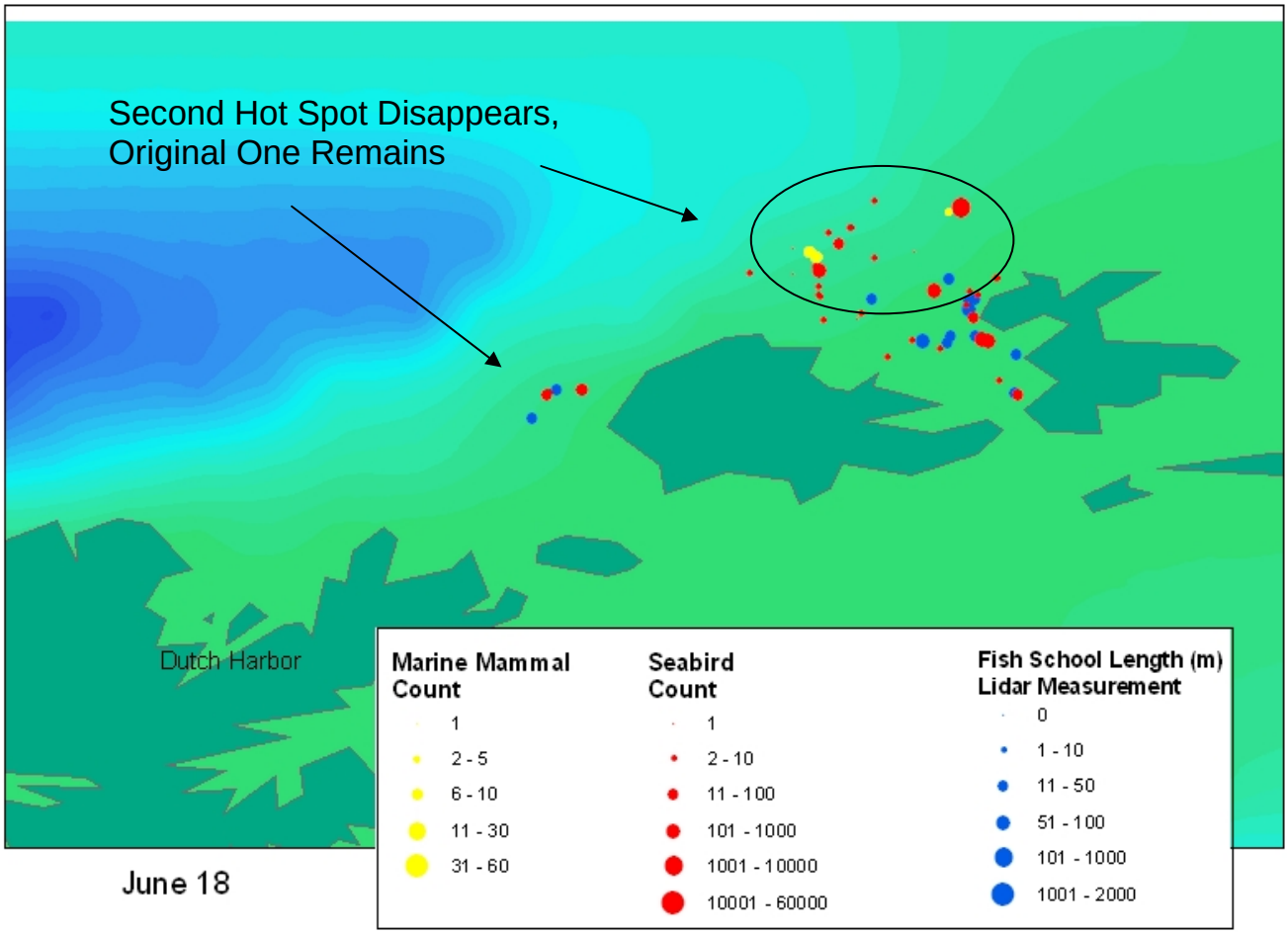

**Figure 13.** On June 19th, the hot spot drifted to the west in approximately the same direction as the residual ocean current.

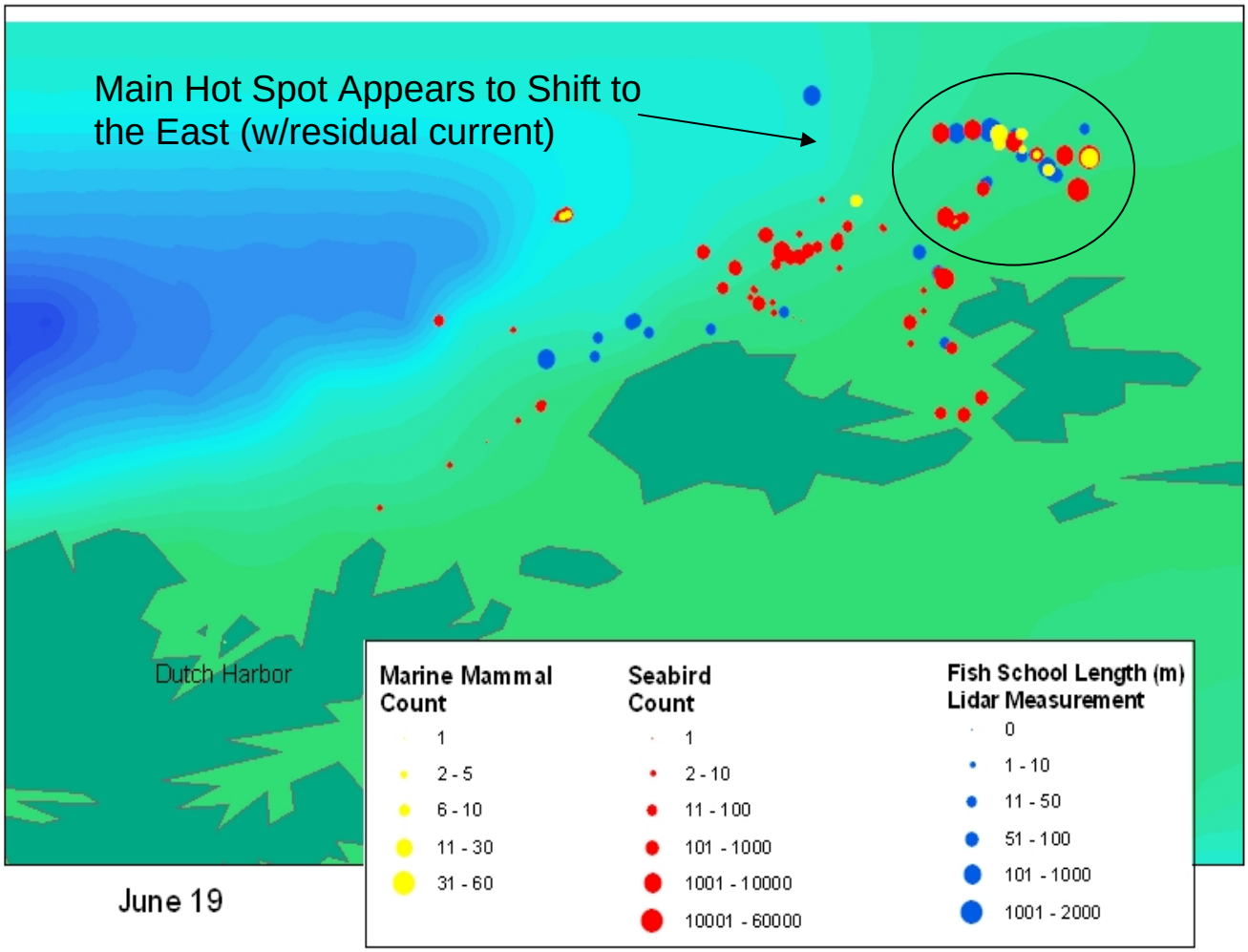

**Figure 14.** An example of a LIDAR echogram shows a large school at a depth of 30 – 40 m and a large number of birds at the surface.

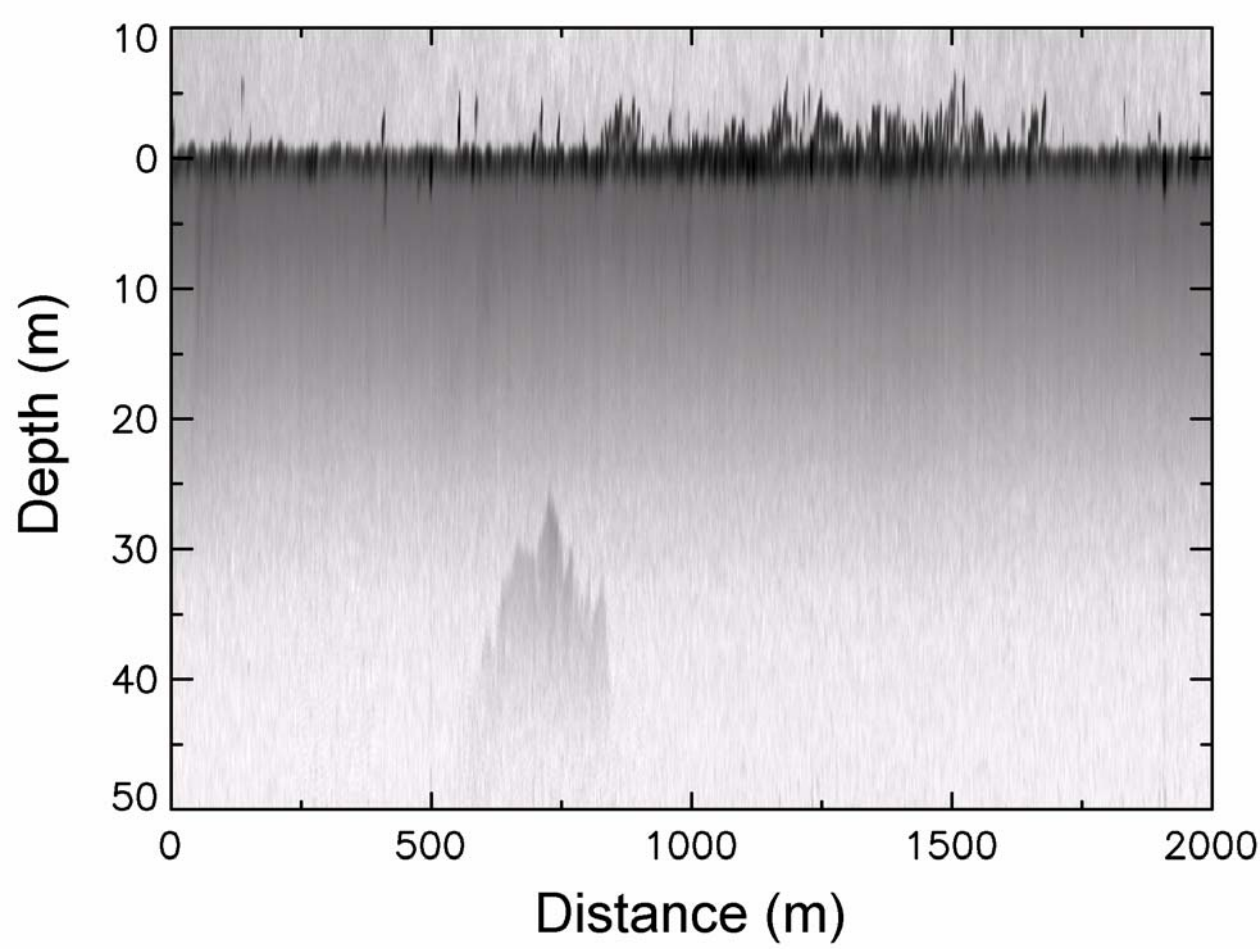

# Mesozooplankton distributions in the southeastern Bering Sea estimated using a Multinet sampler and an evaluation of semi-automated processing with ZooImage software

Mark C. Benfield[1], Nicola Hillgruber[2], Marianne Alford[3], Sara Arndt[4], Jeffrey Bacon[3], and Sean F. Keenan[1,5]

[1]Department of Oceanography and Coastal Sciences, Louisiana State University, Baton Rouge, LA 70803
[2]School of Fisheries and Ocean Science, University of Alaska Fairbanks, Juneau, AK 99801
[3] College of Agriculture, Louisiana State University, Baton Rouge, LA 70803
[4]College of Basic Sciences, Louisiana State University, Baton Rouge, LA 70803
[5]Present Address: Fish and Wildlife Research Institute, Florida Fish and Wildlife Conservation Commission, St. Petersburg, Florida 33701

## Abstract

A series of vertically stratified mesozooplankton samples collected in the Bering Sea north of Akutan Island were processed to estimate the vertical zonation of dominant taxa in the upper 40m of the water column. Traditional manual processing using a microscope was compared with semi-automated processing using a flatbed scanner and ZooImage software. The latter approach used digitized images of plankton to generate abundance estimates. Results from this comparison suggest that it can produce abundance estimates comparable with those produced by manual counting. Vertical zonation patterns obtained by manual processing suggested considerable differences in structure within the near-surface waters from samples collected over a 2 day period. These data will be used to evaluate changes in lidar backscatter from nearby areas.

## Introduction

Collection of zooplankton samples is generally accomplished using various types of nets, pumps and traps (Wiebe and Benfield, 2003). Such devices filter the contents of large volumes of water producing samples that may contain thousands to hundreds of thousands of individuals. Such samples contain a wealth of potential information that can be related to distributions of higher trophic levels, physical and chemical hydrography, and signals from remote sensing systems such as acoustics and lidar. Moreover, zooplankton time-series can provide valuable data on ecosystem responses to climate change and regime-shifts (Hays et al. 2005). Before this information can be obtained and analyzed, the samples must be processed. Processing normally consists of subdividing the sample into a representative aliquot, which is then sorted, identified, measured and enumerated. Sample processing requires a patient and well-trained expert capable

of working with a microscope for extended periods. Skill in recognizing taxonomic identification features is essential if the organisms are to be correctly assigned to taxonomic categories. Sample processing is the bottleneck in studies of zooplankton ecology and delays associated with processing generally limit the rate at which information about the sample can be extracted.

There have been a number of attempts to reduce the amount of time required to process zooplankton samples. Ortner et al. (1979) developed a silhouette photographic technique that created a direct contact sheet image of the contents of a sample aliquot by pouring the sample on a photographic emulsion, exposing it to light, and developing the image. This had the advantage of providing a permanent record of the sample contents, which could be counted, measured, and identified by viewing the silhouette image under a microscope. While the level of taxonomic detail present in the silhouette was lower than in the preserved sample, it provided sufficient information to identify to species for organisms where distinctive morphological features were present, and to broader taxonomic levels, such as calanoid copepods, euphausiids, chaetognaths, in most cases. Moreover, the silhouettes could be quantitatively subsampled by overlaying a grid of cells and randomly selecting some cells for analysis. This approach was combined with a an early micro-computer-based measurement and recording system that employed acoustic localization to determine the position of a cursor on the silhouette (Peter Wiebe, Woods Hole Oceanographic Institution, Pers. Comm.). In this way samples could be analyzed for abundance, size and taxonomic composition in a reproducible and shorter time period than traditional microscope-based analyses.

With the advent of digital scanners, silhouette images could be digitized at high-resolution and analyzed using software packages that subsample the image, and permit the user to identify and measure the contents of the digital image. Abundance can be determined from counts and a knowledge of the area subsampled, sample aliquot, and the original sample volume. The Matlab-based Digitizer software developed by the Woods Hole Oceanographic Institution (http://globec.whoi.edu/software/digi_prog/WHOI_Silhouette_DIGITIZER.htm) is an example of such a system.

Direct scanning of samples suspended in liquid was problematic with the early scanners because vibrations induced by the stepper motor that moved the scanning head, blurred the digitized image. New scanners are capable of digitizing images without perceptible vibration making direct digitization of the contents of plankton samples feasible. Moreover, specialized

waterproofed scanners such as the ZOOSCAN (Gorsky and Grosjean, 2003; Grosjean et al. 2004) have been designed to facilitate rapid scanning of plankton samples.

Production of a 2D image of the contents of a plankton sample or aliquot is but one step in reducing the time required to process a sample. Some or all of the contents of the image must still be counted, identified, and measured. This step remains an obstacle to rapid processing of zooplankton samples. Recent advances in machine vision and pattern recognition have lead to parallel advances in computerized analysis of plankton images. The ZOOSCAN system has specialized software for locating, extracting, measuring and counting particles within an image. Such regions of interest (ROIs) may then be used for visual classification by a human, or computerized classification by a machine using some feature-based classifier (e.g. Culverhouse et al. 1996; 2003; Blaschko et al. 2005).

ZooImage is public-domain software developed for semi-automated or fully-automated processing of digitized zooplankton samples. Semi-automated processing consists of ROI extraction and measurement by ZooImage followed by sorting into taxonomic groups by a human. Fully-automated processing consists of the former steps to produce a taxonomically-verified set of training images, which are then used to classify unknown ROIs into taxonomic categories by ZooImage. In this paper we present the results from studies that compared traditional plankton sample processing with semi-automated processing by ZooImage.

## Methods

### *Study Area*

This study was undertaken in the southeastern Bering Sea along the north coast of the Aleutian Islands (Fig. 1) in waters NE of Dutch Harbor. Four zooplankton sampling stations were selected for use in this analysis. These stations corresponded to dates and times where an airborne lidar system was operated. (see Hillgruber et al. 2006, Table 1 for details of zooplankton sampling station characteristics).

### *Zooplankton Sampling*

An opening/closing net system (Hydrobios MultiNet) equipped with five 335 µm mesh nets was deployed from the side of the F/V Great Pacific. Each cast was designed to collect samples from different parts of the water-column along a double-oblique trajectory (Fig. 2). The net was deployed with all nets closed and net 1 was opened near the bottom of the downward

portion of the trajectory with subsequent nets opened electronically along the ascending portion of the tow (Fig. 2). Upon recovery the samples were washed out of the net with seawater, concentrated by sieving, and preserved in 5% formalin.

***Manual Zooplankton Processing***

Manual processing refers to sample processing performed by a human observer. Our observers were undergraduate student employees in our laboratory who all had been trained in zooplankton sorting and processing for at least one year. All samples were initially examined and sorted under a dissecting microscope for fish, fish eggs, and large pteropods, which were separated and retained. Samples were then split into two equal aliquots using a Folsom plankton splitter. One split from each sample was sent to the University of Alaska Fairbanks, Juneau Center for archiving and the remaining splits were used in this study. All sample processing performed by humans was conducted using plankton sorting trays under a dissection microscope with counters to tally the abundance of taxa in each category. Since the data from these samples was required for a related study examining the signals produced by plankton in response to lidar illumination, our requirement for taxonomic resolution was coarse. The taxonomic categories we used were: copepods, thecosomate pteropods, hyperiid amphipods, chaetognaths, euphausiids, larvaceans, crab zoea, fish, and other zooplankton.

***ZooImage***

ZooImage is a software package written in R that employs the Java-based ImageJ software package for some analyses. Details of ZooImage can be found in the website http://www.sciviews.org/zooimage/. We used ZooImage version 0.3-1 prerelease. ZooImage was run on a computer equipped with a 1.6GHz Pentium 4 processor and 1GB RAM running Windows XP Service Pack 2. The computer was linked via USB to a flatbed scanner (Epson Perfection 4870 Photo).

Samples were scanned directly within transparent polystyrene tissue culture tray lids (Nunclon™ 140156: 12.7mm x 8.5 mm x 7 mm deep). Prior to scanning, each sample was split five more times using a Folsom plankton splitter resulting in a $1/64^{th}$ split. The contents of the split were apportioned into a series of tissue culture tray lids in such a way that no single tray contained objects that were in physical contact with other zooplanktors. Objects that were touching others were moved using a fine-tipped paintbrush or forceps so that they were isolated. This did not always result in equal numbers of taxa in each tray. Scanning was performed while

the samples were suspended in ethanol. Samples were then scanned from within ZooImage using the Vuescan driver (Ver. 8.1.26) at 2400 dpi, 16 bits per pixel. The resultant scans were saved as uncompressed 16bit grayscale TIFF images. Each image was cropped slightly within Adobe Photoshop to remove edges of the tissue culture tray that were visible in the scan. TIFF files were processed individually using the Process Images option in ZooImage. Process Images invokes ImageJ and we used the 16bit grayscale 2400 dpi plug-in module to process images.

Once the images had been extracted to ROIs, a human sorted them into categories using a Thumbnail browsing program (Thumbs Plus Version 6). Additional categories were created for artifacts associated with the scanning process: bubbles, debris, fibers, smudges, tray edges. The number of individuals in each category was determined by summing the numbers of ROIs after sorting. Some ROIs contained two or more individuals. In such cases the number of individuals within a ROI was taken into account when estimating the abundance in that category.

Accurate counts generally required that individuals be extracted as single target ROIs. ROIs containing multiple targets complicated the counting process and introduced delays in the time taken to process a sample. The solution to this was to carefully separate individuals within the tray prior to scanning and to ensure that no tray contained excessive numbers of individuals. In-order to determine how many zooplanktors could be scanned in a tray, we conducted a series of experiments in which increasing numbers of individuals were scanned and the number of individuals counted by ZooImage was compared with the number of individuals known to be in the tray. In this study, the total number of ROIs was summed and each ROI was assumed to contain only one individual. Errors in the number of individuals in each ROI would be evident as deviations between then known and estimated targets in each tray. This experiment was conducted using small (copepods) and large (chaetognaths) zooplankton, separately. Densities of copepods per tray were varied from 0-140 while chaetognaths were varied from 0-80 individuals.

***Manual Versus Semi-Automated Processing***

After determining the approximate densities of individuals that could be scanned and extracted as single ROIs using ZooImage, we proceeded to compare densities estimated from the same samples that were processed using ZooImage and manual methods. Half of a sample from a single MultiNet net, was split five more times yielding a 1:64 aliquot. The contents of this aliquot were divided into approximately equal parts and poured on to tissue culture trays, separated so that individual targets were not touching others, scanned, and processed using

ZooImage to the point where targets were extracted. These were then sorted and counted on the computer by a human who counted the numbers of each taxon present in the extracted ROIs using a Thumbs Plus software. Once scanning was complete, the same split was recombined, sorted, classified, and counted visually by a human (observer 1) working on a dissecting microscope. In a second experiment, the same split was first processed manually and then semi-automatically. The manual counting by observer 2, produced a sorted sample that did not contain a lot of debris and fragments of organisms. This *clean* sample was recombined and distributed among the tissue culture tray lids for scanning and ZooImage processing.

***Processing of MultiNet Samples***

All samples from the four MultiNet casts were processed using traditional manual microscopy. Samples were split according to Table II. Abundance estimates were derived from counts corrected for the degree of splitting and divided by the volume filtered by each net. Densities were estimated for: hyperiid amphipods, chaetognaths, copepods, crab larvae, euphausiids, fish (larvae and juveniles), and pteropods. Densities were estimated for larvaceans, fish eggs and other taxa, however, those samples are being re-examined because they were not consistently counted by all student workers.

## Results

***Manual Versus Semi-Automated Processing***

ZooImage produced clear scans of plankton samples (Fig. 3) containing sufficient features for classification into the taxonomic categories we used. Sufficient detail is likely present in the scans to permit an even finer taxonomic resolution. The size of individual scanned images was large (typically 120MB) which imposed limits on how large an area could be scanned. As a result, the area of the tissue culture trays appears to be the largest practical size that the memory allocated to the ImageJ software could process.

Increasing the density of scanned copepods and chaetognaths revealed that approximately 100 individual copepods could be reliably censused by ZooImage without the need for a human to assess the number of targets present in each ROI (Fig. 4). For larger taxa such as chaetognaths, the maximum density was lower (50 per tray, Fig. 4).

Both semi-automated and manual processing produced estimates of abundance that were comparable (Figs. 5, 6). The variability between semi-automated and manual estimates was low

and generally less than the variability between manual counts performed by two different human observers (compare Fig. 5 and 6). The relatively large variability in copepod abundance derived from manual counts by two different individuals is probably due to difficulty in distinguishing copepods that were live prior to collection from exuvia.

***Vertical Distributions of Zooplankton***

The upper 30 m of the water column displayed considerable biological structure in terms of the distributions of mesozooplankton and micronekton (Fig. 7). Problems with three of the nets at station 13, preclude any inference about vertical zonation patterns at that site. The distributions at station 17.1 suggest a surface maximum with most taxa reaching maximum densities in the shallowest two nets (Fig. 7). Samples from stations 17.2 and 17.3 display a similar pattern with a subsurface density maximum centered at 20m. This is not surprising given the short time and space separation of these two samples. All stations were dominated by copepods, euphausiids, chaetognaths and pteropods.

## Conclusions

Mesozooplankton sample processing can be accomplished using semi-automated methods such as ZooImage. The time required for this processing is comparable to manual processing and could be faster with the use of a more powerful processor. Results from semi-automated processing are comparable to those achieved by manual processing and errors are lower than would be obtained by replicate processing by different human observers.

The vertical structure of the water column at the sites examined, suggests that changes in the lidar signal could be associated with changes in the distributions of mesozooplankton taxa. Further analysis to correlate the lidar and zooplankton distributions is planned.

## References

Blaschko, M.B., G. Holness, M.A. Mattar, D. Lisin, P.E. Utgoff, A.R. Hanson, H. Schultz, E.M. Riseman, M.E. Sieracki, W.M. Balch, and B. Tupper. 2005. Automatic in situ identification of plankton. Seventh IEEE Workshops on Application of Computer Vision (WACV/MOTION'05) – Vol., 1:79-86.

Culverhouse P.F., R. Williams, B. Reguera, R.E. Ellis and T. Parisini. 1996. Automatic categorisation of 23 species of dinoflagellate by artificial neural network. Marine Ecology Progress Series, 139:281–287.

Culverhouse P.F., R. Williams, B. Reguera, V . Herry, and S. Gonzalez-Gill. 2003. Do experts make mistakes? A comparison of human and machine identification of dinoflagellates. Marine Ecology Progress Series, 247:17–25.

Gorsky, G. & P. Grosjean. 2003. Qualitative and quantitative assessment of zooplankton samples, GLOBEC Newsletter, April 2003.

Grosjean, P., M. Picheral, C. Warembourg, and G. Gorsky. 2004. Enumeration, measurement, and identification of net zooplankton samples using the ZOOSCAN digital imaging system. ICES Journal of Marine Science, 61: 518–525.

Hays, G.C., A.J. Richardson, and C. Robinson. 2005. Climate change and marine plankton. Trends in Ecology and Evolution, 20: 337-344.

Hillgruber, H. J.J. Vollenweider, and W. Fournier. 2006. Chapter 3: Distribution, composition and energy density of zooplankton in the southeastern Bering Sea. Final Project Report to North Pacific Research Board for project F0401.

Wiebe, P.H. and M.C. Benfield. 2003. From the Hensen net towards 4-D biological oceanography. Progress in Oceanography, 56: 7-136.

Table I. MultiNet sample characteristics. Cells shaded in gray indicate a potentially contaminated sample that was not enumerated.

| Date | Station | Start Time | Net Number | Minimum Depth (m) | Maximum Depth (m) | Mean Depth (m) | Volume Filtered ($m^3$) |
|---|---|---|---|---|---|---|---|
| June 16 | 13 | 23:16:38 | 1 | 21.3 | 30.7 | 27.3 | 87 |
| | | | 2 | 20.7 | 21.5 | 21.1 | 36 |
| June 17 | 17.1 | 22:27:40 | 1 | 16.5 | 22.4 | 20.2 | 41 |
| | | | 2 | 12.3 | 27.3 | 20.0 | 128 |
| | | | 3 | 9.5 | 16.8 | 14.6 | 106 |
| | | | 4 | 3.9 | 9.6 | 7.4 | 114 |
| | | | 5 | 0 | 4.4 | 2.4 | 74 |
| June 18 | 17.2 | 00:12:26 | 1 | 22.1 | 36.2 | 29.6 | 100 |
| | | | 2 | 15.7 | 22.2 | 19.8 | 67 |
| | | | 3 | 9.9 | 16.0 | 13.4 | 60 |
| | | | 4 | 4.4 | 10.3 | 7.9 | 53 |
| | | | 5 | 0 | 5.1 | 2.3 | 41 |
| June 18 | 17.3 | 02:13:05 | 1 | 15.3 | 45.6 | 31.3 | 203 |
| | | | 2 | 15.5 | 20.8 | 19.6 | 59 |
| | | | 3 | 10.8 | 16.1 | 14.8 | 61 |
| | | | 4 | 5.2 | 11.2 | 9.6 | 61 |
| | | | 5 | 0 | 9.4 | 4.6 | 61 |

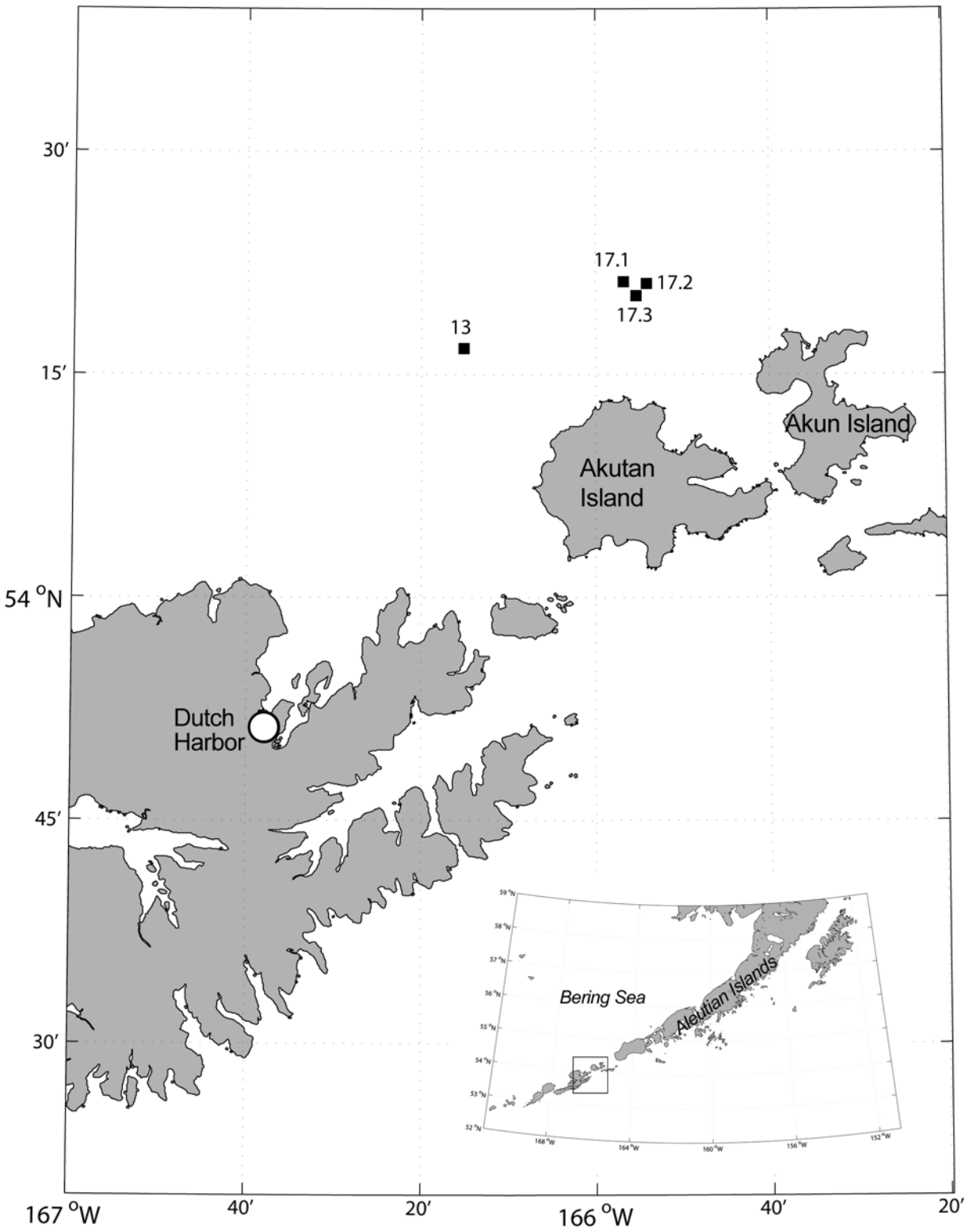


Figure 1. Location of zooplankton sampling stations. Station 13 was sampled on 06/16, station 17.1 was sampled on 06/17, and stations 17.2 and 17.3 were sampled on 06/18. Inset map shows the location of the study area in relation to the Aleutian Island chain.

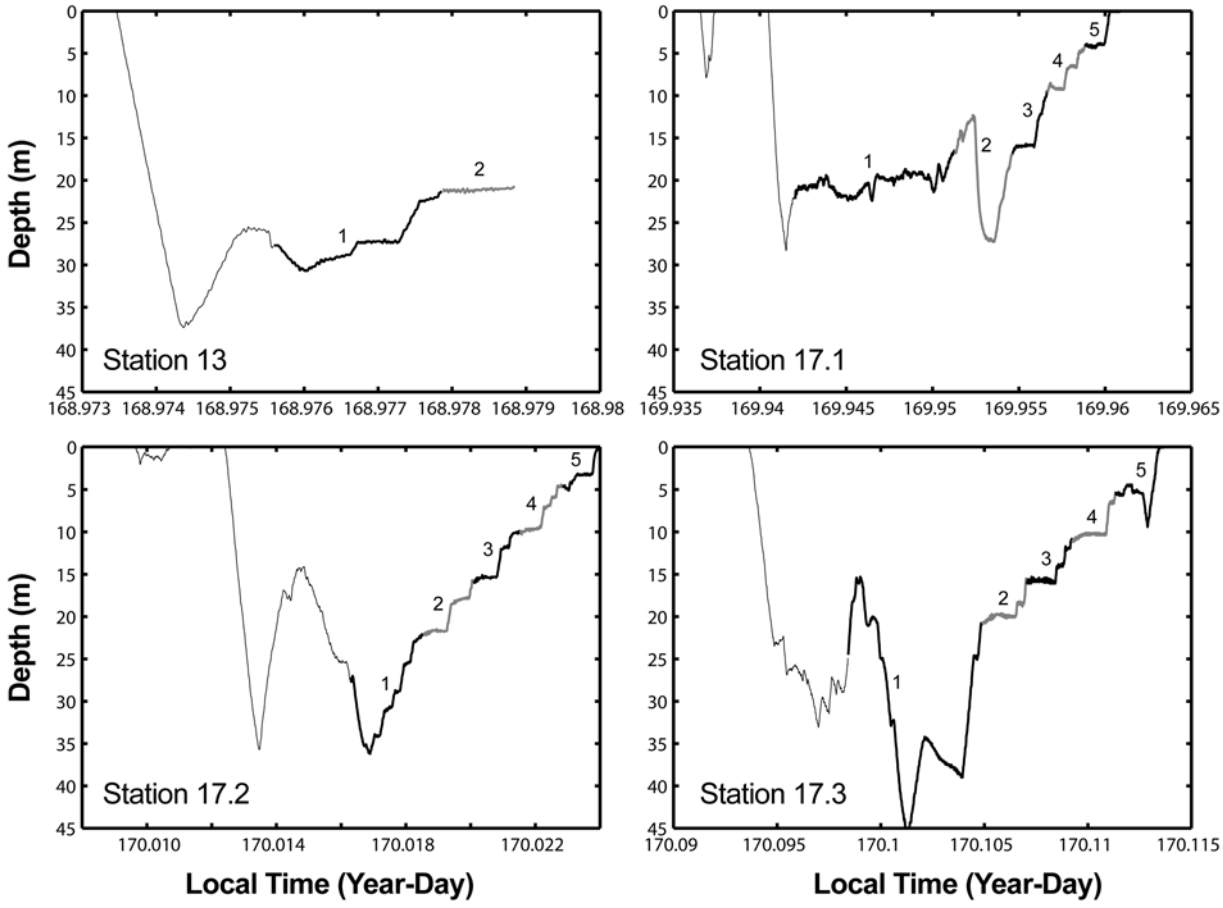


Figure 2. Time-depth trajectory of the Multinet during plankton sampling samples at station 13, June 16: 23:16:38 – 23:29:32; station 17.1, June 17: 22:27:40 – 23:03:46; station 17.2, June 18: 00:12:26 – 00:35:14; and station 17.3, June 18: 02:13:05 – 02:43:46. Sequential nets (1 – 5) are indicated by changes in the line color (black or gray) and numerals.

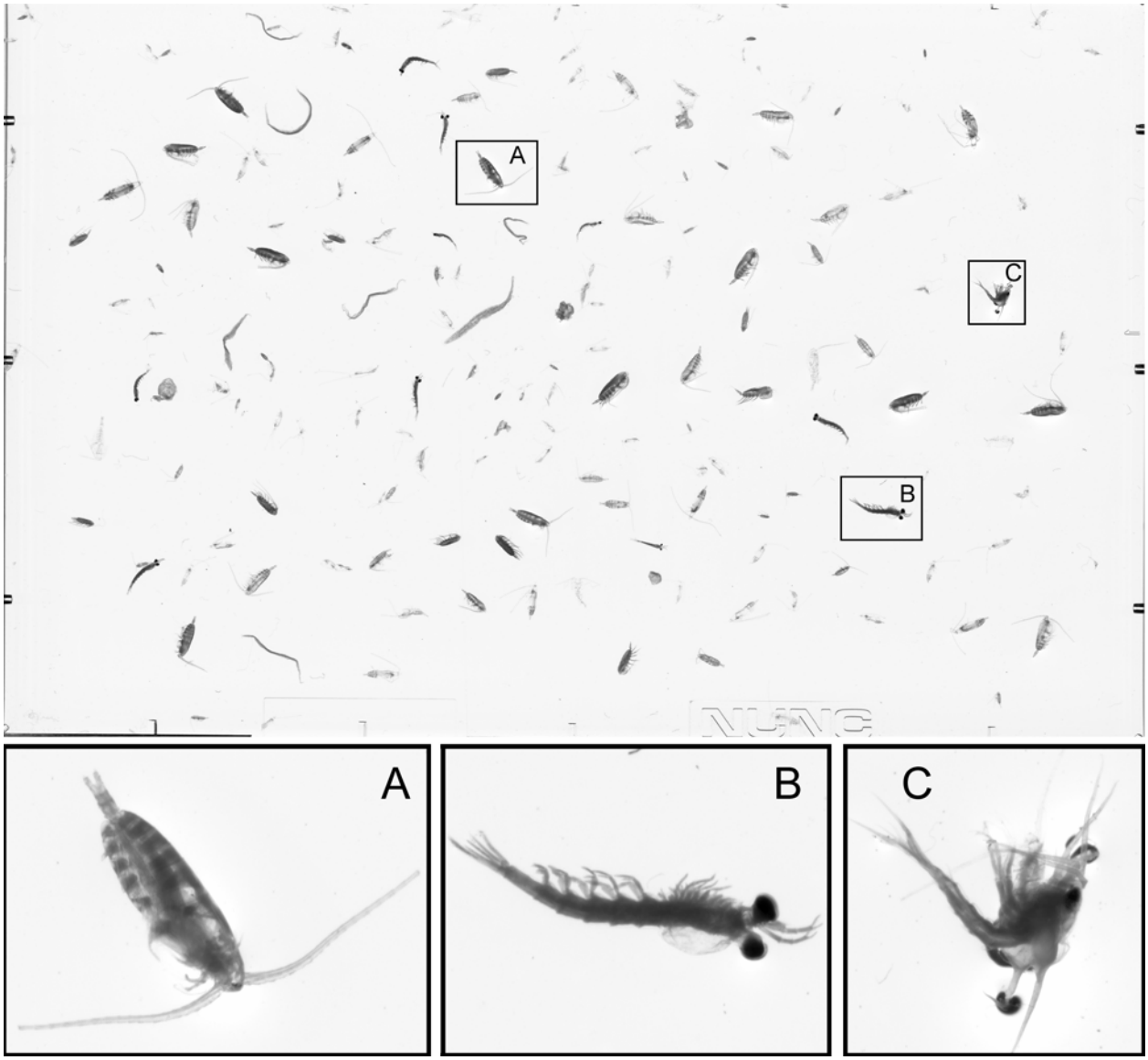


Figure 3. Top: An example ZooImage scan of the contents of a tissue culture tray. In this early test scan the animals near the edge of the tray were not moved away from the border as was done in subsequent scans. Insets A, B, C are enlarged in the bottom panels to show the fine detail of the scanned images of a copepod, euphausiid, and crab larva, respectively.

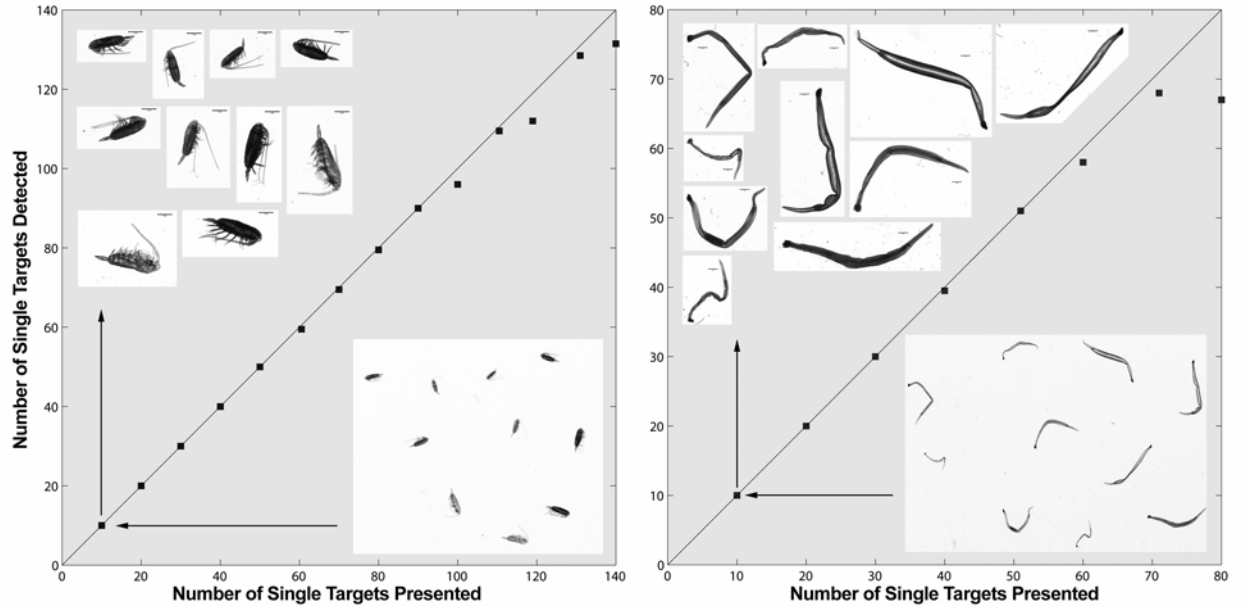


Figure 4. Comparisions of efficiency of ZooImage single target detection based on numbers of ROIs extracted from trays containing increasing densities of small targets such as copepods (left panel) and large targets such as chaetognaths (right panel). The straight line represents a 1:1 relationship between number of targets presented and the number of targets detected.

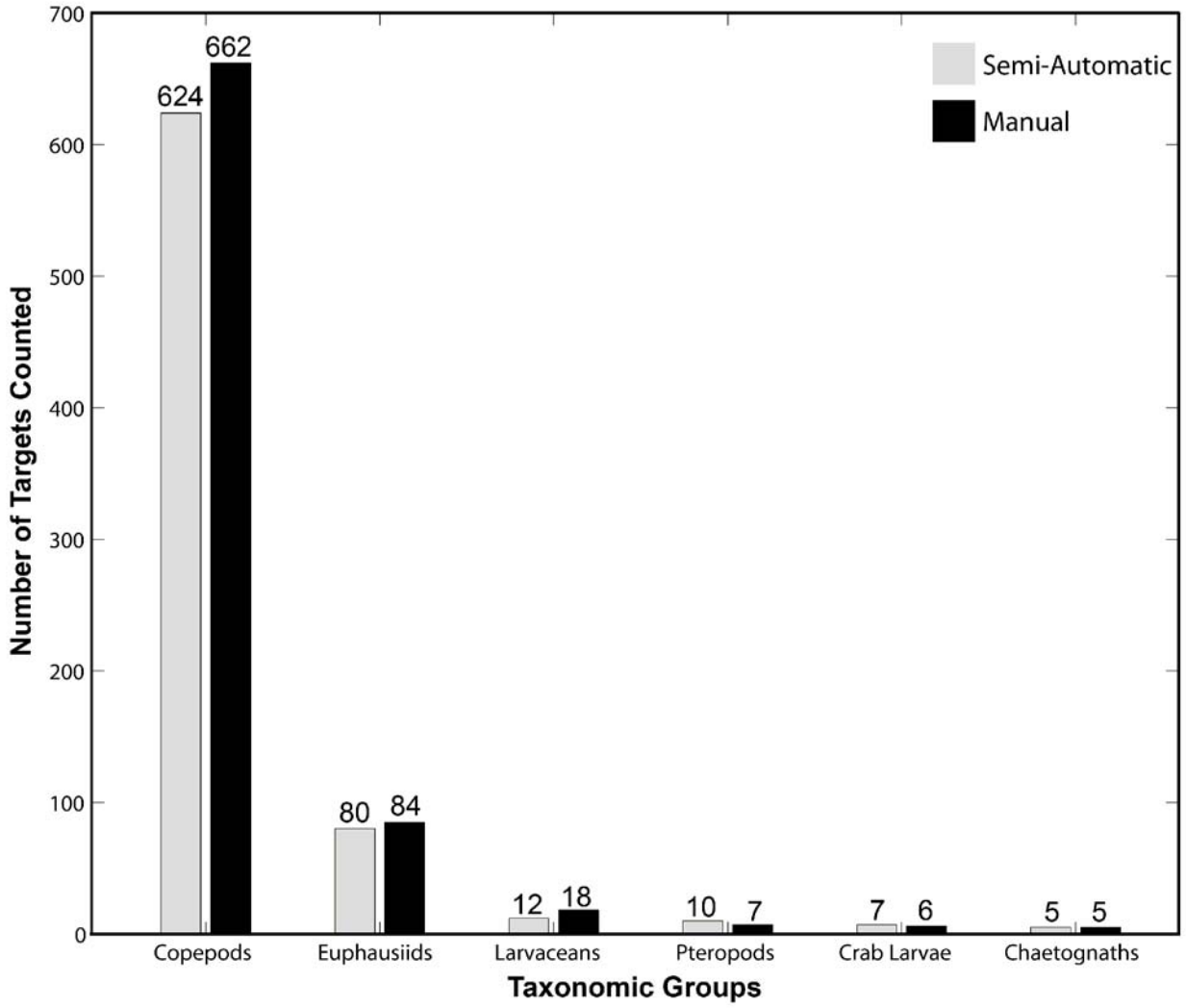


Figure 5. Density estimates for different taxa estimated using manual and semi-automated sample processing. This sample from a single net was a 1/64$^{th}$ aliquot that was first processed with ZooImage, then recombined and processed manually by observer one.

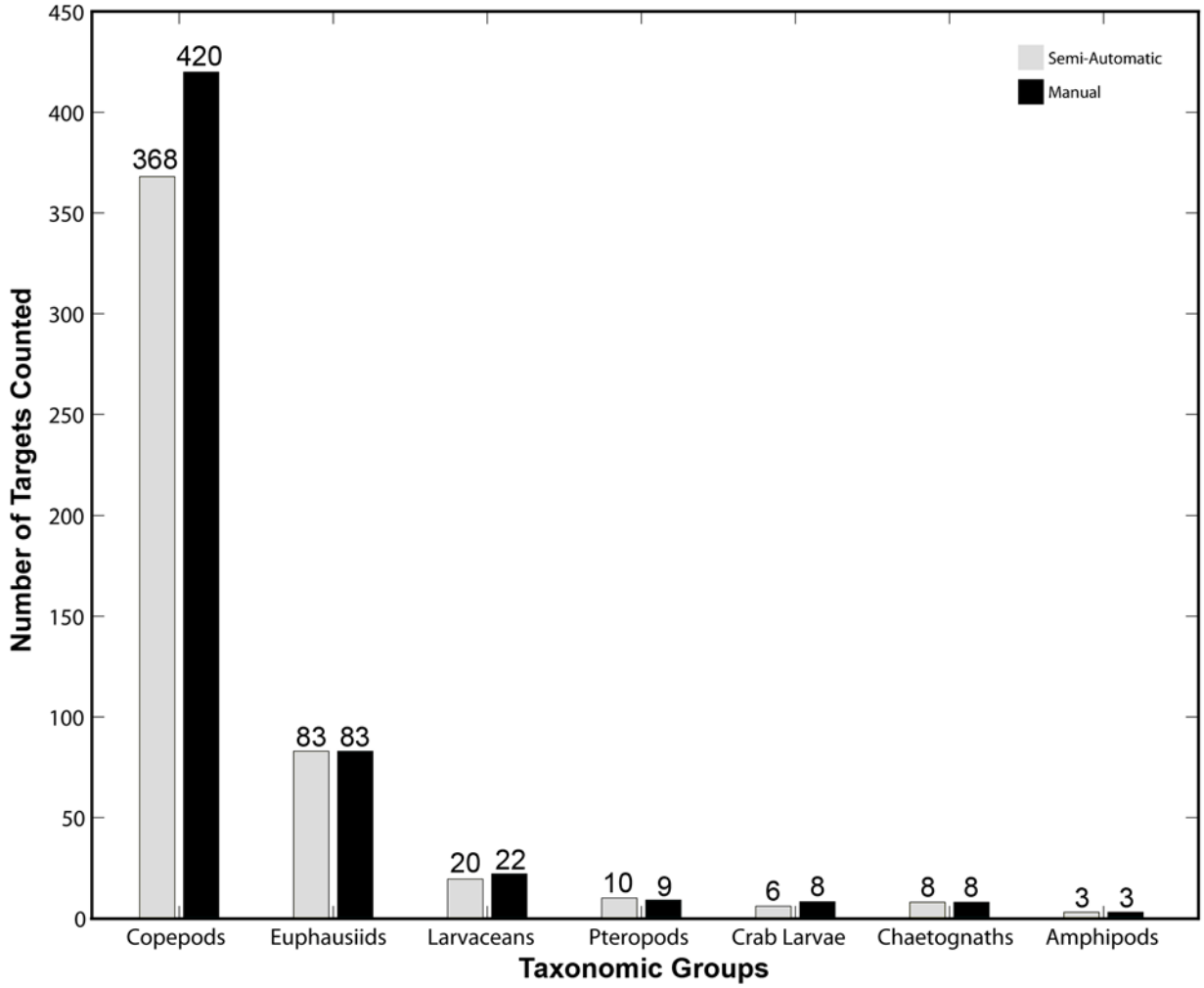


Figure 6. Density estimates for different taxa estimated using manual and semi-automated sample processing. This sample from a single net was a 1/64$^{th}$ aliquot (the same one used for results shown in the preceding figure). The sample was first processed manually by observer two and then recombined and processed with ZooImage.

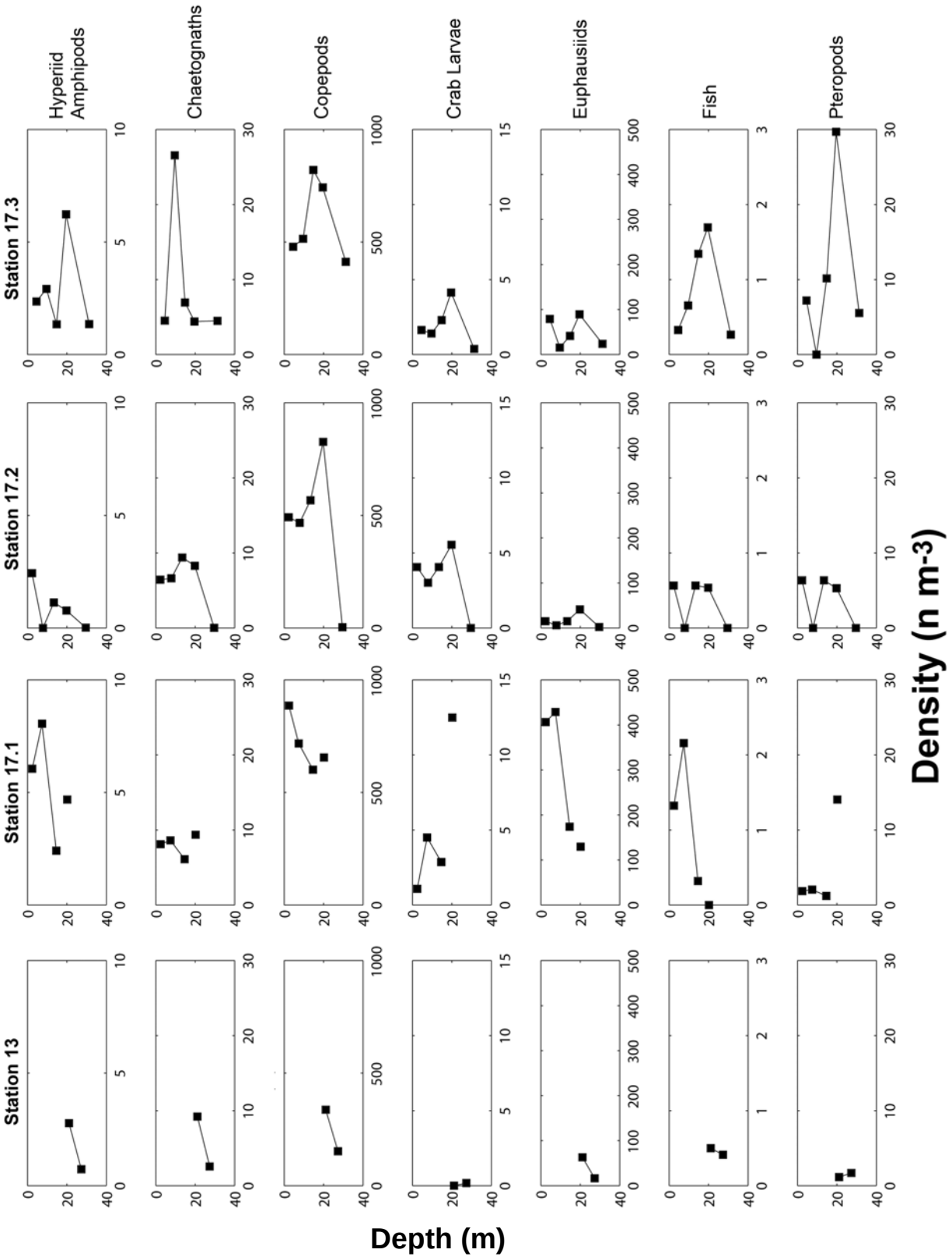


Figure 7. Vertical distributions of dominant mesozooplankton and micronekton in the near-surface waters at four stations. Densities are plotted at the mean depth of each net fished.